To Hell and Back: The genomic and phenotypic landscape of *E.coli* lineages recovering from Muller's Ratchet

A thesis submitted in partial fulfilment of the requirements for the Degree of

Master of Science
in Cellular and Molecular Biology

at the
University of Canterbury

by
S.J. Elley

2017

Table of Contents

Acknowledgements

I would like to thank Ant for providing me with this opportunity to study a truly awesome area of Science. When Ant presented me with a paper by Arlin Stoltzfus entitled - *Constructive Neutral Evolution: exploring evolutionary theory's curious disconnect* – I immediately became intrigued by this idea that complex molecular systems can emerge via random evolutionary processes and not necessarily by positive selection. I read further and realised that there is massive debate among evolutionary biologists concerning the evolutionary processes that drive biological innovation. When I discovered these long-standing theories can be experimentally tested in the lab, I realised I had found the perfect area of biology for me – combining experimental evolution with genomics to disentangle the evolutionary processes that drive the emergence of complex molecular systems. Overall, I wish to thank Ant for his support, patience and the many opportunities he has provided me with. The trip to Australia for the SMBE conference was particularly memorable.

I would like to thank Alicia Lai who allowed me to continue working on her amazing project. Thank you for setting me up with this project and teaching me how to work in a lab. Apologies for the countless silly questions – I appreciate that you would always answer them enthusiastically.

A huge thanks to Nicole who helped me tremendously once I was out of the lab and into the analyses. Without your help and ability to generate useful data very quickly,

my thesis would be very limited indeed. Thank you for allowing me to use your delta-bitscore method and for your help with the genomics and Biolog work.

I would also like to thank Alannah for helping me with numerous aspects of this project; in particular the DNA extractions and genome assembly.

Thank you to Paul Gardner, Nellie and other members of the lab group who have provided input and encouragement over the past few years.

Finally, I wish to thank my family for their continual support throughout this time. Thanks Jayden for the design help which has allowed me to communicate my science much more effectively and Zak for keeping me company while I write this thesis. Thank you Mum and Dad for your huge support and patience.

Abstract

We assessed the genomic and phenotypic landscape of fitness-impaired *E.coli* lineages recovering from the deleterious effects of Muller's ratchet via a combination of experimental evolution, genomics and global phenotypic screening. We found a seemingly paradoxical scenario where protein function appears to worsen in lineages as fitness increases. However, further investigation via functional perturbation analyses revealed that the deleterious effects of mutations that accumulated under the ratchet are probably being mitigated through novel molecular mechanisms – this gives the superficial impression that protein function is worsening. We argue that compensatory evolution explains this novelty, and we suspect compensatory mutations drive a substantial proportion of fitness and protein function recovery in the evolving lineages.

Additionally, based on the Biolog colour change assay, which measures substrate-dependent respiration, and rates-based measurements collected through time, we observed rapid and widespread metabolic erosion in populations subjected to the ratchet. Moreover, we found that phenotypic impairment was not mitigated following a period of fitness recovery.

The results presented here suggest that both the genomic and phenotypic landscape for lineages recovering from the effects of Muller's ratchet are novel compared to that of ancestral lineages. We comment on implications of these results with respect to various ideas on the emergence of biological complexity, and offer suggestions for

future work. To our knowledge, this is the first report of how mutational changes that accumulate in recovering populations impact on protein function, and no other study to date has assessed the capacity for recovering populations to grow in a very broad range of environments.

Chapter 1

Introduction: How mutation and drift drive Evolutionary Innovation

Motivation

Elevated mutation rates may increase the capacity for populations to adapt to new environments (Taddei et al., 1997; Tanaka, Bergstrom, & Levin, 2003). However, as the majority of mutations are deleterious, species must balance adequate mutation rates to facilitate adaptation, with fine-tuned error correction mechanisms to prevent fitness decline (Denamur & Matic, 2006). Because of such fitness costs, most organisms maintain low mutation rates via high fidelity DNA repair mechanisms that are normally favoured by selection (Denamur & Matic, 2006). However, in evolutionary contexts where selection is ineffective, elevated mutation rates are sometimes unavoidable and slightly deleterious mutations can irreversibly drift to fixation. In small, asexual populations this is commonly known as Muller's ratchet (Felsenstein, 1974; Muller, 1932; Muller, 1964). Under the ratchet, populations accumulate deleterious mutations at a rate that exceeds back mutations which can ultimately result in fitness decline and in some cases, mutational meltdown (Lynch, Bürger, Butcher, & Gabriel 1993).

The concept of Muller's ratchet has been supported by numerous studies that include computer simulations, theoretical studies (for review see Nei, 2005), experimental evolution (e.g. Andersson & Hughes, 1996; Funchain et al, 2000; Kibota & Lynch, 1996) and genomics (e.g. Jaramillo, Domingo, Munoz-Egea, Tabares, & Gadea, 2013; Lynch, 1996; Tenaillon et al., 2016). However, few studies to date have examined how genotypic changes that accumulate under the ratchet impact on protein function and phenotype, and none have screened for rare beneficial mutations that may help a population survive in a novel environment – such events might be possible under elevated mutation rates. Moreover, no study to date has examined how these phenomena might operate in populations recovering from the ratchet - the aim of this study is to address exactly these issues. Using experimental evolution coupled with whole-genome sequencing, we tracked and correlated genomic and phenotypic changes over the course of two experimental regimes. The first regime is a mutation accumulation (MA) experiment in which initially identical lineages of *E.coli* strain REL606 + pGEM::*mutD5* were subjected to repeated single-cell genetic bottlenecks on rich media (Lai, 2017). This effectively reduces the ability of natural selection to purge spontaneous mutations and increases their chances of drifting to fixation, and is thus analogous to Muller's ratchet (Halligan & Keightley, 2009). In the second regime, these MA lines were allowed to evolve further under a bottleneck relief regime. In this case, selection is predicted to operate with more efficiency (Clarke et al., 1993a).

Our lab group has already provided intriguing results from the bottleneck scheme. For example, we observed the emergence of slippage-type-editing (a process analogous

to RNA editing that rescues frameshift mutations) after approximately 4000 generations of bottlenecking (Lai, 2017). Additionally, when a frameshift mutation was introduced into wild-type *E.coli,* a loss of fitness attributable to RNA editing was observed (Lai, 2017). This suggests more generally that increases in complexity (in this case the emergence of RNA editing) may result under conditions that favour drift, and that such events are more probable under elevated mutation rates. These observations are congruent with a more general theme of constructive neutral evolution, a model that proposes non-adaptive (selectively neutral) processes are fundamental in shaping some complex biomolecular systems, with natural selection of secondary importance (Stoltzfus, 1999). One goal here was to extend our previous observations by assessing whether phenotypic innovation is also achievable by a species subjected to Muller's ratchet. In other words, as mutation rates become elevated under the ratchet, are we likely to see any novel gain-of-function phenotypes that might otherwise be avoided under conditions that favour natural selection.

Overall, the combination of bottleneck and bottleneck relief experiments, coupled with genomic and phenotypic analyses, provides opportunities to comprehensively assess the evolutionary implications of Muller's ratchet which previously has been limited to one or two areas. Combining experimental evolution with whole genome sequencing has previously provided incredible insight into how genotypic changes cause phenotypic changes in viruses, bacteria, yeast and flies (summarized in Barrick & Lenski, 2013). However, few studies have correlated genotypic changes with phenotypic changes under both a bottleneck and bottleneck relief regime. Moreover,

few studies have assessed the impact of genomic changes on protein function under such regimes, and how these changes may impact on phenotype. We implemented a newly described delta-bitscore (DBS) metric that assesses the functional severity of mutations, based on residue conservation and indel rates within a sequence (Wheeler, Barquist, Kingsley, & Gardner, 2016). Critically, this tool discriminates neutral from beneficial and deleterious mutational changes, and is favoured over the commonly employed dN/dS method that is unreliable over short evolutionary timescales (Rocha et al., 2006; Wheeler, Barquist, Ashari Ghomi, Kingsley, & Gardner, 2015). By assessing the impact of mutation of protein function, we can better understand how mutational changes that accumulate under the ratchet impact phenotype.

In Chapter 2 of this thesis, I explore the genomic basis that might allow severely bottlenecked populations to escape from "the click of the ratchet", via bottleneck relief. In Chapter 3, I assess the phenotypic capacities of the bottlenecked populations as well as populations that have evolved under the bottleneck relief regime. I continue chapter 1 by discussing the importance of mutation and drift in evolution in general. This is important to appreciate because under Muller's ratchet, natural selection is ineffective and thus evolution is expected to proceed more or less in a neutral fashion. However, mutation and drift that drive the ratchet are important evolutionary forces and there is substantial argument that these forces shape numerous complex biological phenomena with natural selection of secondary importance (Lynch, 2007; Nei, 2007; Stoltzfus, 1999). Motoo Kimura argued these forces are the main drivers of

evolution at the level of DNA and presented his case under a general model called neutral theory (Kimura, 1968). Nei 2007 goes further and argues that mutation and drift are the fundamental forces for phenotypic evolution also. One possible mechanism of how mutation and drift might facilitate evolutionary innovation at levels of biological organisation above that of DNA is presented under the constructive neutral evolution hypothesis (Lukeš, Archibald, Keeling, Doolittle, & Gray, 2011; Stoltzfus, 1999), which also has experimental support (Finnigan, Hanson-Smith, Stevens, & Thornton, 2012). Lynch (2007) and Doolittle (2012) argue that mutation and drift can facilitate the emergence of biological complexity particularly in small populations as natural selection is less efficient and slightly deleterious mutations can accumulate. As previously mentioned, however, this is problematic and potentially catastrophic for asexual organisms that are subjected to the deleterious effects of Muller's ratchet. I explore these themes in more detail below.

The Neutral Theory of molecular evolution

The neutral theory asserts that the majority of evolutionary change at the level of DNA is caused by random mutation and drift, with selection having a negligible role (Kimura, 1983). The theory was originally proposed by Kimura in 1968 and independently by J.L. King and T.H. Jukes in 1969 (Kimura, 1968; King & Jukes, 1969) and it received heavy criticism at the time, probably because it departed from classical Neo-Darwinism thinking that emphasizes the awesome power of natural selection in driving evolution (Zhang, 2016). For example, Simpson (1964) argued it improbable that proteins should have non-functional parts because completely neutral genes must be very rare. Therefore, it was claimed, that "natural selection is the composer of the genetic message, and DNA, RNA, enzymes and other molecules in the system are successively its messengers" (Simpson, 1964). This type of neutralist-selectionist debate amplified immediately following the conception of neutral theory and exists to this day. Since its inception, neutral theory has been adapted to include the nearly neutral theory (Ohta, 1992), expanded to account for evolutionary change at the phenotypic level (Nei, 2007), and applied to various aspects of genome architecture (Lynch, 2007; summarized in Zhang, 2016). Before discussing modern-day interpretations of neutral theory, I shall mention some important contributions that led to the development of the theory.

The first major attempt to describe how biological systems evolve dates back to the early 19th century when Jean Baptiste Lamarck, in his book called *Philosophie Zoologique*, proposed that acquired characters caused by use or disuse are inherited,

which is ultimately influenced by environmental factors (Lamarck, 1809; for review see Kimura 1983). The Lamarckian description of evolution was rejected following the development of the modern synthesis and Charles Darwin's evolution by natural selection became the new frontier in evolutionary thought. Darwin's interpretation of evolution was that because variation exists between individuals and this variation may be inherited, variation that contributes optimally to survival and reproduction is more likely to be propagated. Over time, small-beneficial variations accumulate in a continuous process of adaptive evolution (Darwin, 1859; for review see Kimura 1983). The eventual merger of Darwinism and Mendelism (which could explain principles of heredity) contributed to the formation of classical population genetics (for review see Kimura, 1983). This field was pioneered by three key figures: R.A. Fisher, J.B.S Haldane and Sewall Wright. The former two emphasized the importance of natural selection in evolution while Wright argued that evolution is explained by a number of factors, including random genetic drift (Wright 1977; for review see Kimura, 1983). By the 1960s, the consensus among evolutionary biologists was that evolution is primarily influenced by adaptation through natural selection. Some, for instance, argued that neutral mutations are very rare (e.g. Mayr, 1962) while others such as Fisher (1930b) argued for the importance of positive selection and downplayed any significant role of mutation in driving evolution. Kimura (1983) pointed out, however, that studies around this time were mainly focused on phenotypic models, and thus overlooked how evolution operates at the molecular level. As such, Kimura presented a thesis that proposed the nucleotide substitution rate in the mammalian genome exceeds the

upper limit of adaptive evolution that was originally put forward by Haldane (Haldane, 1957b). This suggests that most genetic changes are selectively neutral and not under positive Darwinian selection (Kimura, 1968; Zhang, 2016). Unsurprisingly, this proposal was met with criticism. For example, Maynard Smith (1968) argued that Haldane's upper limit of adaptive evolution is too low, suggesting the rapid nucleotide substitution rate in mammals which Kimura observed is possible under an adaptive model. Nevertheless, there were also studies around this time that parallel aspects of neutral theory (e.g. King & Jukes, 1969; Zuckerkandl & Pauling, 1965) and more recent work is also in favour of neutral theory (reviewed in Nei, Suzuki, & Nozawa, 2010b). In contrast, recent criticism of neutral theory can be found in Hahn 2008.

Expansion of the Neutral Theory

Ohta (1973) adapted neutral theory to include nearly neutral mutations. Ohta argued that slightly-deleterious mutations can go to fixation by drift if their selection coefficient is small enough, based on the assumption that the majority of mutations fall in the range of deleterious to selectively neutral (Akashi, Osada, & Ohta, 2012). In line with this, it was also suggested that effective population size is an important variable with respect to the likelihood of nearly-neutral mutations becoming fixed. For instance, Ohta (1972a) identified a negative correlation between rates of protein evolution and population size, which was observed in *Drosophila* and mammals. This has since been verified in several genome-scale comparison studies that have

identified an inverse relationship between the ratio of non-synonymous to synonymous substitutions per nucleotide site (dN/dS) and population size, for example, in the Chimpanzee sequencing and analysis consortium 2005, and Rhesus Macaque Genome sequencing and analysis consortium 2007 (for review see Akashi et al., 2012; Zhang, 2016). Wright & Andolfatto 2008 argue this relationship extends to plants and bacteria also, the latter of which has been reported in studies that show faster rates of evolution in endosymbiont bacteria compared to their free-living relatives (Moran, 1996).

Neutral theory has also been expanded to include the new mutation theory of phenotypic evolution that proposes phenotypic evolution is mainly driven by mutation (Nei, 2007). It is interesting that this contradicts arguments from the pioneers of neutral theory - Kimura, Jukes and King, who argued against the importance of selectively neutral forces at the phenotypic level. For example, Kimura states "Opportunism in evolution is an eloquent testimony that evolution at the level of form and function is largely determined by Darwinian natural selection that brings about adaptation of organisms to their environments" (Kimura, 1983). The arguments presented by Kimura stem from extrapolations based on the fossil record, for which there are numerous examples of opportunism and convergence. One such example is seen in the adaptive radiation of marsupials in Australia that show comparisons to placental mammals such as the mole-like Marsupials, squirrel-like Marsupials and dog-like marsupials (Kimura, 1983). Despite this, Kimura later conceded that phenotypic evolution could, in some circumstances, be predominately driven by mutation and

drift rather than selection. One possibility, Kimura argued, is by gene duplication. Mutations in a newly duplicated gene allows that gene to drift into unique evolutionary space, which could conceivably facilitate adaptation (Kimura, 1991).

Nei 2007 strongly argued for the importance of mutation and drift in phenotypic evolution in general. Nei proposes that the vast amount of phenotypic diversity that exists is a result of novel mutations which can facilitate adaptation to new environmental conditions. He put forward this proposal by examining the evolution of multigene families in Eukaryotes involved in basic developmental processes; for example, homebox genes that encode transcription factors involved in morphogenesis (Nei, 2007). These genes are highly conserved, however, there is generally a relationship between the number of gene copies and the complexity of the physiological or morphological character controlled by that family (Nei, 2007). Ultimately, changes in the number of member genes in a particular family is due to random deletion and duplication events under a process called random genomic drift and therefore the evolution of the homebox genes and the phenotypic characters they encode is largely determined by selectively neutral processes (Nei, 2007). One such example is seen in the evolution in the *HOX* gene family - a group of developmental genes in animals controlling anterior-posterior segmentation in the homebox superfamily. Vertebrates, which have more complex body plans than Invertebrates, typically contain much higher numbers of *HOX* gene copies. For example, Mammals contain 39 gene copies compared to 8 in Fruit flies. To some, this suggests random duplication events have facilitated the ability of mammals to exploit complex

morphological body plans, which in turn allows adaptation to novel environments (Nei, 2007).

Nei (2007) also presents several other arguments that highlight the importance of mutation and drift in driving phenotypic evolution. For example, Nei points out that increases in the number of genes involved in complex genetic networks generally equates with increases in phenotypic character complexity, and this increase in gene number is a result of random gene duplication events (Nei, 2007). This is also argued in several other studies (Nei, 1969; Ohno, 1970; Pires-daSilva & Sommer, 2003). Finally, in a review by Nei (2005), Nei highlights how simple mutational events alone can contribute to significant changes at the phenotypic level. Perutz (1983) for example, found that in haemoglobin in crocodiles, just 5 amino acid substitutions can explain a gain-of-function phenotype (bicarbonate binding) that mitigates the effects of blood acidity that occurs during extended periods under water. Moreover, Hedge & Spratt (1985) found that only four amino acid substitutions are required to be introduced into Penicillin binding protein 3 of *E.coli* for resistance to beta-lactam antibiotics.

The Emergence of Biological Complexity: Positive selection or Neutral evolution?

A common misconception in evolutionary biology is that natural selection encourages organisms to become more complex (Gould, 1996). However, some argue that reductions in the efficiency of natural selection facilitates the emergence of complex systems (e.g. Lynch, 2007). This is certainly true in small populations, as selection is ineffective at preventing deleterious mutations from becoming fixed when the effective population size is very small (Lynch, 2007). For example, multicellular Eukaryotes that experience reduced populations sizes have complex genomes that contain mobile elements, introns and other features that add to overall genome complexity (Lynch, 2007). Some argue, albeit controversially (see Hickey (1982) for alternative hypothesis) , that this complex architecture emerged partly due to the effect of reduced population sizes that Multicellular species experience (Lynch, 2007). Prokaryotes that normally reside as large populations on the other hand have less elaborate genome architecture. These arguments are somewhat in line with models of constructive neutral evolution and the Zero Force Evolutionary Law (McShea & Brandon, 2010; Stoltzfus, 1999). The former describes how mutation and drift can facilitate the design of intricate intracellular systems and the latter argues for a tendency for life to become more complex when selection is ineffective. I explore these concepts in more detail below.

The CNE model proposes that some examples of complex biological systems in nature emerged probably by selectively-neutral processes, with positive selection playing a

subsidiary role. This model contradicts arguments from Neo-Darwinists who argue complexity correlates with operational fitness (Stoltzfus, 1999). Nonetheless, there is compelling evidence that CNE can explain the origins of spliceosome splicing, the emergence of RNA editing, the retention of gene duplicates, and possibly even the elaborate structure of the ribosome (Stoltzfus, 1999). These complex systems might, at first glance, appear as fine-tuned products of natural selection, however, some argue that "pre-suppression" presents a simpler, more plausible explanation (Lukeš et al., 2011).

Lukeš and colleagues (2011) present a hypothetical model illustrating how CNE might operate (Figure 1.1). To summarize, let's assume an enzyme called [A] facilitates a biological reaction independently of another enzyme called [B]. Fortuitous and neutral interactions may allow [A] and [B] to interact. A mutation in [A] might cause [A] to depend on an interaction with [B] for the reaction to occur. Further mutations in [A] could increase this dependency, and if there are many amino acid sites at which [A] becomes dependent on [B] then the capacity for [A] to revert to an independent state is unlikely (Figure 1.1). Due to this irreversibility, CNE is often described as an evolutionary ratchet, possibly in a nod to Muller's ratchet (Lukeš et al., 2011). Let us consider one example where this might be possible - that of Neurospora mitochondrial group I introns which depend on a mitochondrial tyrosyl tRNA synthetase (mtTyRS) for splicing (Akins & Lambowitz, 1987). By designating the self-splicing introns as [A] and the mtTyRS as [B], and assuming [A] and [B] react fortuitously, then mutations in [A] that prevent self-splicing are suppressed by [B]. It is unlikely the ability to self-splice

would be salvaged following further mutations in the introns, and hence, a 1-component system becomes a more complex 2-component system following a selectively neutral walk through evolutionary space (Lukeš et al., 2011). An alternative explanation might be that mtTyRS evolved to compensate for defects in the intron sequence through positive selection (Paukstelis & Lambowitz, 2008). However, Lukeš and colleagues 2011 argue this "puts the cart before the horse" - that is, mutant introns would likely be removed by natural selection before mtTyRS had time to evolve its compensatory power.

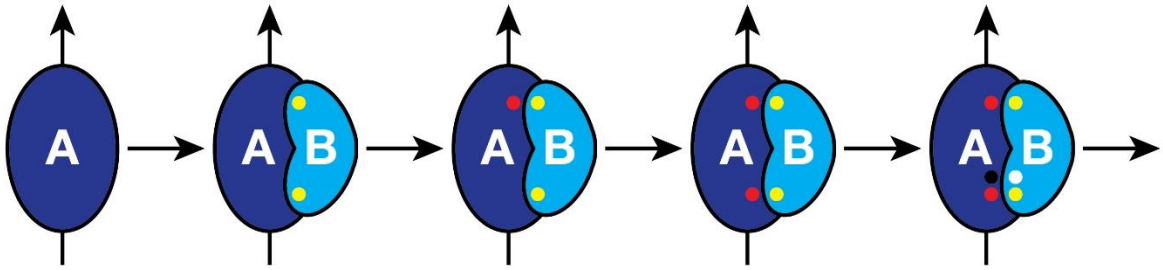

Figure 1.1. Depiction of how constructive neutral evolution could theoretically operate. [A] and [B] are enzymes that react fortuitously through neutral interactions (yellow dots). A mutation in component [A] (red dot) causes a dependency on [B] for an enzymatic reaction to take place that [A] could previously facilitate independently. Further mutations in [A] increases this dependency (more red dots). Interactions between [A] and [B] are maintained by negative selection, and [A] and [B] begin to co-evolve (black and white dots). Figure is adapted from Lukeš et al. (2011).

CNE is elegant in theory, however, few studies have directly tested it. Several studies show that spliceosomal splicing is less efficient than self-splicing by group 2 introns (e.g Baurén & Wieslander, 1994; Beyer & Osheim, 1988; Schmidt, Podar, Stahl, & Perlman, 1996), suggesting the highly complex spiceosomal machinery which comprises five small RNAs and over 300 proteins emerged not entirely through the action of positive selection (Nilsen, 2003; Stoltzfus, 1999). Possibly, the most convincing experimental evidence for CNE is provided by Finnigan and colleagues (2012). This group showed through ancestral gene reconstruction and manipulative genetic experiments, that a 3-component protein complex in Fungi evolved from a simpler 2-component system by simple mutation and drift events. The system this group disentangled was the vacuolar H^+-ATPase (V-ATPase) which is a multi-paralogue ring complex that acidifies subcellular compartments. They proposed that each component is expressed by a single gene, two of which emerged from a single gene following a gene duplication event. Following this event, each component encoded by the two daughter copies subsequently lost an ability to bind to specific interfaces of other proteins following an accumulation of neutral (or nearly-neutral) mutations. These losses resulted in each component having a specific spatial orientation and gave rise to the emergence of a more complex hetero-oligomeric complex (Figure 1.2). By introducing historical mutations into resurrected ancestral proteins, the group argued that simple, high-probably mutations are a more likely the cause for increased complexity than positive selection (Doolittle, 2012; Finnigan et al., 2012).

As already mentioned, our lab group also found experimental evidence for the emergence of slippage-type editing in *E.coli* which appears have to resulted under conditions that minimises the efficiency of selection (Lai, 2017). Lai (2017) found that while slippage-type editing rescues frameshift mutations, it leads to a general loss of fitness when these mutations are introduced into wild-type bacteria. Through GFP reporter systems, it was also found that protein production is reduced. These results imply that slippage-type editing evolved through the action of random mutation and drift, a finding that is congruent with the constructive neutral evolution model and proposal by Finnigan and colleagues (2012) that the V-ATPase in Fungi became more complex as a result of mutation and drift.

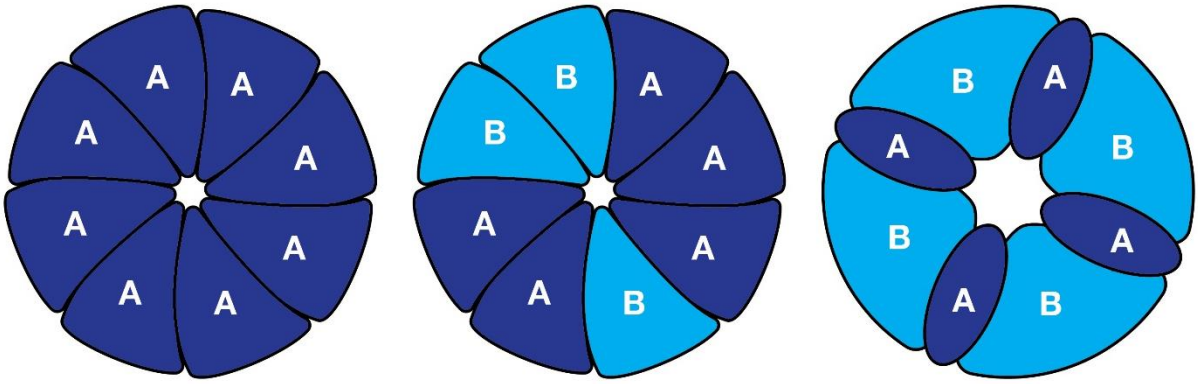

Figure 1.2. Depiction of how a molecular machine could become more complex. Left: All subunits [A] are encoded by a single gene. Middle: A gene duplication event allows subunits [A] and [B] to diverge via an accumulation of neutral (or nearly-neutral) mutations without impairing the original function of the protein complex, resulting in a hetero-oligomeric complex. Right: Further mutations may prevent subunits from binding to their own type. It is unlikely further mutations would cause a reversion of the complex to a homo-oligomeric state. This simple depiction reveals how mutation and drift can drive complexity in a molecular machine without invoking natural selection. In small populations, even sub-lethal mutations could theoretically accumulate in duplicated genes. Figure is adapted from Doolittle (2012).

CNE is in line with the Zero Force Evolutionary Law (ZFEL) hypothesis which proposes that life in general tends to increase in complexity when selection is inefficient (Fleming & McShea, 2013; McShea & Brandon, 2010). For example, Fleming & McShea (2013) present a study in which they assess the morphological complexity of laboratory mutants in *Drosophila Melanogaster* compared to wild-type lines. They observed laboratory strains (which are subjected to reduced selection pressures) to be more complex than wild-type strains where complexity is equated with the number of different part types as well as shape and colour. This parallels work from our group in which we observed the emergence of slippage-type editing because both studies were performed in environments that maximise drift and minimise selection (Lai, 2017). Often advocates of ZFEL emphasize a latent potential for adaptation to new environments when complexity increases in a neutral fashion. Fleming & McShea (2013) write: "Who is to say that a mutant fly with one leg shorter than the others - suitably stabilized in development by selection - could not in some ecological context become the next adaptive innovation for *Drosophila?*." This is in line with work by Masatoshi Nei who emphasises the power of mutation and drift in generating phenotypes that might be advantageous in some novel environment (Nei, 2007).

In summary, there is strong support for the emergence of biological complexity by neutral processes. As natural selection is ineffective under Muller's ratchet, it may be that complexity emerges under populations subjected to the ratchet. One aspect of this project involved testing this prediction by screening for any rare beneficial phenotypes that might emerge by chance under a bottlenecking regime.

Replicating Muller's Ratchet in the lab

So far I have discussed the importance of mutation and drift in evolution. I have also mentioned how the effects of these forces are amplified in small populations. Here I focus on one implication of small population size, called Muller's Ratchet - the irreversible accumulation of sub-lethal mutations in small, asexual populations (Felsenstein, 1974; Muller, 1964). Occurrence of the ratchet has been widely reported in bacterial, viral and protozoan populations (Andersson & Hughes, 1996; Chao, 1990; Lewis, 1990; Moran, 1996). Moran (1996) for example, compared Aphid endosymbionts to their free-living relatives and found that the endosymbionts evolved rapidly and accumulated low ratios of synonymous to non-synonymous substitutions, consistent with Muller's ratchet. In another study, Chao (1990) investigated the role of Muller's ratchet on the evolution of sex in RNA bacteriophage Φ6 and report that fitness decline associated with Muller's ratchet is unable to be mitigated by beneficial, backward and compensatory mutations.

However, several studies have demonstrated that avoidance of the ratchet can be achieved by a variety of mechanisms, the most prominent example of which is the ability of sexual organisms to undergo recombination, which can yield mutation-free individuals (Felsenstein, 1974). As such, implications of Muller's ratchet have been proposed to account for the advantages of why some organisms undergo sexual reproduction (Felsenstein, 1974). Some asexual organisms also have similar avoidance mechanisms. For example, Asexual Amoebae and other protists avoid the ratchet through gene conversion events that are possible due to their Polyploid state. In gene

conversion, a mutated sequence is replaced by a wild-type sequence through homologous recombination (Maciver, 2016). Other asexual Organisms may achieve avoidance of the ratchet via horizontal gene transfer (Overballe-Petersen & Willerslev, 2014; Overballe-Petersen et al., 2013), host-level selection on bacterial endosymbionts of insects that experience population bottlenecks upon infection (Allen, Light, Perotti, Braig, & Reed, 2009; Rispe & Moran, 2000), or via back and compensatory mutations that mitigate the deleterious effects of mutations (Bull, Badgett, Rokyta, & Molineux, 2003; Pfaffelhuber, Staab, & Wakolbinger, 2012).

Reproducing a Muller's ratchet-type scenario in the laboratory is possible via Mutation Accumulation (MA) Experiments. In MA experiments, conditions are adjusted to minimise the impact of selection such that mutations can accumulate in replicated lines over several generations. Therefore, MA experiments allow researchers to investigate the rates and properties of new mutations, as well their effects on fitness, transcriptome abundance, phenotype or any other measurable biological property (Figure 1.4) (Halligan & Keightley, 2009).

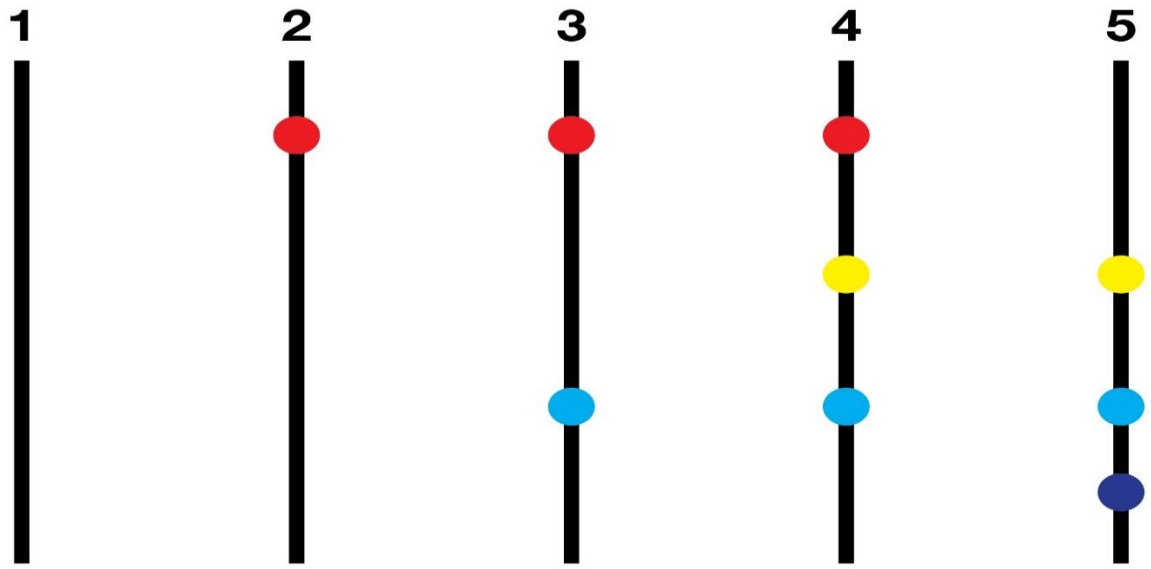

Figure 1.3. Depiction of how Muller's ratchet operates. A mutation (red) appears in generation 2 in the genome (black) of members of a population. This is passed on to generation 3. Another mutation appears in the third generation (light blue). Further mutations (yellow and purple) emerge in generation 4 and 5, respectively. The original mutation (red) reverts in generation 5 however under conditions that minimise the efficiency of selection, the general trend of mutation accumulation continues irrespective of the impact of these mutations on fitness.

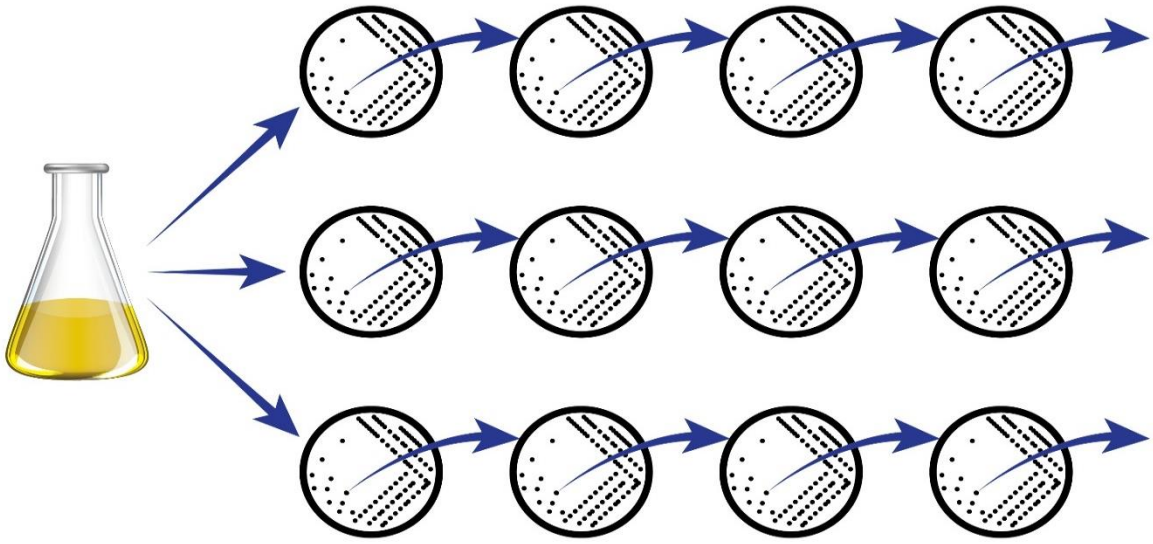

Figure 1.4 Depiction of a classic Mutation Accumulation (MA) experiment. Initially isogenic lines (Erlenmeyer flask) are subjected to multiple population bottlenecks by continuously passaging a very small number of individuals (horizontal arrows) to fresh media. Over time, fitness decline is normally observed due to the accumulation of sub-lethal mutations. In asexual systems, this is known as Muller's ratchet. Given mutations evolve neutrally with respect to fitness, the average rate of increase in numbers of mutations per line is equivalent to the mutation rate (Lynch et al., 2016). The procedure is often followed up by genome sequencing, fitness assays and phenotypic analysis.

So far I have addressed studies that have confirmed Muller's ratchet through use of MA manipulations (e.g. Andersson & Hughes, 1996; Bull et al., 2003; Chao, 1990; Clarke et al., 1993c). MA experiments also allows one to assess how changes at the genomic level impact on phenotype, and thus potentially provide a useful tool for examining how genomic changes accumulated under the ratchet impact phenotype. Several studies have examined the phenotypic impact of mutations by utilizing MA experiments, some of which have addressed gene expression (e.g. Denver et al., 2005;

Rifkin, Houle, Kim, & White, 2005), and others of which have examined metabolism (e.g. Cooper & Lenski, 2000; Funchain et al., 2000; Leiby & Marx, 2014). For example, Rifkin et al. (2005) examined transcriptome abundance across 12 initially identical *Drosophila* lines that have independently accumulated mutations over 200 generations. They observed that spontaneous mutations can cause widespread variation in gene expression, but such expression is constrained by stabilizing selection. In another study, *Caenorhabditis elegans* MA lines were compared to natural isolate lines (Denver et al., 2005). The authors reported massive variation in gene expression in MA lines compared to wild-type lines, conclusions in line with Rifkin et al. (2005) who argue that selective pressures prevent gene expression levels from varying significantly in wild populations (for review see Halligan & Keightley, 2009). In a MA-based study assessing metabolism, Funchain and colleagues (2000) examined the function of over 700 genes in mutator *E.coli* lineages following continuous cycles of single-cell bottlenecking. They observed populations with reduced fitness, increased auxotrophic requirements, colony size reductions and loss-of-function phenotypes that limited carbon utilization capacities. Leiby & Marx (2014) examined the ability of *E.coli* to utilize various carbon sources after 50 000 generations of growth on glucose. Whilst they found novel gain-of-function phenotypes associated with organic acids, strains that showed elevated mutation rates triggered declines in metabolic capacities.

Conclusions

Muller's ratchet is characterized by elevated mutation rates, small population size, intense genetic drift and irreversibility. The former components have been shown to drive evolutionary innovation at all levels of biological organisation. The latter component (irreversibility) is problematic (and potentially catastrophic) for asexual organisms that lack the mechanisms to halt the ratchet. In chapter 2 of this thesis we examine the mutational basis that might allow a bottlenecked population of *E.coli* to escape the ratchet under a bottleneck relief regime. How mutations that accumulate under such a regime impact on protein function, and how such changes relate to fitness recovery remains largely ignored in the literature. In chapter 3 we then focus on the phenotypic effects of Muller's ratchet by assessing the capacity for bottlenecked and recovering lineages to grow in hundreds of different metabolic environments.

To achieve such an undertaking, we analysed growth data, sequenced genomes and analysed the functional severity of mutations. To assess the functional impact of mutations, and to distinguish loss-of-function mutations from gain-of-function mutations, we screened our lines using Biolog phenotypic arrays.

Chapter 2

Escaping the Ratchet: Novel molecular pathways to restoring Fitness and Protein Function

Introduction

Small, asexual populations are well known to experience fitness decline when subjected to Muller's ratchet (Lynch, Bürger, Butcher, & Gabriel 1993). However, there are several mechanisms that may allow populations to escape from the deleterious effects of the ratchet. These include horizontal gene transfer events which can reverse the inactivation of genes by mutation, host-level selection pressures, as well as compensatory and reversion mutations (Bull et al., 2003; Pfaffelhuber et al., 2012; Rispe & Moran, 2000; Takeuchi, Kaneko, & Koonin, 2014). It has been demonstrated in several Mutation Accumulation (MA) experiments that compensatory and reversion mutations can partially or completely recapture wild-type fitness in populations recovering from severe population bottlenecks (Bull et al., 2003; Burch & Chao, 1999; Charlesworth, 2009; Clarke et al., 1993b; Perfeito, Sousa, Bataillon, & Gordo, 2014; Pfaffelhuber et al., 2012; Poon & Otto, 2000). Compensatory mutations are particularly prominent in these studies for these types of mutations are more likely to restore fitness than back mutations (Pfaffelhuber et al., 2012; Poon & Chao, 2005).

Haigh (1978), for example, stated that back mutations are rare because the "deleterious mutation rate is proportional to the full length of the genome of a clonally reproducing individual, while the compensatory mutation rate (which in this case means back mutation) scales with the length of a single base within the full genome" (for review see Pfaffelhuber et al., 2012). Even in bacteriophages that comprise small genomes the rate of compensatory mutations exceeds that of back mutations (Bull et al., 2003; Poon & Chao, 2005). For example, Poon & Chao (2005) investigated the frequency at which compensatory mutations restore fitness in mutant populations of bacteriophage ϕX174 compared to reversion mutations. Following the introduction of 21 deleterious missense substitutions into the ϕX174 genome, they observed that when lineages regained fitness the frequency of compensatory mutations was ~70%. These types of observations are also reported in other studies (e.g. Bull et al., 2003; Escarmís, Dávila, & Domingo, 1999; Moore, Rozen, & Lenski, 2000). Compensatory mutations are particularly relevant to our research due to their capacity to reduce the deleterious effects of mutations that could potentially be adaptive. For example, antibiotic resistance-causing mutations can sometimes have deleterious consequences in a wild-type background, the effects of which can be remedied by compensatory mutations (Maisnier-Patin & Andersson, 2004; Poon & Chao, 2005).

Several possible mechanisms for which compensatory mutations might operate are described in Maisnier-Patin & Andersson (2004). The first possibility is through intragenic point mutations that recapture structural or functional defects of protein or RNA molecules. A second possibility is by intergenic mutations that repair mutated

multi-subunit complexes or organelles. Thirdly, compensatory mutations can trigger the recruitment of alternative pathways to circumvent existing pathways affected by mutation. Another possibility is through increased enzyme production that can compensate for lowered activity caused by a defect enzyme. There is substantial experimental evidence that these occurrences can provide a potential escape route for organisms subjected to the ratchet. This is true for fitness-impaired viruses (Bull et al., 2003; Burch & Chao, 1999; Clarke et al., 1993b; Poon & Chao, 2005), bacteria (Bjrkman, Hughes, Andersson, & Roth, 1998; Levin, Perrot, & Walker, 2000; Maisnier-Patin, Berg, Liljas, & Andersson, 2002; Moore et al., 2000) and even multicellular organisms (Estes & Lynch, 2003).

In summary, back and compensatory mutations provide a potential escape route for populations subjected to Muller's ratchet. Such mutations aid in fitness recovery and compensatory mutations may even allow the persistence of adaptive mutations in populations that have a deleterious effect in a wild-type background. Numerous studies support this, and many of these studies have achieved this by observing these types of mutations in MA lines that have been subjected to further evolution under a bottleneck relief-type regime (Bull et al., 2003; Estes & Lynch, 2003; Poon & Otto, 2000). Here, we undertook a similar procedure. However, as little is known about how mutations that accumulate under a relief regime (such as back, compensatory and other mutations) impact protein function, we decided to focus on exactly this. In turn, the aim here is to assess the mutational basis that might allow populations subjected to Muller's ratchet to escape from a trajectory towards mutational meltdown, by

exploring the impact of these mutations on protein function and relating this to fitness recovery. To achieve such a goal, we employed a newly-described delta bitscore (DBS) tool (Wheeler et al., 2016). The DBS method utilizes Profile hidden Markov models to assess the functional severity of mutations by considering residue conservation and indel rates within a sequence, and is defined by the following equation:

$$DBS = x_{ref} - x_{var}$$

"Where DBS is delta-bitscore, and x_{ref} and x_{var} are bitscores for reference and variant sequences derived from alignments to the same profile HMM" (Wheeler et al., 2016). As such, mutations in highly conserved positions in a protein sequence alignment are scored with a greater penalty than those in positions that are free to vary. Critically, the DBS-based approach for assessing the functional impact of mutations has several advantageous over the commonly employed dN/dS tool for examining recently diverged strains. Often, dN/dS ratios are accompanied by high rates of false-positives and false negatives in addition to contradicting results (Kryazhimskiy, Plotkin, Smith, Simonsen, & Miller, 2008; Nei et al., 2010; Rocha et al., 2006; Wheeler et al., 2016).

To this end, we decided to recover bottlenecked populations of *E.coli* close to extinction by repeatedly transferring large populations of cells under competitive conditions, which we call bottleneck relief and will sometimes refer to as BR. We sequenced genomes of recovering lines, performed fitness experiments and assessed the functional severity of mutations that emerged under this regime. We compare changes to the ancestral and wild-type populations. The ancestral line represents a

severely fitness-impaired mutator population that has accumulated thousands of mutations over 50 cycles of single-cell bottlenecking and thus represents an extreme case of Muller's ratchet (Lai, 2017). Wild-type populations represent day 0 and the beginning of the bottleneck period. To control for media adaptation, we also compared changes to control lines that have been evolved in the same environmental conditions without being subjected to the bottleneck regime.

Methods

Strain and media

The strain used throughout this experiment was *E.coli* strain REL606 containing a pGEM::*mutD5* plasmid. In short, this plasmid contains a mutation in the *dnaQ (mutD)* gene which reduces the ability of its encoded product, DNA polymerase III holoenzyme, to correct DNA replication errors (Degnen & Cox, 1974). The strain is derived from the bottleneck regime aforementioned and provided by Alicia Lai who carried out the bottleneck experiments.

For cells growing in liquid media, Luria-Bertani (LB) media was used. For solid media, cells were grown in LB supplemented with agar added to a concentration of 1.5%w/v. All media was supplemented with antibiotics streptomycin and ampicillin at concentrations *of 100*µg/mL (Peptides International). All chemicals used in the experiments were purchased from Sigma-Aldrich Co. except where otherwise stated.

Bottleneck Relief Regime

The experiments undertaken are a continuation of a MA (bottleneck) experiment carried out by a member of our lab group, Alicia Lai. Under that regime, single colonies of wild-type REL606 + pGEM::*mutD5* were isolated daily on LB agar for 50 cycles, thus forcing populations through severe bottlenecks. In total, 10 lines were forced through bottlenecks while 5 controls lines were passaged by transferring 100 µl of culture onto fresh LB agar for 50 cycles also.

For the bottleneck relief regime, the most severely impaired line at day 50 of the bottleneck regime was used as a starting point (designated BN50). This line has accumulated approximately 3790 mutations with an average overall impact of protein coding mutations calculated at a DBS value of 21.25 (note that > 5 is considered a functionally significant change based on benchmarking work by Wheeler, Barquist, Ashari Ghomi, Kingsley, & Gardner (2015). For controls, we selected one line from the five bottleneck control lines mentioned above as a starting point (designated BNC50). This line accumulated 80 mutations and the average impact of those mutations that encode proteins was measured at a DBS value of 0.098. The control lines served as a media control, to help distinguish changes that arise due to general laboratory adaptation versus those that arise in response to the effect of bottlenecking and subsequently, bottleneck relief. To this end, 10 independent lines derived from BN50 were maintained in large population sizes, by transferring a 20µl suspension of cells to a new source of media, daily, for a total of 50 cycles. In parallel, 10 independent control lines derived from BNC50 were propagated in the same fashion.

The experiments were initiated by scraping 10µl of frozen-down BN50 and BNC50 cultures and inoculating two separate McCartney bottles containing fresh LB supplemented with streptomycin and ampicillin. Cultures were grown to saturation at 37°C in a shaking water bath. 20µl of culture was dispensed into 20 separate wells containing 2mls of LB supplemented with antibiotics. Two cell-culture plates containing the wells were used, with one plate containing the control lines and the other plate containing the bottleneck relief lines. 10 wells were inoculated with cells

derived from BN50 while the other 10 wells were inoculated with cells derived from BNC50. Cells were grown for 24hrs in a shaking incubator at 37°C. Subsequently, 20µl of cells were dispensed into a new set of wells containing 2mls of fresh LB with antibiotics and the experiment was repeated as above for a total of 50 cycles. As such, 10 independent bottleneck relief lines and 10 independent control lines were allowed to evolve for 50 days. Glycerol stocks for each line were prepared on a daily basis and stored in a -80°C freezer to provide a 'fossil' record of the evolving populations.

The bottleneck relief lines shall be designated as BR followed by the associated relief cycle followed by the lineage number. For example, BR50.1 represents lineage 1 from bottleneck relief day 50. The control lines shall be designated as BRC followed by the associated relief cycle followed by the line number. For example, BRC50.1 represents lineage 1 from bottleneck relief day 50.

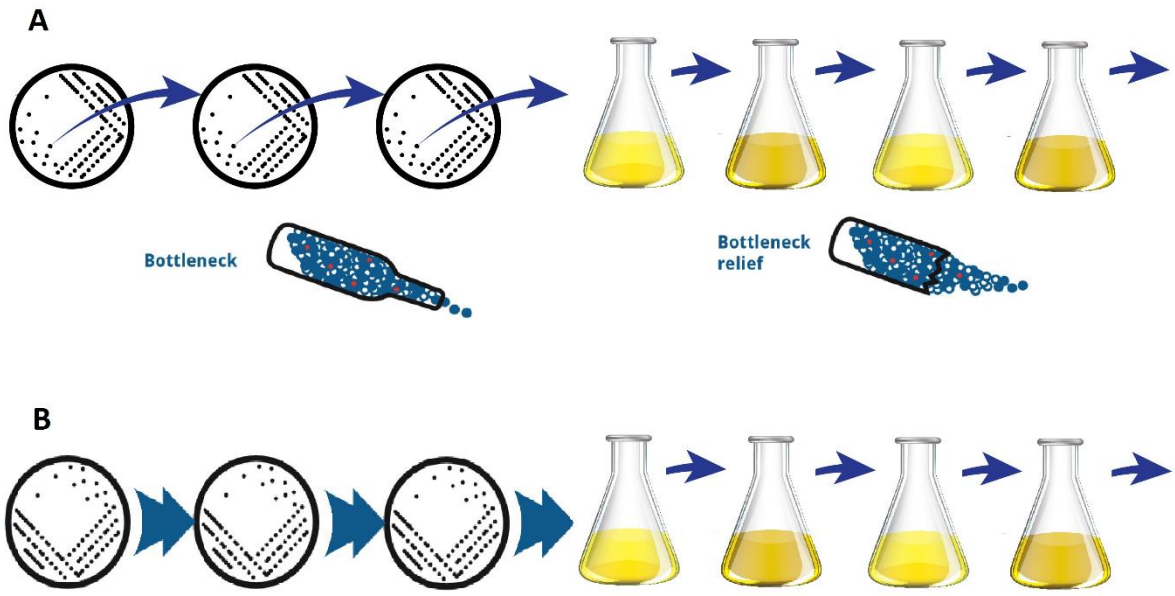

Figure 2.1. Overview of the Experimental Regime. A) REL606 + pGEM*::mutD5* populations were subjected to a bottleneck regime in which a random single-colony was repeatedly picked and streaked onto fresh LB agar for 50 cycles (Lai, 2017). Subsequently, 10 independent lines were then allowed to further evolve under a bottleneck relief regime in shaking, liquid media. **B)** In parallel, control populations were propagated by repeatedly transferring large populations to fresh media. Populations that evolved on solid media represent controls for the bottleneck regime while populations that evolved in liquid media represent controls for the bottleneck relief regime. The coloured circles in the "bottleneck" and "bottleneck relief" bottles may represent different populations that are continually propagated. In the bottleneck regime the blue circles could represent unfit populations that are transferred while remaining populations that are more fit (red and white circles) are left behind. On the other hand, under the bottleneck relief regime, the fitter red and white populations are able to be passaged and are thus expected to outcompete the fitness-impaired (blue) populations over time.

Contamination tests

To check for contamination, independent contamination tests were performed on a regular basis throughout the relief regime, as well as prior to and after extracting DNA for genome sequencing. Cells were readily streaked out on solid LB agar to single colonies for visual examination of potential unwanted contaminants. In addition, cells were readily checked for sensitivity to bacteriophages T4 and T5: Briefly, 15µl of T4 and T5 cultures are dispensed on separate LB agar plates and plates are turned upright to allow liquid to slide down a straight line in the centre of the plate. 1µl of bacterial culture is dispensed to the side of the plates and streaked through the vertical line of the phage. Plates are then incubated at 37°C overnight. Confirmation that cells are *E.coli* is determined by observing no colonies forming beyond the vertical phage line. This protocol was obtained from Richard Lenski's lab group and is available online: myxo.css.msu.edu/ecoli/contam.html. This test does not distinguish between *E.coli* strains. Therefore, to confirm cells are not other strains of *E.coli* commonly found in the laboratory, PCR screens were also performed. In brief, cultures were streaked out to single colonies on LB agar followed by a PCR screening using *trkD* and *rbsD* primers that amplify REL606 strains with a band of approximately 3 kb. Finally, cells were regularly plated for single colonies on TA (tetrazolium and arabinose) agar which distinguishes Ara^- from Ara^+ strains. As REL606 + pGEM::*mutD5* is an Ara^- strain, colonies are expected to be red whereas formation of white colonies could be due to contamination from arabinose-utilizing organisms (Lenski, Rose, Simpson, & Tadler, 1991).

Fitness Experiments

Fitness was assessed by measuring growth rates every 10 days of the relief regime. For controls, growth rates were measured at day 50 only. Briefly, saturated cultures of all 20 lines were dispensed into a 24 well cell culture plate at a 1:100 dilution in 1ml of LB with antibiotics supplemented. The OD595 of each line was measured using a FLUOstar Omega Microplate Reader (BMG Labtech). Runs were carried out at 37°C for 24 hours with shaking. OD595 measurements were calculated every 6 minutes. 2 biological replicates were tested for each line, however, for relief lines measured at day 50, four replicate tests were performed. As day 50 lines underwent genome sequencing, it was important to obtain highly reliable data to ensure genome-fitness comparisons were robust

DNA extractions and Whole Genome Sequencing

All 10 relief lines and 10 control lines from day 50 were streaked out to single colonies on LB agar. A single colony was then used to inoculate liquid LB and cells were grown to saturation. DNA extractions for all 20 lines was carried out using the Wizard Genomic DNA purification kit (Promega) for gram negative bacteria. The procedures for extracting DNA were performed according to the manufactures instructions. Subsequently, isolated DNA was quantified using the Nanodrop 1000 spectrophotometer (ThermoFisher Scientific) and Qubit 2.0 Fluorometer (Thermofisher Scientific). Line BR50.5 and BRC50.2 did not meet the requirements for genome sequencing and due to time constraints, DNA extractions for these lines could not be repeated. As such, DNA from 9 relief lines and 9 control lines in total was sent

to Macrogen for whole-genome sequencing via the Illumina Miseq platform. Raw sequence data was later processed in Geneious version 9.1.7 (Kearse et al., 2012). In brief, The BBDuk plug-in for Geneious (Bushnell 2014) was implemented to filter and trim sequence data. Trimmed reads were then mapped to reference genomes using the Bowtie2 plug-in for Geneious (Langmead & Salzberg, 2012). For the relief lines, reads were mapped to the genome of BN50 while reads for the control lines were mapped to the genome of BRC50. Annotation and SNP calling was performed using Geneious software. For polymorphism detection, the minimum variant frequency was set to 0.75.

Delta-bitscore Analyses

To assess the functional severity of mutations, we employed a newly-described delta-bitscore tool (Wheeler et al., 2016). This tool utilizes Profile hidden Markov models to assess the functional severity of mutations by considering residue conservation and indel rates within a sequence. HMM profile models for gamma-proteobacterial protein sequences were retrieved from the EggNOG database (Huerta-Cepas et al., 2016). Each of our protein sequences were aligned to their respective profile HMM to produce bitscore values, and by subtracting the bitscores of ancestral protein sequences from that of the evolved protein, a measure of divergence between the proteins is produced (Wheeler et al., 2016). In general, a high positive DBS value (>5) is indicative of sequence change that is likely to impair protein function while a high negative DBS value suggests an improvement in protein function. Changes that have a minor impact on function are likely to be scored with a minimal absolute DBS value.

Results

10 initially identical lines of fitness-impaired BN50 were subjected to a bottleneck relief regime consisting of a series of independent passages that involved transferring a suspension of cells to 2ml of fresh LB for 50 cycles (Figure 2.1a). Additionally, 10 initial identical lines of BNC50 were passaged as stated above – this served as a media control (Figure 2.1b). After 50 cycles, DNA was extracted from 9 bottleneck relief and 9 control lines. Whole-genome sequencing was carried out on the Illumina Miseq Platform and reads were assembled using BN50 as a reference genome for the bottleneck relief (BR) lines and BNC50 for the control lines. Raw data statistics can be found in supplementary material.

Fitness increases observed in bottleneck relief lines

Growth rate was measured at 10-day intervals using a plate-reader. For controls, data was obtained from day 50 only. Growth rate was measured as the minimum doubling time over a 30 minute period. From BR day 20 onwards, growth rates were consistently measured as being above that of BN50. However it appears that beyond day 20, growth rates level off (Figure 2.2). A Wilcoxon rank sum test comparing doubling times of lines representing BR day 20 and BR day 50 yielded a *P*-value of 0.150, indicating no significant difference in growth rate between these time points.

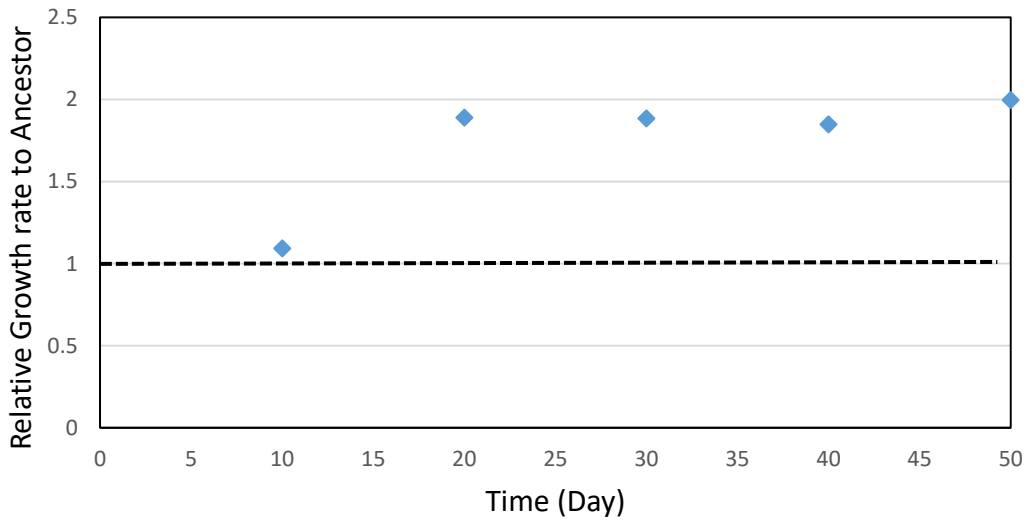

Figure 2.2. Average Increase in growth rate of BR lineages relative to BN50 is observed from day 20 onwards. BR lines (light blue diamonds) show an increase in growth rate compared to BN50 (dashed line) at day 20, 30, 40 and 50 of the bottleneck relief regime. Values above 1 represent an increase in relative growth rate and values below 1 represent a decrease in relative growth rate. Each point represents the average of the 10 lines.

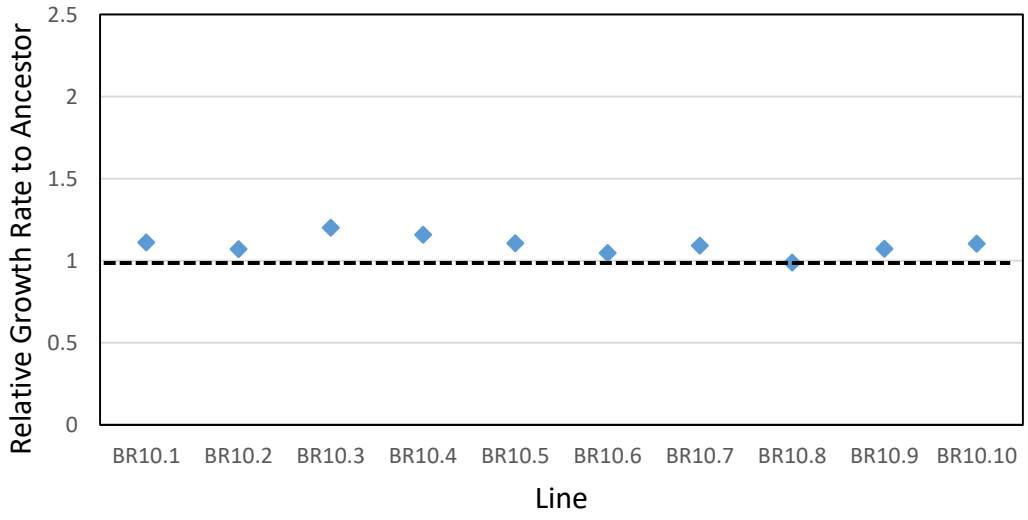

Figure 2.3. No major increase in growth rate observed following 10 days of bottleneck relief. BR lineages at day 10 (light blue diamonds) do not appear to deviate significantly from BN50 (dashed line) although BR10.3 and BR10.4 show a slight increase in growth rate. Values above 1 represent an increase in relative growth rate and values below 1 represent a decrease in relative growth rate. Each point represents the average of two replicates.

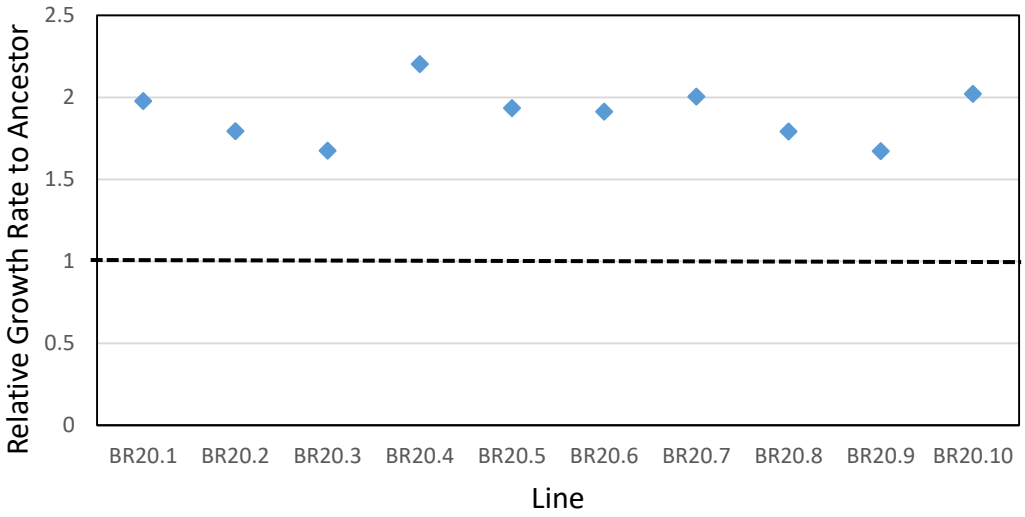

Figure 2.4. Increase in growth rate observed following 20 days of bottleneck relief. All BR lineages at day 20 (light blue diamonds) have increased in growth rate compared to BN50 (dashed line) with BR20.4 showing the greatest increase. Values above 1 represent an increase in relative growth rate and values below 1 represent a decrease in relative growth rate. Each point represents the average of two replicates.

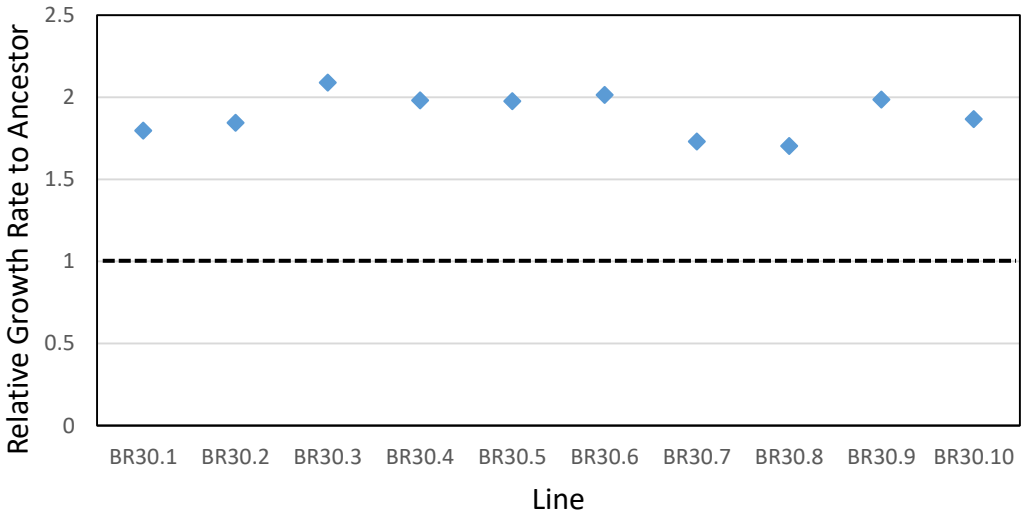

Figure 2.5. Increase in growth rate observed following 30 days of bottleneck relief. All BR lineages at day 30 (light blue diamonds) have increased in growth rate compared to BN50 (dashed line) with BR30.3 showing the greatest increase. Values above 1 represent an increase in relative growth rate and values below 1 represent a decrease in relative growth rate. Each point represents the average of two replicates.

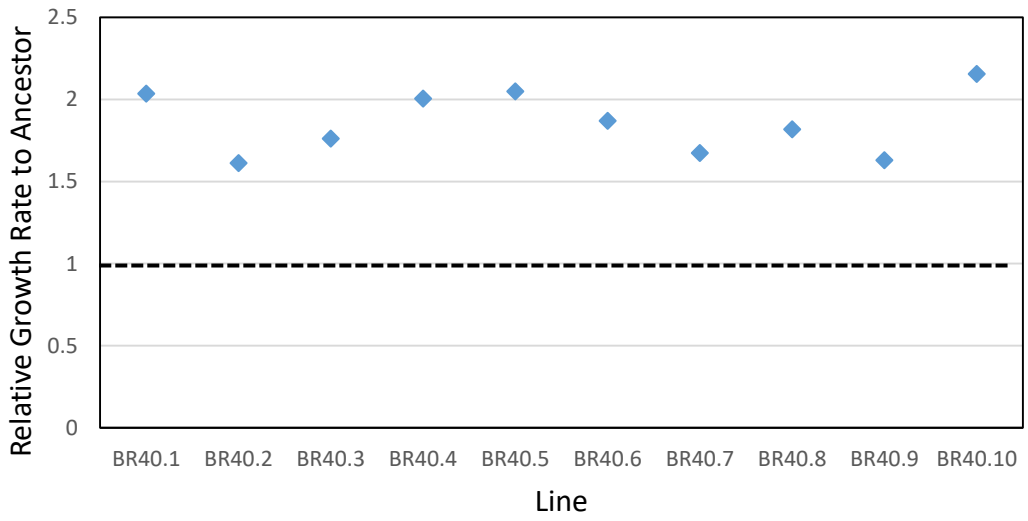

Figure 2. 6. Increase in growth rate observed following 40 days of bottleneck relief. All BR lineages at day 40 (light blue diamonds) have increased in growth rate compared to BN50 (dashed line) with BR40.10 showing the greatest increase. Values above 1 represent an increase in relative growth rate and values below 1 represent a decrease in relative growth rate. Each point represents the average of two replicates.

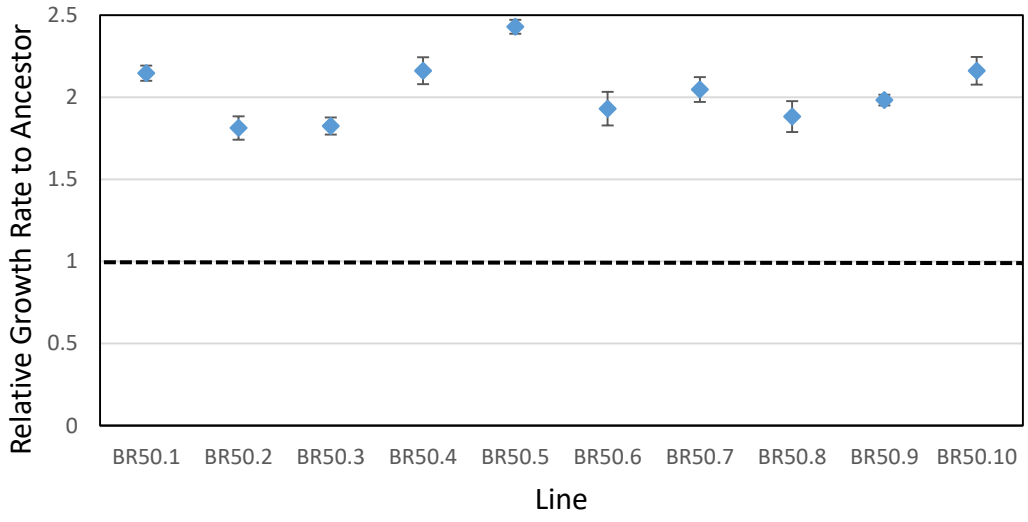

Figure 2.7. Increase in growth rate observed following 50 days of bottleneck relief. All BR lineages at day 50 (light blue diamonds) have increased in growth rate compared to BN50 (dashed line) with BR50.5 showing the greatest increase. Values above 1 represent an increase in relative growth rate and values below 1 represent a decrease in relative growth rate. Each point represents the average of four replicates ($\bar{x} \pm SE$).

BR lines show lower growth rates than wild-type and control populations

To assess whether the relief lines recaptured wild-type fitness (or captured control fitness), growth rates at BR day 50 were compared to wild-type and to control growth rates measured at day 50. All BR lineages show lower relative growth rates compared to both wild-type (Figure 2.9) and controls (Figure 2.8). To show significance, a Wilcoxon rank sum test was performed by comparing growth rates of BR day 50 lines and control lines. We found a statistically significant difference between each group (*P*-value = 0.000977).

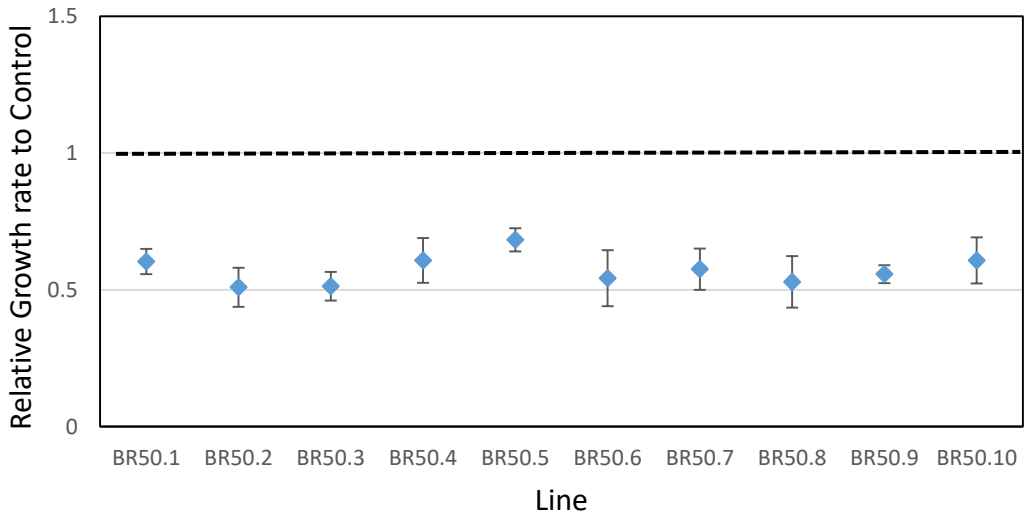

Figure 2.8. BR lineages at day 50 show lower growth rates compared to the average BR control growth rate. BR growth rates are depicted as light blue diamonds referenced against the average BR control growth rate (dashed line). Values above 1 represent an increase in relative growth rate and values below 1 represent a decrease in relative growth rate. Each point represents the average of four replicates ($\bar{x} \pm SE$).

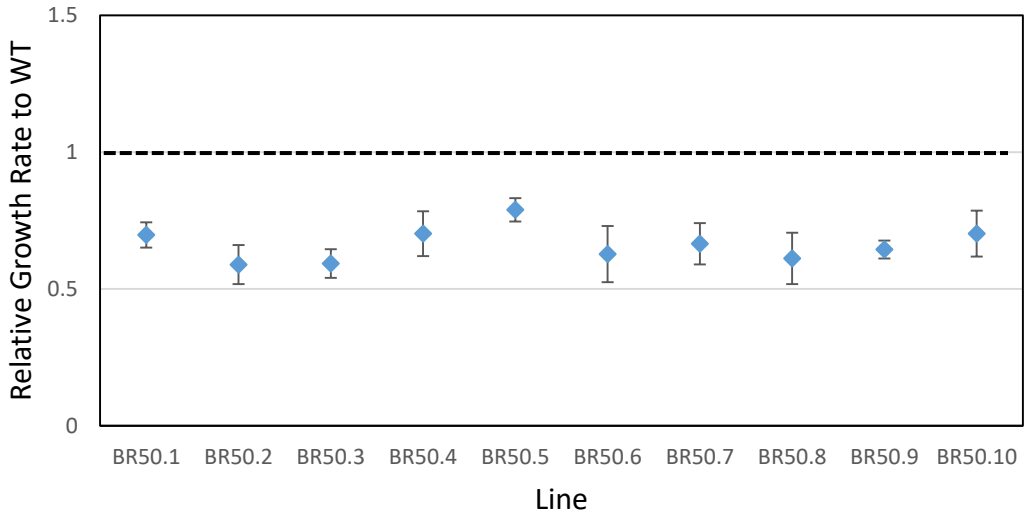

Figure 2.9. BR lineages at day 50 show lower growth rates compared to WT. BR growth rates are depicted as light blue diamonds referenced against the average WT growth rate (dashed line). Values above 1 represent an increase in relative growth rate and values below 1 represent a decrease in relative growth rate. Each point represents the average of four replicates ($\bar{x}$ ± SE).

Fitness of Control lines remain similar to ancestral and Wild-type Levels

To assess fitness changes that might be attributable to adaptation to media, growth rates of BR control lines at day 50 were compared to the average ancestral (bottleneck control) growth rate (Figure 2.10), and to wild-type (Figure 2.11). No major differences in fitness were observed, however, growth rates are marginally above wild-type levels and slightly below ancestral levels.

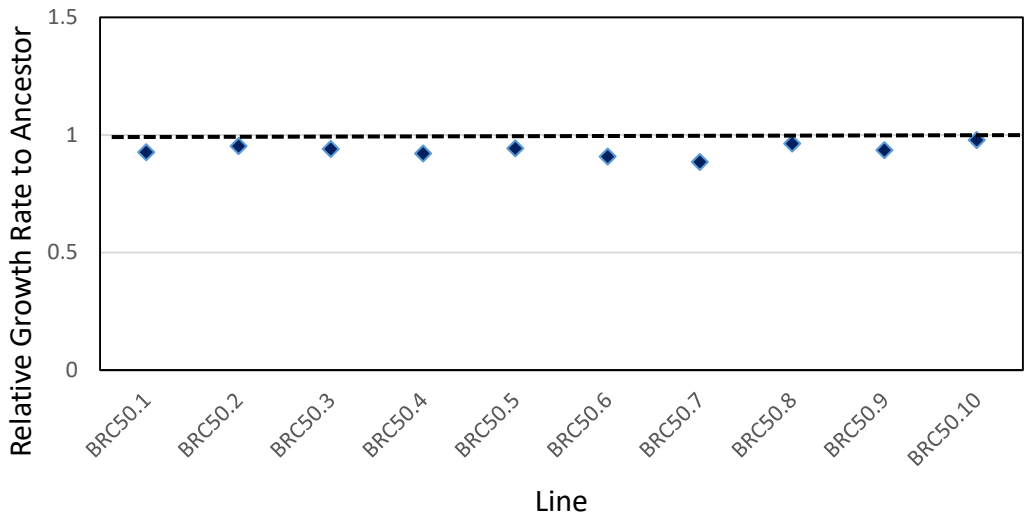

Figure 2.10. BR control lineages at day 50 show similar growth rates compared to BNC50. Control growth rates are depicted as dark blue diamonds referenced against the average ancestral (BNC50) growth rate (dashed line). Values above 1 represent an increase in relative growth rate and values below 1 represent a decrease in relative growth rate. Each point represents the average of two replicates.

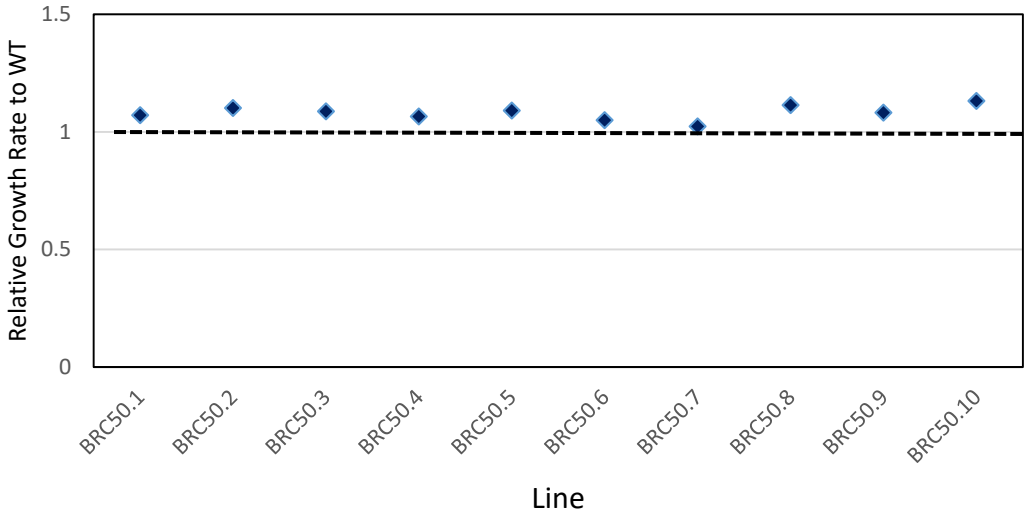

Figure 2.11. BR control lineages at day 50 show similar growth rates compared to WT. Control growth rates are depicted as dark blue diamonds referenced against the average WT growth rate (dashed line). Values above 1 represent an increase in relative growth rate and values below 1 represent a decrease in relative growth rate. Each point represents the average of two replicates.

Whole-Genome Sequencing reveals an accumulation of Mutations following 50 cycles of bottleneck relief

Whole-genome sequencing was carried out on the Illumina Miseq Platform and reads were assembled using the genome sequence of BN50 as a reference for the BR lines and the genome of BNC50 as a reference for the control lines. SNP calling and analyses were carried out in Geneious version 9.1.7 (Kearse et al., 2012). The relief lines showed higher mutation rates than controls ($P < 0.05$, Wilcoxon rank sum), and a greater number of mutations accumulated over fewer generations (Table 2.1). For the BR lines, BR50.6 showed the highest mutation rate while BR50.4 has the lowest mutation rate. For the control lines, BRC50.1 has the highest mutation rate while BRC50.10 has the lowest mutation rate. All the BR lines have a lower mutation rate than BN50 (1.11×10^{-6}). However, all control lines have a higher mutation rate compared to BNC50 (7.02×10^{-9}).

Table 2.1. General overview of mutational changes observed in the day 50 relief and control genomes

Lineage	Number of Generations	Number of Substitutions	Number of Insertions	Number of Deletions	Total Number of Mutations	Mutation Rate
BR50.1	1518	556	39	26	621	8.83×10^{-8}
BR50.2	1266	448	21	25	494	8.42×10^{-8}
BR50.3	1288	568	42	34	644	1.08×10^{-7}
BR50.4	1498	492	29	15	536	7.72×10^{-8}
BR50.6	1320	587	36	43	666	1.09×10^{-7}
BR50.7	1426	565	42	1	608	9.68×10^{-8}
BR50.8	1298	423	23	22	468	7.78×10^{-8}
BR50.9	1408	507	23	34	564	8.64×10^{-8}
BR50.10	1499	499	27	27	553	7.96×10^{-8}
BRC50.1	2350	272	5	4	281	2.58×10^{-8}
BRC50.3	2377	214	3	8	225	2.04×10^{-8}
BRC50.4	2331	238	8	9	255	2.36×10^{-8}
BRC50.5	2394	232	8	8	248	2.24×10^{-8}
BRC50.6	2304	207	3	6	216	2.02×10^{-8}
BRC50.7	2245	242	9	4	255	2.45×10^{-8}
BRC50.8	2445	241	3	5	249	2.20×10^{-8}
BRC50.9	2366	219	8	5	232	2.12×10^{-8}
BRC50.10	2483	218	4	5	227	1.97×10^{-8}

SNP calling is based on mutational changes relative to ancestral genomes (BN50 for BR50.1-BR50.10 and BNC50 for BRC50.1-BRC50.10). The number of generations calculated is based on doubling time calculated every 24 hours for the experimental regime. The total number of mutations is calculated by diving the number of mutations by the number of generations and number of nucleotides in the genome of *E.coli* REL606.

DBS Analysis reveals mutations in relief lines diverge from Ancestral Sequence Constraints

Mutations that emerged under the relief regime were analysed using a newly-described delta-bitscore metric that assesses the functional-severity of mutations based on protein sequence conservation (Wheeler et al., 2016).

We found that BR lines accumulated mutations with typically high associated positive DBS values while relatively few mutations were scored as having negative DBS values (Figure 2.12). As the DBS method is based on sequence conservation, these results suggest that protein sequences are diverging from sequences favoured in the evolutionary history of those proteins, and that overall protein function is not improving relative to BN50 (see discussion for why this observation is superficial). Moreover, the average DBS of all the BR lines examined increased relative to the mean DBS of BN50, and this correlates with the number of SNPs emerging throughout the experimental regime (Figure 2.13). In contrast, the control lines appear to have accumulated substantially fewer deleterious mutations (Figure 2.12) and have a much lower mean DBS (Figure 2.13).

Mapping BR DBS values to their corresponding COG category shows functionally significant DBS scores commonly found in sequences associated with energy production, amino acid transport/metabolism , carbohydrate transport/metabolism and in sequences that have unknown functions (Figure 2.12). For control populations, functionally significant DBS values mostly belong to sequences associated with

unknown function, signal transduction and cell wall/membrane processes (Figure 2.12).

For the relief lineages, the most extreme DBS values fall under COG categories associated with unknown function, amino acid transport/metabolism, energy production and cell well/membrane biogenesis. The lowest negatively scored DBS values are associated with carbohydrate transport/metabolism and cell wall/membrane biogenesis (Figure 2.12). High positive DBS values are in many cases a result of insertion or deletions causing Frame Shifts. The highest DBS values (1890.5 and 1616.2) are associated with a hypothetical protein and bifunctional protein PutA, respectively, and are due to substitution mutations causing truncations (Table 2.2). The truncation mutation identified in the gene *putA* was found to occur in all nine sequenced BR lines (Table 2.2).

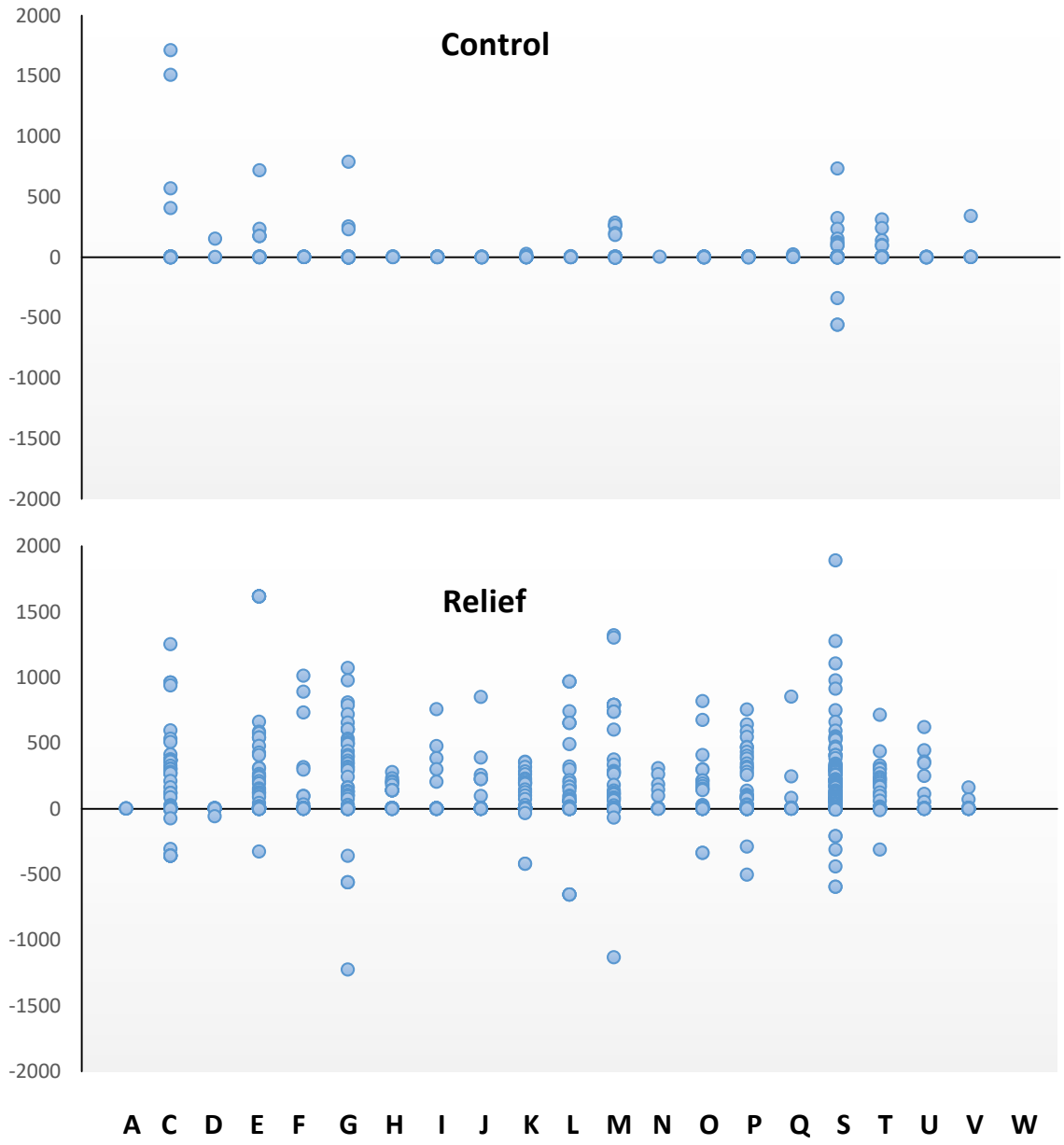

Figure 2.12. Scatterplot Depicting DBS values for BR and control lineages. Each point represents a DBS value for a particular protein sequence. DBS values in this depiction are relative to DBS values calculated for mutations in ancestral sequences which have been assigned here to 0. For functional categorization, DBS values are mapped to the COG category that its corresponding protein sequence belongs to. A = RNA processing/modification, C = Energy production, D = Cell cycle control , E = Amino acid transport/metabolism, F = Nucleotide transport/metabolism, G = carbohydrate transport/metabolism, H = Coenzyme transport/metabolism, I = Lipid transport/metabolism, J = Translation, ribosome structure, K = Transcription, L = Replication, recombination, M = Cell wall/membrane, N = Cell motility, O = Posttranslational modification, P = Inorganic ion transport/metabolism, Q = secondary metabolites, S = Function unknown, T = Signal transduction, U = intracellular trafficking, V = Defence mechanisms, W = Extracellular structures.

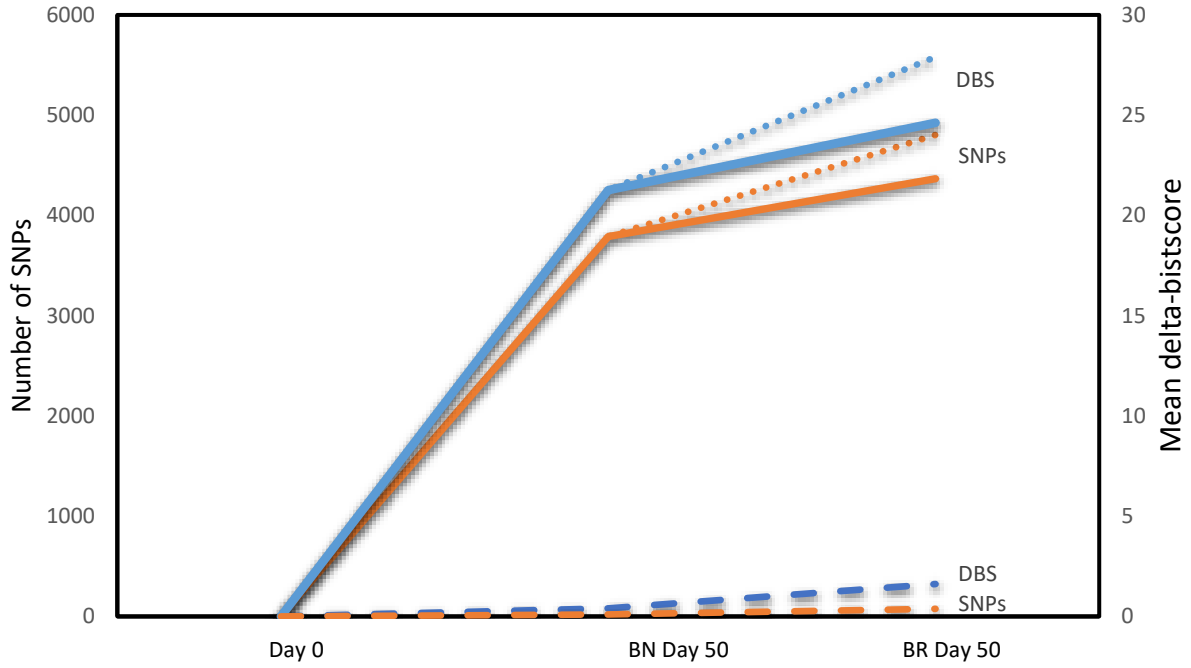

Figure 2.13. Relationship between mean delta-bitscore (blue lines) and the average number of SNPs (red lines) for WT (Day 0), bottleneck day 50 (BN Day 50) and bottleneck relief day 50 (BR Day 50). Thick lines represent WT, bottleneck day 50 and Bottleneck relief day 50. Dotted lines represent data from our lab group (Lai, 2017) if BN50 was bottlenecked further for 50 cycles as opposed to undergoing bottleneck relief. Dashed lines (bottom of figure) depict the average number of SNPs and mean DBS for BNC50 (bottleneck control) and the BR control lines that evolved in parallel to the bottleneck and Bottleneck relief regime.

Table 2.2. Summary of the highest DBS Values (>1000) for the relief lines

CDS	COG category	Change	Protein Effect	DBS	Line(s)
Hypothetical Protein	Function Unknown	G -> A Substitution	Truncation	1890.5	BR50.8
PutA	Amino acid transport/metabolism	C -> T Substitution	Truncation	1616.2	All
RHS element protein	Cell Wall/Membrane	(C)5 -> (C)4 Deletion (Tandem Repeat)	Frame Shift	1321	BR50.6
RHS element protein	Cell Wall/Membrane	(C)4 -> (C)3 Deletion (tandem repeat)	Frame Shift	1302.9	BR50.10
inverse autotransporter adhesin-like protein YeeJ	Function Unknown	(A)8 -> (A)9 Insertion (tandem repeat)	Frame Shift	1276.3	BR50.10
trimethylamine N-oxide reductase I catalytic subunit	Energy Production	(G)6 -> (G)5 Deletion (tandem repeat)	Frame Shift	1252.7	BR50.4
membrane protein	Function Unknown	(G)3 -> (G)2 Deletion (tandem repeat)	Frame Shift	1106.2	BR50.9
lacZ	Carbohydrate Transport Metabolism	C -> T Substitution	Truncation	1072.1	BR50.7
ribonucleotide-diphosphate reductase subunit alpha	Nucleotide transport/Metabolism	(T)6 -> (T)7 Insertion (tandem repeat)	Frame Shift	1013.1	BR50.8

Above is an outline of the highest DBS values (calculated to be > 1000) in all the BR genomes analysed. It shows the coding sequence associated with these values and the mutational basis that are the cause for such changes, as well as the BR lines in which these mutations occurred.

Sum of absolute delta-bitscore does not correlate with fitness of relief lineages

To assess the relationship between DBS and fitness (measured by doubling time), a Pearson's correlation test was performed on BR and control lineages based on the Σ|DBS| calculated for each line and the corresponding doubling time (Table 2.3). A significant positive relationship was observed ($P < 0.05$, $R^2 = 0.9387$) (Figure 2.14). In other words, populations calculated to have higher absolute DBS values typically also

had higher doubling times. However, when the Σ|DBS| and doubling times for the control lines were excluded from the Pearson's test, and only the values for relief lines were included, a non-significant relationship was calculated ($P > 0.05$, R^2=0.034907) (Figure 2.15).

Table 2.3. Sum of Absolute DBS and Doubling Time calculated for BR lines and Control lines

Lineage	Σ|DBS|	Doubling Time (minutes)
BR50.1	98776	47.2 ± 2.10
BR50.2	97859	56.88 ± 4.18
BR50.3	97859	55.91 ± 2.82
BR50.4	100490	48.06 ± 4.13
BR50.6	106955	54.56 ± 5.62
BR50.7	108146	50.48 ± 3.92
BR50.8	96489	55.47 ± 4.95
BR50.9	101258	51.13 ± 1.67
BR50.10	99992	48.03 ± 3.98
BRC50.1	2614	30.64 ± 0.51
BRC50.3	2840	30.29 ± 1.37
BRC50.4	1245	30.88 ± 1.19
BRC50.5	1130	30.08 ± 0.10
BRC50.6	2231	31.25 ± 0.28
BRC50.7	2076	32.08 ± 0.55
BRC50.8	2038	29.45 ± 0.24
BRC50.9	1199	30.43 ± 1.25
BRC50.10	821	28.99 ± 0.14

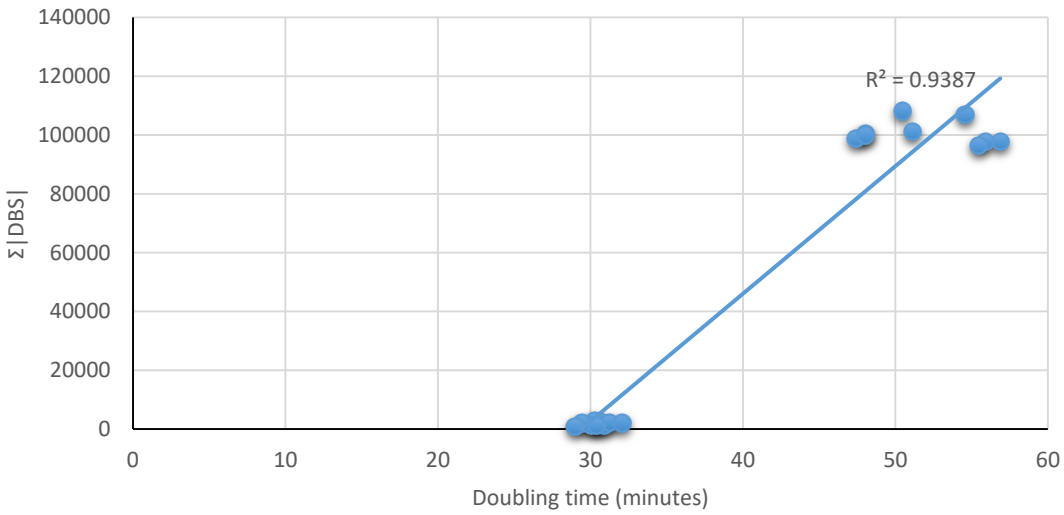

Figure 2.14. Relationship between Sum of absolute DBS (y-axis) and Doubling time (x-axis). A significant correlation was identified ($P < 0.05$, $R^2 = 0.9387$). Σ|DBS| and doubling times for all BR and control populations are included in calculation.

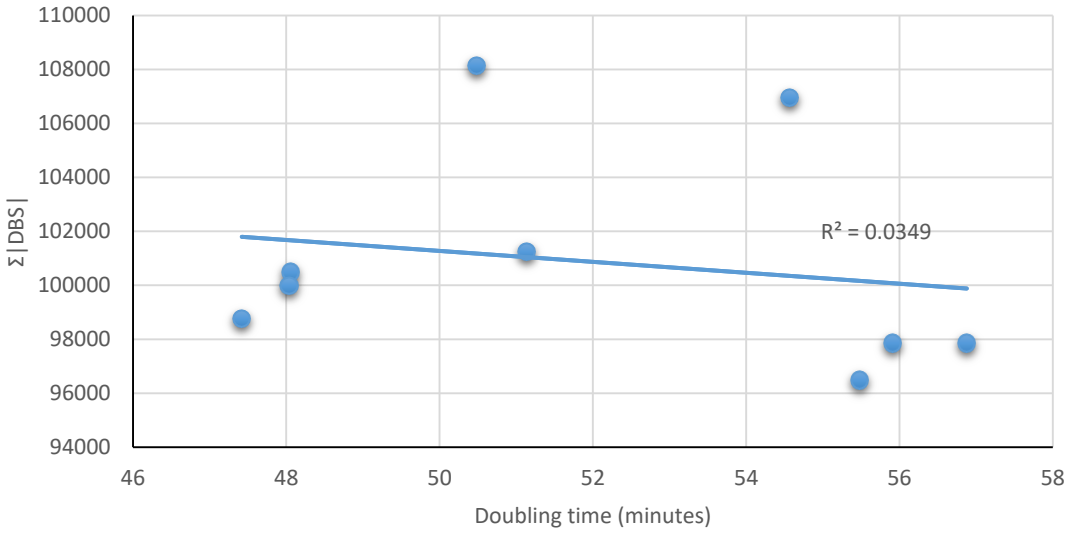

Figure 2.15. Relationship between Sum of absolute DBS (y-axis) and Doubling time (x-axis). A non-significant correlation was identified ($P > 0.05$, $R^2 = 0.034907$). Σ|DBS| and doubling times for all BR lines are considered while values for control lines are excluded from calculation.

To assess whether DBS values that are outliers (such as those in table 2.2) might be contributing to fitness differences between the relief lines, two scatterplots depicting DBS values greater than |500| were aligned to a graph depicting doubling time (Figure 2.16). DBS values > 500 and < -500 were used because this is the range in which the fewest DBS scores fall into. Visual inspection reveals no clear relationship (Figure 2.16). For example, BR50.8 which has a high doubling time and the highest DBS calculated (hypothetical protein, DBS = 1890.5, table 2.2), also has the second most significantly improved protein function predicted (cellulose synthase catalytic subunit, DBS = -1131.1).

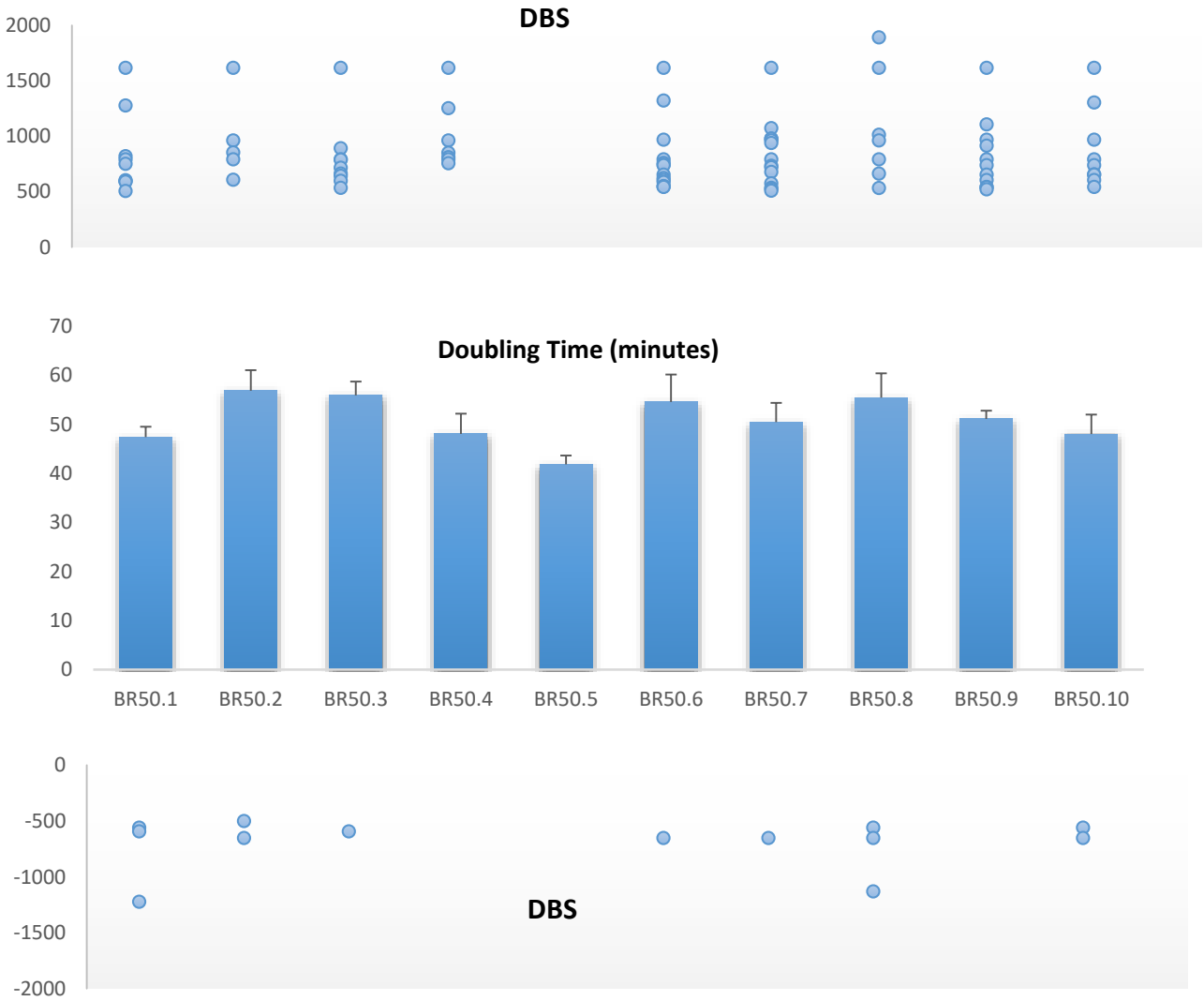

Figure 2.16. Comparison of doubling time and extreme DBS values calculated for the relief lines. Blue points represent DBS values greater than |500|. The top scatterplot represents positive DBS values while the bottom scatterplot depicts negative DBS values. Doubling time (middle) is the mean doubling time calculated for that lineage. Standard error is included also.

The occurrence of Parallel mutations in some cases appear deleterious

We next investigated how reversion and parallel mutations could be impacting fitness. In total we identified 881 reversion mutations throughout all BR lines. For example, we identified 57 SNPs in BN50 that reverted in at least one relief line while only 8 SNPs present in BN50 reverted in all 9 relief lines (Figure 2.17). An overview is provided in figure 2.17 and some examples are provided in table 2.4.

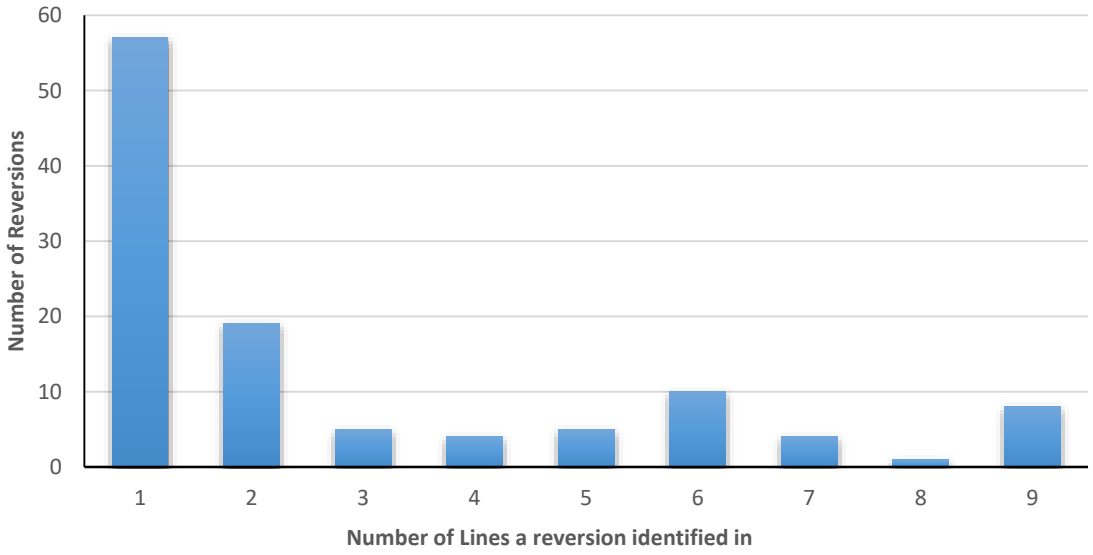

Figure 2.17. Number of cases in which a SNP that has occurred in BN50 has reverted to a wild-type sequence composition, and how many lineages that reversion was identified in.

In addition to parallel reversions being identified, we also identified mutations that were absent in BN50 but present in all nine relief lineages. Some of these had a functionally-significant DBS value (>5). For example, in gene *putA*, a C to T transition SNP causing a truncation is found in all 9 BR lines (Figure 2.18). The DBS score for this sequence is 1616.2. Likewise, all lines possess an aldehyde dehydrogenase gene containing a G to A transition SNP that is also predicted to code for a truncated protein

(Figure 2.19). The DBS score for this mutation is 368.7. Finally, a frame shift in a gene of unknown function caused by a T insertion was found in all lines (Figure 2.20). The DBS value for this mutation is 790. These results are surprising in that some of the most predicted functionally severe mutations are present throughout multiple relief lines.

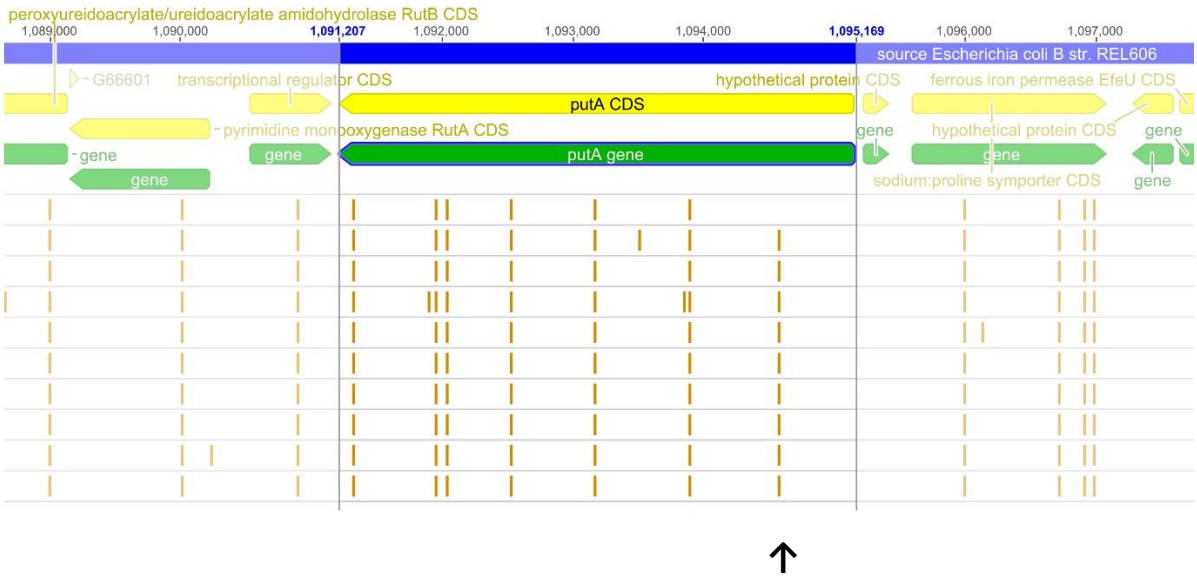

Figure 2.18. Depiction of SNPs in the *putA* gene within the genomes of the BR lines. Shown here is the *putA* gene (green bar), CDS (yellow bar) and surrounding sequences. In blue is the WT REL606 genome that reads were mapped to. Orange dashes represent SNPs and each white horizontal segment represents a BR line. The SNPs shown by the black arrow are responsible for premature stop codons which have resulted in a truncated protein for each of the nine BR lines sequenced. In the top white horizontal segment there is no SNP – this segment represents the genome of BN50 for which this mutation is absent.

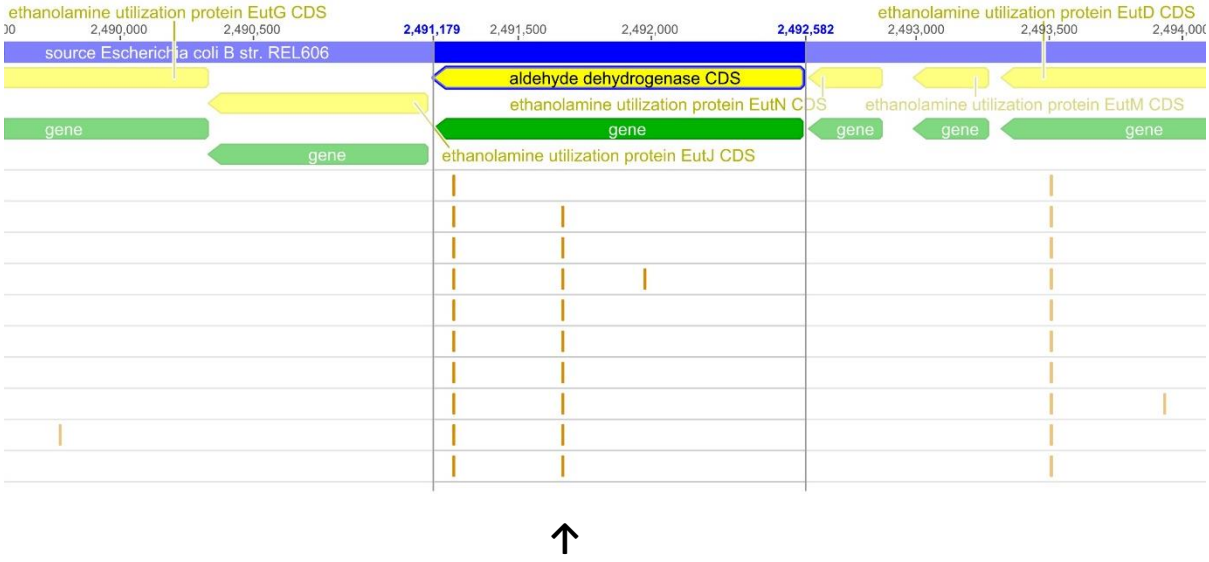

Figure 2.19. Depiction of SNPs in an aldehyde dehydrogenase gene within the genomes of the BR lines. Shown here is an aldehyde dehydrogenase gene (green bar), CDS (yellow bar) and surrounding sequences. In blue is the WT REL606 genome that reads were mapped to. Orange dashes represent SNPs and each white horizontal segment represents a BR line. The SNPs shown by the black arrow are responsible for premature stop codons which have resulted in a truncated protein for each of the nine BR lines sequenced. In the top white horizontal segment there is no SNP – this segment represents the genome of BN50 for which this mutation is absent.

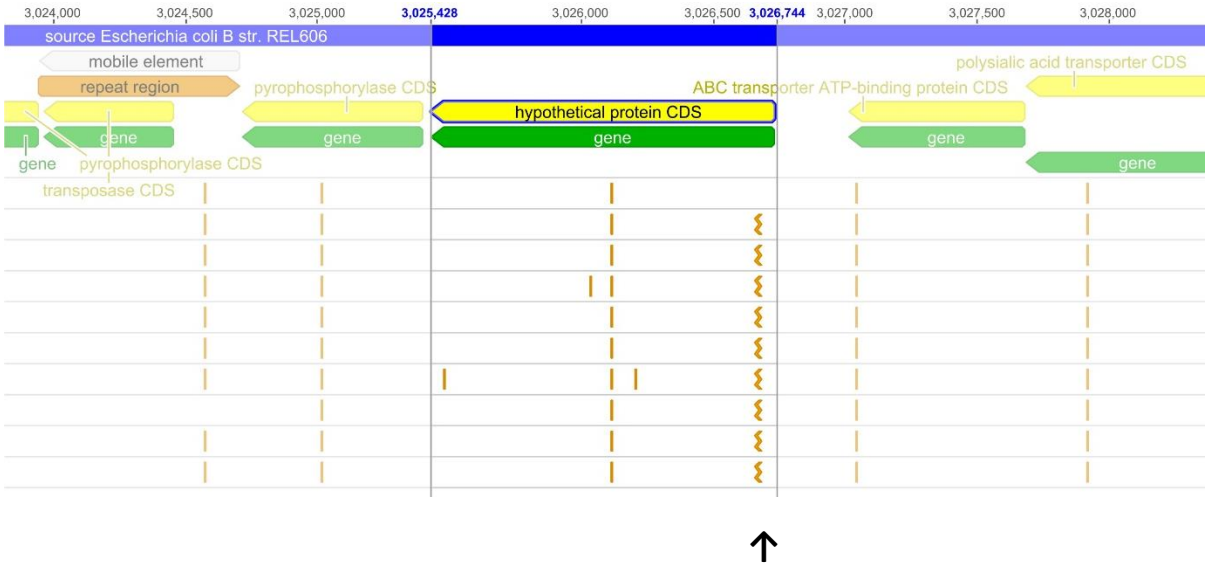

Figure 2.20. Depiction of SNPs in a hypothetical protein-encoding gene within the genomes of the BR lines. Shown here is a hypothetical protein-encoding gene (green bar), CDS (yellow bar) and surrounding sequences. In blue is the WT REL606 genome that reads were mapped to. Orange dashes represent SNPs and each white horizontal segment represents a BR line. The SNPs shown by the black

arrow are responsible for premature stop codons which have resulted in frame shifts for each of the nine BR lines sequenced. In the top white horizontal segment there is no SNP – this segment represents the genome of BN50 for which this mutation is absent.

Table 2.4. Examples of parallel reversions of mutations that occurred in BN50

CDS	COG Category	Mutation in BN50	Lines showing Reversion
phage tail protein	Function Unkown	T -> C Substitution	All
Zn-dependent Hydrolase	Amino acid transport/metabolism	G -> A Substitution	All
NADPH-dependent oxidoreductase	Energy Production	A -> G Substitution	All
protein AegA	Function Unkown	G -> A Substitution	All
transposase	Replication, Recombination	T -> C Substitution	BR50.1, BR50.3, BR50.4, BR50.7, BR50.8, BR50.9,
polymerase		(A) Insertion	BR50.2, BR50.4, BR50.5, BR50.7, BR50.8, BR50.9,
transferase	Function Unkown	C -> T Substitution	BR50.2, BR50.4, BR50.5, BR50.7, BR50.8, BR50.9,
dTDP-4-dehydrorhamnose 3,5-epimerase	Cell wall/membrane	A -> G Substitution	BR50.2, BR50.4, BR50.5, BR50.7, BR50.8, BR50.9,
glucose-1-phosphate thymidylyltransferase	Cell wall/membrane	T -> C Substitution	BR50.2, BR50.4, BR50.5, BR50.7, BR50.8, BR50.9,
dTDP-glucose 4,6-dehydratase	Cell wall/membrane	G -> A Substitution	BR50.2, BR50.4, BR50.5, BR50.7, BR50.8, BR50.9,
wcaM	Cell wall/membrane	C -> A Substitution	BR50.2, BR50.4, BR50.5, BR50.7, BR50.8, BR50.9,
colanic acid biosynthesis pyruvyl transferase	Cell wall/membrane	G -> A Substitution	BR50.2, BR50.4, BR50.5, BR50.7, BR50.8, BR50.9,
transposase	Replication, Recombination	C Insertion	BR50.2, BR50.6, BR50.7, BR50.8, BR50.10
transposase	Replication, Recombination	A -> C Substitution	BR50.1, BR50.4, BR50.7, BR50.8, BR50.10

Discussion

The aim here was to assess the mutational basis that might allow populations subjected to Muller's ratchet to escape from a trajectory towards mutational meltdown. While an abundance of studies report that compensatory and reversion mutations are important, few studies have assessed how mutations that accumulate under an escape regime impact protein function. Through delta-bitscore analyses, our lab group has previously shown that protein coding sequences accumulate functionally-severe mutations in populations subjected to Muller's ratchet (Lai, 2017). We predicted then that halting the ratchet might be facilitated by mutations that improve protein function, and that the functional-severity of mutations that accumulate under an escape regime will be minimal. To address these issues, 10 initially identical populations of *E.coli* close to extinction as a result of multiple population bottlenecks were subjected to a bottleneck relief regime. We performed fitness assays, sequenced genomes and examined the functional impact of mutations using the DBS method.

We observed improvements in overall fitness in all 10 bottleneck relief lines which echoes previous studies where bottlenecked populations have been further evolved under larger population sizes (e.g. Bull et al., 2003; Burch & Chao, 1999; Clarke et al., 1993). We found that fitness increase is most rapid between days 10 – 20 of the bottleneck relief regime, and that beyond day 20 fitness levels off (Figure 2.2). However, at day 50, average growth rate was calculated to be above that of day 40 (Figure 2.2) suggesting further propagation of large population sizes might increase

fitness in these lines even more. This observation of rapid fitness increase is also reported in other studies (Burch & Chao, 1999; Estes & Lynch, 2003; Whitlock & Otto, 1999), however, these studies also report that on average populations completely or nearly recapture wild-type fitness which was not the case in our study (Figure 2.9). We also found that although on average lineages increase in fitness at some point between days 10 – 20, individual differences between in fitness between lines was observed throughout the regime, including at day 10. For example, at day 10, lineage BR10.8 was calculated to have a doubling time of 102 minutes while BR10.3 was calculated to have a doubling time of 84 minutes. As such, BR10.3 has become fitter compared to its bottlenecked ancestor (BN50) which has a doubling time of 100 minutes. On the other hand, BR10.8 shows no increase in fitness relative to BN50 (Figure 2.3). Likewise, at day 50, the highest calculated doubling time is 56 minutes observed for BR50.2 while the lowest doubling time was observed for BR50.5 which is 41 minutes (figure 2.7). In addition, there is no obvious parallel pattern of fitness increase between lines over time, and in some cases fitness in a particular line decreased between two time points. For example, BR40.3 shows a lower growth rate relative to BN50 compared to BR30.3 - the same line tested 10 days earlier in the bottleneck relief regime (Figure 2.5, 2.6). Such stochasticity could be attributable to the continual accumulation of deleterious mutations in the relief lines, or could be an artefact resulting from background noise occurring during growth rate trials - more fitness assays are required to determine this. Overall, the rapid average improvement in fitness, and the observed

individual differences between lines, is consistent with other studies (Bull et al., 2003; Estes & Lynch, 2003).

To account for adaptation to the laboratory environment, control lines were also propagated similarly to the relief lines, the difference being the ancestral background from which the two sets of lineages are derived from. As the bottleneck regime was performed on solid LB agar, it was important to establish whether adaptation to a liquid, shaking environment that relief lineages were evolved under, might explain some fitness observations. The overall average growth rate of the BR control lines was calculated to be slightly less than their ancestral equivalent (BNC50) (Figure 2.10), and slightly greater than wild-type (Figure 2.11). For example the average calculated doubling time for the BR controls at day 50 was calculated to be 30.38 minutes. In contrast, the average doubling time for BNC50 is 28.37 minutes while wild-type populations have an average doubling time of 32.8 minutes. This negligible decrease in fitness of the control lines suggests fitness restoration in the BR lines is not driven mainly by general laboratory adaptation, and that reversion and compensatory mutations could be influencing fitness recovery (Estes & Lynch, 2003).

We found a statistically significant difference in mutation rate of the BR lines compared to the control lines (*P*-value < 0.05, Wilcoxon rank sum), with BR lines showing a higher average mutation rate of 8.97×10^{-8} compared to an average of 2.22×10^{-8} for the controls (Table 2.1). In addition, we found the BR lines to have a lower average mutation rate compared to the ancestral (BN50) rate while the control lines

showed an increase in mutation rate relative to their ancestor (BNC50). This increase in mutation rate for the controls is surprising, however, it could reflect the minor decrease in fitness observed between the controls and BNC50. The lowered mutation rates observed in the relief lines reflects both the efficiency of selection that is expected to increase under the relief regime, and the relaxed genetic load that is predicted to occur as species adapt to new conditions (Kimura, 1967.,Taddei et al., 1997).

Although the average mutation rates have decreased in the BR lines, the average rate is still above that of wild-type *E.coli* (10^{-10} per nucleotide per generation) (Foster, Lee, Popodi, Townes, & Tang, 2015). This is not surprising, however, as all genomes including controls were found to carry the *mutD5* mutator allele that was introduced into the wild-type genome at the very beginning of the experiment - including in bottleneck and control lines. Moreover, mutations were identified in DNA mismatch repair genes in the genome of BN50, many of which did not appear to revert in any of the BR lines. For example, in the *mutS* gene, which performs the mismatch recognition step during the DNA repair process (Hsieh, 2001), a nonsynonymous mutation with an associated DBS score of 3.9 was found in the genome of BN50 and all BR lines. Pinpointing the cause of the observed decline in mutation rate observed in the relief lines relative is not straightforward. For instance we found parallel mutations in all BR lines in repair genes *mutY* and *mutD5* however only *mutD5* was identified as being important in terms of functional change (DBS = -0.4). Overall, the mutations in *mutY* and *mutD5* were predicted to have no effect on protein function.

To assess the overall impact of all mutations on protein function, a delta-bitscore analysis of protein-coding sequences was undertaken in all 18 sequenced genomes. We predicted that as relief populations become fitter, protein function would generally improve relative to BN50 which accumulated numerous functionally severe mutations throughout the bottleneck regime. In other words - that fitness recovery would correlate with improved protein function. Surprisingly, we found that overall protein function does not appear to improve in the relief lines, and that functionally-severe mutations continue to accumulate (Figure 2.12). Initially, this seemed somewhat as a paradox – how could protein sequences continue to accumulate functionally-severe mutations as lineages become fitter? - However, with further investigation into the literature these seemingly unusual observations became more transparent. For instance, the high number of positive DBS scores observed in the relief lines (Figure 2.12) is congruent with previous work that shows reversion mutations are rare when populations are able to recover from the deleterious effects of population bottlenecks (Haigh, 1978; Pfaffelhuber et al., 2012; Poon & Chao, 2005). If reversion mutations were commonly occurring under this experimental regime then we might expect to see more negative DBS values for the protein sequences, however, this is not the case (Figure 2.12). As such, we suspect that fitness recovery is occurring primarily through compensatory mutations. Some of these compensatory mutations could have fitness costs in a wild-type background, and some might be masking the deleterious effects of mutations that emerged in the bottleneck regime. This, in turn, might explain the apparent lack of protein function improvement observed, despite

overall increases in fitness (Poon & Chao, 2005; Szamecz et al., 2014). Moreover, Fisher's geometric model of adaptation predicts that the number of compensatory mutations increases with increasing distance from fitness optimum (Fisher, 1930). As relief populations were initially at about 30% wild-type fitness levels, then we should expect that compensatory mutations will be a common occurrence under the relief regime (Poon & Chao, 2005; Szamecz et al., 2014). Szamecz and colleagues (2014) write: "when a population with a gene defect is further away from a fitness peak, compensatory evolution may proceed through a wider range of mutations, including ones that have deleterious side effects." Nonetheless, we did observe a large jump in fitness between days 10 to 20 suggesting some reversion events with large effects might have occurred during this time period. However, several studies have argued that even compensatory mutations can explain massive jumps in fitness (Burch & Chao, 1999; Estes & Lynch, 2003; Maisnier-Patin & Andersson, 2004). Moreover, some argue that the accumulation of deleterious mutations under conditions favouring drift and the subsequent emergence of compensatory mutations may trap populations in an inferior fitness peak (Poon & Chao, 2005; Szamecz et al., 2014). This could explain the fitness plateau we observed between days 20 to 50 and why the relief lines show growth rates lower than wild-type and control levels (Figure 2.8, 2.9). However, further long-term culturing accompanied with fitness experiments are required to determine long-term fitness trajectories of the relief populations. Finally, we argue that compensatory mutations explain at least some fitness increases as opposed to general laboratory adaptation because, as Estes & Lynch (2003) point out, general

laboratory adaptation would be expected would affect all lines equally. This was not the case, as figures 2.8 and 2.9 show, there are substantial fitness differences between recovering lines.

A Pearson's correlation test was performed to examine how well protein divergence correlates with overall fitness. We determined protein divergence by calculating the sum of absolute DBS for each line. We then compared these values to the fitness of each line, determined by measuring doubling time over a 30 minute interval (Table 2.3). Previously our lab group found no statistically significant relationship between the sum of absolute DBS and doubling time in bottlenecked *E.coli* (Lai, 2017). Our aim here was to explore whether this relationship holds for lines that have evolved under a bottleneck relief regime. We found a statistically significant relationship when both relief lines and controls are included in Pearson's test (Figure 2.14). However, when BR lines are considered only, the sum of absolute DBS and doubling time do not correlate significantly (Figure 2.15). For example, we found that while BR50.8 has the lowest |DBS| value (96 489) it also has one of the highest mean doubling times (55.47 minutes) (Table 2.3). The differences in statistical correlation between these two tests performed suggests the sum of absolute DBS correlates well between populations with large fitness differences (i.e. controls versus relief lines) but not between populations with smaller fitness differences (i.e. relief lines versus other relief lines). One limitation of the DBS method is that it only considers protein-coding sequences. As mutations were found distributed both within and outside coding sequences, DBS measures do not reflect the global impact of mutation on fitness. This is problematic because

mutations in non-coding regions such as regulatory RNA and promoters can greatly impact critical cellular processes such as translation, metabolism, regulation, DNA replication, among others (Repoila & Darfeuille, 2009; Winkler & Breaker, 2005). Additionally, compensatory mutations can occur in extragenic regions and thus the DBS method fails to capture the impact of all compensatory mutations (Poon & Chao, 2005). Moreover, DBS only looks at individual mutations, not combinations, which might be non-additive in their effect. Finally, the DBS method does not account for environmental context. Although some theoretical studies have argued that the effect of mutation on fitness is independent of environmental background (see Estes & Lynch (2003) for explanation), numerous studies argue that mutation effects are dependent on the environmental background(Burch & Chao, 1999; Elena & Lenski, 2001). As these experiments are conducted in rich media, some genes that might have been essential in the evolutionary history of the species, could now be non-essential. Possibly some of these mutations are contributing to the high DBS values observed in figure 2.12.

Another explanation for the continual accumulation of functionally severe mutations in the relief lines is that although natural selection is expected to operate efficiently under this relief regime, genetic drift is still expected to be an importantly evolutionary force. As lines were severely bottlenecked, mutations rates remained significantly elevated even under the relief regime (Table 2.1). Some of these mutations are likely to be slightly deleterious and drift to fixation. To explore this further, we investigated how the accumulation of functionally-severe mutations in the relief lines compares to populations that were subjected to a further 50 cycles of bottlenecking without

undergoing a relief regime. Data for this was provided by a member of our lab group, Alicia Lai. We found that both under the relief regime, or alternative bottlenecking regime, mean DBS continues to climb (Lai, 2017). However, the rate at which deleterious mutations accumulate is reduced under relief conditions, reinforcing the idea that natural selection is limiting the overall impact of mutation on protein function, but not eliminating it (Figure 2.13).

Could it be that specific mutations accumulating in the relief populations are responsible for fitness differences between lines, compared to many mutations of smaller effect? We found no clear indication of this. For instance, although we found the most severally impaired protein is a hypothetical protein that belongs to line BR50.8, which has one of the highest recorded doubling times, we discovered that the next most impaired protein, PutA, was truncated in all nine lines (Table 2.2, 2.3). Meanwhile, two frame shift mutations identified in the genome of BR50.10 have significantly high DBS values: A frameshift in a gene encoding an RHS element had an associated DBS value of 1302.9 while a mutation in a gene encoding an inverse auto-transporter adhesion-like protein had an associated DBS value of 1276.3 (Table 2.2). Despite these mutations that are predicted to have large effects, BR50.10 has one of the lowest recorded doubling times of 48.03 minutes (Table 2.3). Moreover, BR50.2, the lineage with the highest average doubling time of 56.88 minutes does not carry a mutation with a large predicted effect on protein function (Table 2.2, 2.3). To examine this relationship further, all DBS values greater than 500 or lower than -500 were plotted against doubling times for each lineage (Figure 2.16). Again, there is no clear

evidence that outliers are responsible for fitness differences between lines. For example, BR50.8 which has one of the highest doubling times and the most significantly impaired protein (hypothetical protein, DBS = 1890.5), also has the second most significantly improved protein (cellulose synthase catalytic subunit, DBS = -1131.1). It is intriguing that BR50.1 has a low relative doubling time and carries a functionally-significant reversion mutation (DBS = -1224.2) that probably recaptures functional activity of the enzyme α-xylosidase. This enzyme catalyses the transfer of an alpha-xylosyl residue from alpha-xyloside to various carbon sources and is therefore important in carbohydrate metabolism, and in overall bacterial fitness (Répérant, Porcheron, Rouquet, & Gilot, 2011). However, confirmation requires further experimental investigation via gene knock-in or knock-out experiments coupled with fitness assays. Our lab group previously found that a small number of mutations can have a large effect on fitness when populations are subjected to Muller's ratchet. However, Fisher's geometric model of adaptation predicts that because beneficial mutations are rare compared to deleterious mutations, adaptation proceeds in a gradual, step-wise fashion (Fisher, 1930) - which is also argued in more modern work (e.g. Burch & Chao, 1999; Tenaillon, 2014). As these lines are undergoing bottleneck relief, we could then expect that fitness restoration is achieved in many steps by mutations of small effect, in accordance to Fisher's model. As such, it could be that compensatory mutations of smaller effect are responsible for fitness differences between lines as opposed to outliers (Burch & Chao, 1999, Fisher, 1930). These mutations will inevitably be more difficult to detect compared to outliers that

'stand out in the crowd.' This is only speculation – examining the individual impacts of mutation on fitness requires further experimental investigation.

To summarize these results so far, we found that overall protein function does not appear to improve in the relief lines, and that protein coding sequences continue to accumulate deleterious mutations. However, this could be due to compensatory mutations that are obscuring the deleterious effects of mutations that occurred in the bottleneck regime rather than simple reversion mutations. Moreover, some of these compensatory mutations may themselves be deleterious in a wild-type background. However, as the DBS tool has several limitations, we therefore add that some of these unusual results could be attributed to these limitations.

Finally, we explored whether the mutational basis for fitness recovery might be further unearthed by exploring mutations that occur across parallel lineages. We identified 881 reversions in total, however, we found that most types of reversion mutations were present in one line only. For example, we identified 57 SNPs in BN50 that reverted in at least one relief line while only 8 SNPs present in BN50 reverted in all 9 relief lines (Figure 2.17). To determine whether these parallel reversions might be causing the general trend in fitness recovery observed in all lines (Figure 2.2), we examined more closely the function of the coding sequences for which reversions were present in all 9 relief lines (Table 2.4). We found no clear indication that these reversions are responsible for the general fitness increase. For example, example, we identified an A to G substitution in an NADPH-dependent oxidoreductase-encoding

sequence in the genome of BN50 that reverted in all 9 relief lines. However, although this mutation resulted in a nonsynonymous change at the amino-acid level, we found the associated DBS value to be – 0.5. Therefore, we are not strongly confident that this reversion is likely to cause any functionally significant change that is likely to impact overall fitness. Additionally, we identified a mutation in BN50 for a gene encoding a Zn-dependent hydrolase. This was predicted to have no effect on protein function (DBS = 0). Therefore, a reversion is unlikely to have any impact at the protein level. We also identified a reversion in all nine lines for a gene encoding a phage-tail protein. However, we found that this also had no significant effect on protein function. Moreover, a separate frameshift-causing mutation was identified in this gene also that did not revert in any line suggesting the functional activity of this gene is impaired in the relief lines regardless. Nevertheless, as previously mentioned, DBS only considers protein level changes and ignores DNA-level or RNA-level effects. Additionally, to find reversion mutations in all 9 lines is a stunning number of lines to observe the same reversion in. To determine more robustly how these reversions impact on fitness, gene knock-in/knock-out experiments are required, along with competitive fitness experiments.

In addition to parallel reversions, we also found several examples of parallel SNPs that have large impacts on protein function by causing premature stop codons (Figure 2.18, 2.19, 2.20). As these mutations were found in all relief lines, it could be that these are examples of compensatory mutations where inactivation of one gene is compensating for the loss of another, an idea also proposed in (Szamecz et al., 2014). Because these

mutations are functionally significant, they also contribute to some of the high DBS values observed in figure 2.12. For example, inactivation of the gene *putA* has an associated DBS score of 1616.2 (Table 2.2). We can only speculate on how these mutations are contributing to fitness increases, and as compensatory and reversion mutations can occur in extragenic regions, more work is required to fully decipher the full effects of all mutations that emerged under the relief regime (Poon & Chao, 2005).

In light of all this, it appears that the mutational basis for escaping the ratchet is achieved, at least under the experimental system presented in this study, through compensatory mutations that appear to have been avoided in the evolutionary past of the affected proteins. This is because the delta-bitscore method calculates the impact of mutation based on sequence conservation, and penalises novel sequences that go into the profile hidden markov model (Wheeler et al., 2016). It is likely that many of these compensatory mutations have rarely emerged and become fixed in the evolutionary past of the gamma-proteobacterial lineages that were included in the profile hidden markov model. Throughout this chapter I have argued how overall protein function appears to have worsened in the relief lineages, at least according to the delta-bitscore predictions. However, I suspect that in reality overall protein function is in fact improving via unique molecular pathways that the DBS method is assigning as functionally deleterious, due to the fact that DBS bases such predictions on how well conserved sequences are. Finally, as there are numerous pathways in the mutational landscape for which compensatory mutations may act (Szamecz et al., 2014), and because there are many ways in which a single mutation may be

compensated for (Poon & Chao, 2005), I suspect that intense drift conditions previously experienced by these recovering populations has opened up evolutionary doorways previously inaccessible due to constraints imposed by selection.

Supplementary Material

Supplementary Table 2.1. Raw data Statistics for Sequenced Genomes

Sample	Total Bases	Read Count	GC (%)	AT (%)	Q20 (%)	Q30 (%)
BR50.1	304,372,622	1,223,444	50.93	49.07	91.11	88.55
BR50.2	395,431,399	1,588,884	50.87	49.13	92.36	90.05
BR50.3	330,486,634	1,327,964	50.57	49.43	92.83	90.61
BR50.4	320,775,998	1,289,350	50.76	49.24	93.38	91.28
BR50.6	338,648,601	1,360,634	50.77	49.23	92.64	90.39
BR50.7	321,925,479	1,293,866	50.85	49.15	92.54	90.26
BR50.8	288,750,456	1,161,374	50.76	49.24	90.02	87.31
BR50.9	336,403,996	1,352,834	50.84	49.17	92.78	90.53
BR50.10	304,134,182	1,226,966	50.47	49.53	92.20	89.87
BRC50_1	349,491,908	1,405,018	50.83	49.17	93.0	90.82
BRC50_3	297,068,994	1,193,028	50.86	49.14	92.91	90.69
BRC50_4	339,629,369	1,364,400	50.81	49.19	91.82	89.30
BRC50_5	339,926,700	1,365,186	50.84	49.16	92.56	90.28
BRC50_6	287,797,477	1,155,226	50.83	49.17	92.21	89.87
BRC50_7	272,494,503	1,093,668	50.93	49.07	91.26	88.73
BRC50_8	339,096,891	1,364,328	50.82	49.18	91.56	89.05
BRC50_9	320,245,951	1,285,262	50.84	49.16	91.22	88.66
BRC50_10	347,243,861	1,395,676	50.83	49.17	92.73	90.49

Q20 (%) : Ratio of reads that have phred quality score of over 20

Q30 (%) : Ratio of reads that have phred quality score of over 30

Phred quality score numerically expresses the accuracy of each nucleotide. Higher Q number signifies higher accuracy.

Chapter 3

Phenotypic effects of the Ratchet

Introduction

While there are numerous studies highlighting the fitness effects and mutational properties of Muller's ratchet (e.g. Bull, Badgett, Rokyta, & Molineux, 2003; Clarke et al., 1993; Estes & Lynch, 2003; Perfeito, Sousa, Bataillon, & Gordo, 2014; Poon & Otto, 2000; Poon & Chao, 2005; Rispe & Moran, 2000), there are far fewer studies that address phenotypic changes that occur under the ratchet, and even less that screen for very broad ranges of phenotypes that could be altered. Often studies focus on phenotypes of interest to the authors, in many cases with medical applications (Andersson, Hughest, & Smith, 1996; Bergstrom, McElhany, & Real, 1999; Escarmís, Perales, & Domingo, 2009; Maisnier-Patin & Andersson, 2004). Such studies have provided critical insight into the pathogenesis of important diseases such as foot-and-mouth disease (Escarmís et al., 2009), AIDS (Yuste, Sánchez-Palomino, Casado, Domingo, & López-Galíndez, 1999) and bacterial diseases (Abel, Abel zur Wiesch, Davis, Waldor, & Baranowski, 2015). However, few studies have examined the vastness of phenotypic space that can be altered under the ratchet. Funchain and colleagues (2000) assessed various phenotypes such as auxotrophy, carbon utilization, motility, osmolarity and phage resistance that became impaired following multiple

cycles of single-colony bottlenecking. However, this study lacks in-depth genomic insight into the mutational basis for such impairment, and it lacks a follow-up bottleneck relief regime. This is important because compensatory mutations that emerge under a bottleneck relief regime can potentially provide an avenue for adaptive mutations to emerge that may have deleterious effects in a wild-type background (Maisnier-Patin & Andersson, 2004). Moreover, little is known about the phenotypic landscape that might emerge under a relief regime. On one hand compensatory and back mutations may restore eroded phenotypes, while on the other hand selection may prevent the recovery of impaired phenotypes if that phenotype does not contribute to overall fitness.

Additionally, it is not commonplace to find studies that screen for rare gain-of-function phenotypes that might help a bottlenecked population survive in a new environment. I have already emphasized in chapter 1 how elevated mutation rates and intensified drift can facilitate the emergence of phenotypic innovation. Therefore, it should follow that such innovation might be conceivable under the ratchet. Moreover, it is argued that slightly deleterious mutations may be important in facilitating aspects of biological complexity (Lenski, Ofria, Pennock, & Adami, 2003; Lynch, 2007), and such mutations are synonymous with Muller's ratchet. How might mutation facilitate the ability of bacteria to adapt to new environments? In other words, what is the genetic basis for adaptation?

There is no simple answer to this question, for, the evolution of new traits can emerge by single SNPs (Viana et al., 2015), or multiple mutations (Lenski et al., 2003; Zhang & al., 2003), by larger rearrangements through recombination (Naas, Blot, Fitch, & Arber, 1995) or by gene duplication followed by neo-functionalisation (Zhang & al., 2003), for example. Also, adaptive mutations can occur in both coding and non-coding regulatory regions of a genome (such as in Cis-regulatory elements), the latter of which can facilitate substantial adaptation (Elena & Lenski, 2003). To add to this complexity, mutations can promote adaptation by impacting genes encoding single enzymatic steps or global regulatory genes that control multiple interacting networks, for example genes that are involved in central metabolism (Elena & Lenski, 2003). Finally, adaptive mutations have trade-offs in their relative fitness across different environments, meaning that mutations beneficial in terms of fitness in one environment, could be costly in another – a mechanism known as antagonistic pleiotropy (Cooper & Lenski, 2000; Elena & Lenski, 2003).

Understanding the evolutionary steps required to facilitate functional change can be disentangled by coupling experimental evolution with genomics (Elena & Lenski, 2003). For example, one study identified the genetic causes of aerobic citrate utilization (Cit^+) that appeared in *E.coli* after about 33 000 generations of long-term culturing. By sequencing genomes of Cit^+ mutants and comparing reads to Cit^- strains, the group concluded that tandem duplication events allowed expression of an aerobically-expressed promoter that resulted in the expression of a previously non-functional citrate transporter (Blount, Barrick, Davidson, & Lenski, 2012). In another

study, genome sequencing revealed parallel chromosomal rearrangements in long-term independently evolving *E.coli* populations that resulted in deletions of the ribose-utilization operon, suggesting adaptation to glucose-limited media (Raeside et al., 2014). Similar studies on *E.coli* that explore the mutational-basis for adaptation to media-limiting environments have also identified gain-of-function mutations; For example, mutations that increase the permeability of the LamB porin in glucose limited environments (Notley-McRobb & Ferenci, 1999a, 1999b), and mutations in *ompF* that increases the permeability of the OmpF porin in lactose-limiting media (Zhang & Ferenci, 1999).

The goal here is to screen a very broad range of phenotypes at various time points of the bottleneck and bottleneck relief regime to test for both gain-of-function and loss-of-function phenotypes that might emerge under the ratchet. Moreover, by coupling these experiments with genomics analyses, our aim was to assess the mutational basis for such changes. How mutational changes that accumulate under the ratchet impact on phenotype remains poorly understood. To achieve this, we extracted frozen-down cultures representing various time-points of the bottleneck and bottleneck relief regime. We then screened cells for active (or inactive) respiration in various metabolic environments using Biolog plates (Bochner, 2009). Biolog plates contain 96 wells with each well comprising a unique metabolic environment that cells may or may not respire in. Active respiration is coupled to the reduction of a colourless dye to purple; cells that can utilize a particular metabolic substrate are distinguished from inactive cells by purple colour formation. Biolog-based experiments have provided massive

insight in diverse contexts such as in studies on antibiotic resistance (Guard-Bouldin, Morales, Frye, Gast, & Musgrove, 2007), pathogenicity (Blin, Passet, Touchon, Rocha, & Brisse, 2017), microbial ecology (Keymer, Miller, Schoolnik, & Boehm, 2007), genotype-phenotype relationships (Ceapa et al., 2015), and, most relevant to this study, Biolog plates have also been implemented to screen for phenotypic changes that occur under MA regimes, though not following bottleneck relief (Funchain et al., 2000; Leiby & Marx, 2014). To this end, we report here the results of a screen of 379 metabolic environments covering carbon, nitrogen, phosphorous and sulphur at various time points of the bottleneck and bottleneck relief regime. To assess the mutational basis for our observations, we relate phenotypic changes back to mutational changes.

Methods

96-well Biolog plates PM1 (carbon sources), PM2A (carbon sources), PM3B (Nitrogen sources) and PM4A (Phosphorous and Sulphur Sources) were tested for populations that represent different time points in both the bottleneck and bottleneck relief experiments. These lineages include Day 0 (wild-type, WT), Day 10 (BN10), Day 20 (BN20), and Day 50 (BN50) of the bottleneck period as well as the control lineage that represents Day 50 (BNC50). For the bottleneck relief lineages, BR50.1 and the control lineage BRC50.1 were tested. These represent lines from day 50 of the relief regime.

Experimental procedures were adapted from the protocol for *E.coli* developed by Biolog Inc:

Glycerol stocks from each time point tested were streaked out for single colonies on LB agar and then sub-cultured a second time onto a fresh source of LB agar. Plates were checked visually for contamination. Additionally, genomic data was also used to assess for evidence of contaminants. Cells were incubated at 37°C for 1-3 days depending on growth. For example, wild-type and control lines grow more rapidly than bottleneck and relief lines.

For plates PM1 and PM2A the following procedures were used:

5-10 Colonies were removed from a plate using a sterile inoculation loop and re-suspended in 10mls of Biolog inoculating fluid IF-0a (1.2x) to reach a cell density of 85% transmittance. 4mls of cells were added to a solution containing 16mls of IF-0a and 0.24mls of Biolog Redox Dye Mix A (100x). 3.76mls of water was added to give a

final volume of 24mls. 100ul of final mixture was dispensed into each well for plate PM1 and PM2A.

For plates PM3B and PM4A, the following procedures were used:

5-10 Colonies were removed from a plate using a sterile inoculation loop and re-suspended in 10mls of Biolog inoculating fluid IF-0a (1.2x) to reach a cell density of 85% transmittance. 4mls of cells were added to a solution containing 16mls of IF-0a, 0.24mls of Biolog Redox dye Mix A and 0.24mls of sodium succinate/ferric citrate (100x) – these are carbon sources required for plates PM3B and PM4A. 3.52mls of water was added to give a final volume of 24mls. 100ul of final mixture was dispensed into each well for plates PM3B and PM4A.

Plates were incubated at 37°C and the optical density (OD595) was measured with a FLUOstar Omega Microplate Reader (BMG Labtech) every 12 hours for 48-60hrs depending on the plate and strain being analysed. Where possible, technical replicates were performed. However, due to time constraints some time points were tested once only. Biolog plates were also visually inspected and photographed. Photos were taken several days following the experiments and as such, are not a complete reflection of results. PM3B and PM4A in particular show unusual patterns following incubation, including wells that form individual purple specs and in some cases, the negative control wells turn slightly purple. Therefore, only plate reader data for PM3B and PM4A is provided here. PM1 and PM2A, on the other hand, appear more reliable to examine visually, and therefore both visual and kinetic data is provided for

experiments conducted on these plates. When interpreting results, readers are encouraged to refer to the appendix for the names of the particular phenotypes being tested. Alternatively readers may download their own copies via www.biolog.com.

Results

Biolog data reveals Widespread Metabolic Erosion in Bottlenecked and Bottleneck Relief Populations

379 metabolic environments were screened using Biolog plates PM1, PM2A, PM3B and PM4A. Populations corresponding to 7 different time points in the bottleneck and bottleneck relief regimes were tested. These include wild-type, BN10, BN20, BN50, BNC50, BR50.1 and BRC50.1. To assess metabolic activity, optical density (OD595) was measured every 12 hours for 60 hours total using a FLUOstar Omega Microplate Reader (BMG Labtech). Absorbance values for well A1 (negative control) are subtracted from aborbance values for each other well in a plate to cancel out the impact of background noise. Note that for plate PM4A, well F1 is also a negative control.

Biolog data reveals that for each of the four plate types: PM1, PM2A, PM3B and PM4A, all phenotypic capacity that wild-type populations can undergo is rapidly lost throughout the course of the bottleneck regime. Moreover, the majority of wild-type phenotypes are lost by 20 cycles of bottlenecking which means that a 100% loss in phenotypic capacity for all the Biolog reactions tested probably occurs much earlier than bottleneck day 50. In addition, no phenotype that is eroded is recaptured in the bottleneck relief regime and no gain-of-function phenotype was identified.

For PM1, we counted about 65 carbon sources that could be utilized by wild-type cells and for PM2A we counted about 20 different carbon sources. As such, the

bottlenecking regime resulted in a loss of about 85 different carbon-based metabolic reactions that we measured (Figure 3.1, 3.2, 3.3, 3.4, 3.5, 3.6, 3.7 and 3.8). For PM3B, about 35 positive reactions were counted for wild-type cells. Therefore, at least 35 different nitrogen-based sources could no longer be metabolized following the bottleneck regime (Figure 3.9). For PM4A, wild-type cells were demonstrated to utilize about 30 different phosphorous and sulphur sources, the capacity of which became impaired by about day 20 of the bottleneck regime (Figure 3.10). These counts are conservative, because for some environments, respiration is slow and therefore purple colour formation can form beyond the recommended incubation time (48hrs). In some cases we observed purple colour change emerging beyond this time point. As results become less reliable past this time, we have avoided (where possible) assigning a reaction as positive if there is uncertainty. Counts are based on visual inspection immediately following incubation, photographic evidence and by assessing kinetic changes over time via optical density-based measurements.

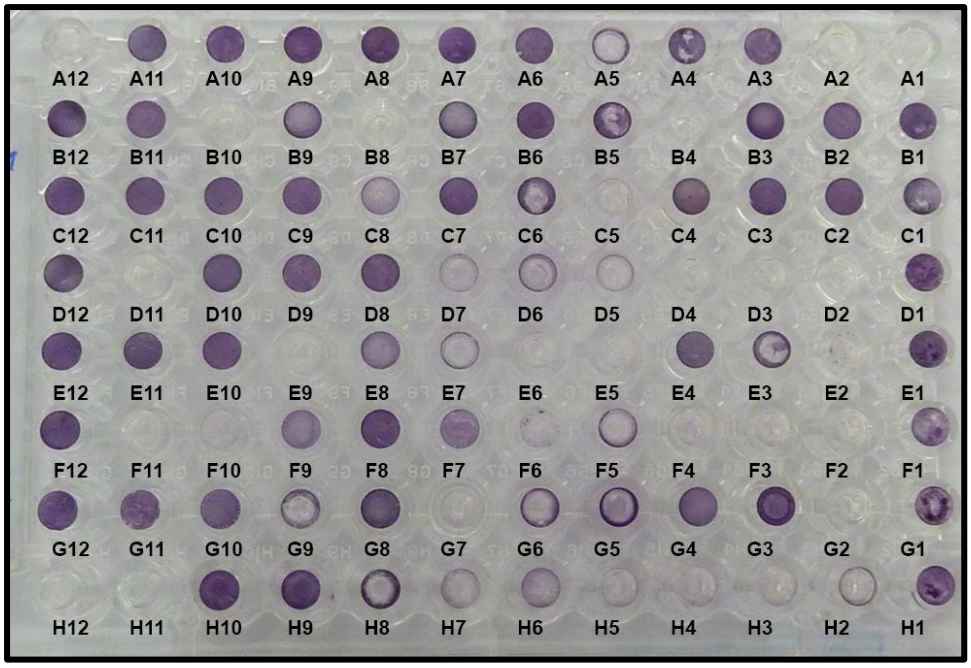

Figure 3.1. Biolog phenotypic array (PM1) for wild-type. Each well contains a different carbon source (see appendix). The ability to utilize a carbon source is determined by purple colour formation. A1 is a negative control containing no source of carbon.

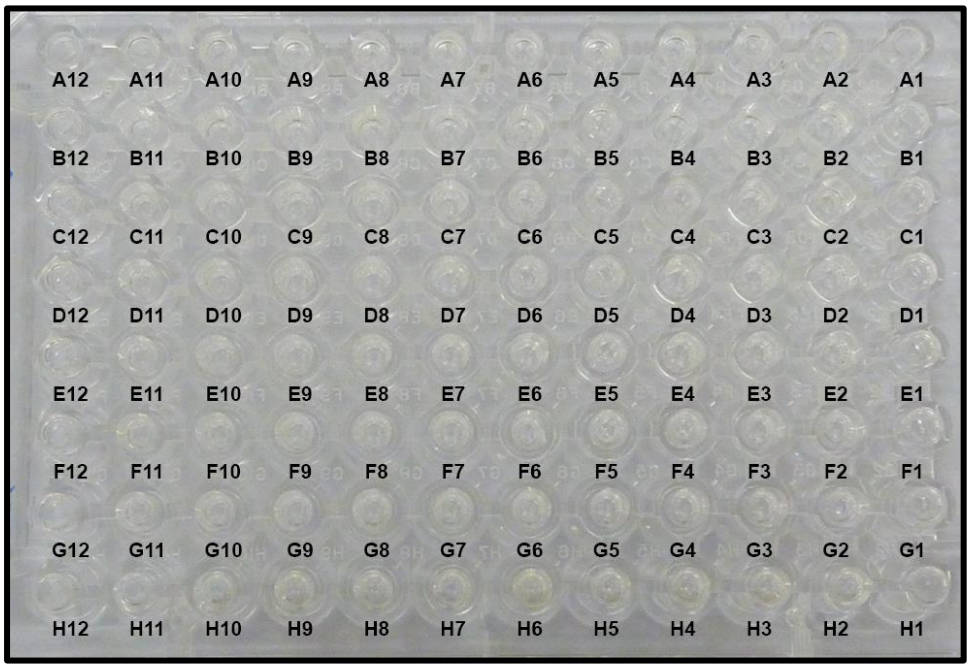

Figure 3.2. Biolog phenotypic array (PM1) for BN50. Each well contains a different carbon source (see appendix). The ability to utilize a carbon source is determined by purple colour formation. A1 is a negative control containing no source of carbon.

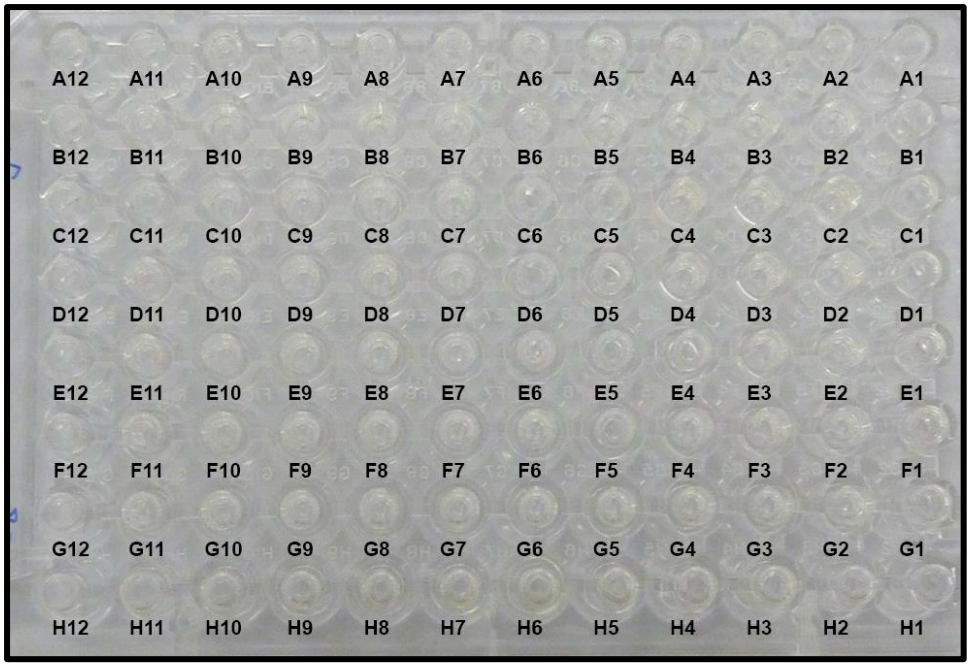

Figure 3.3. Biolog phenotypic array (PM1) for BR50.1. Each well contains a different carbon source (see appendix). The ability to utilize a carbon source is determined by purple colour formation. A1 is a negative control containing no source of carbon.

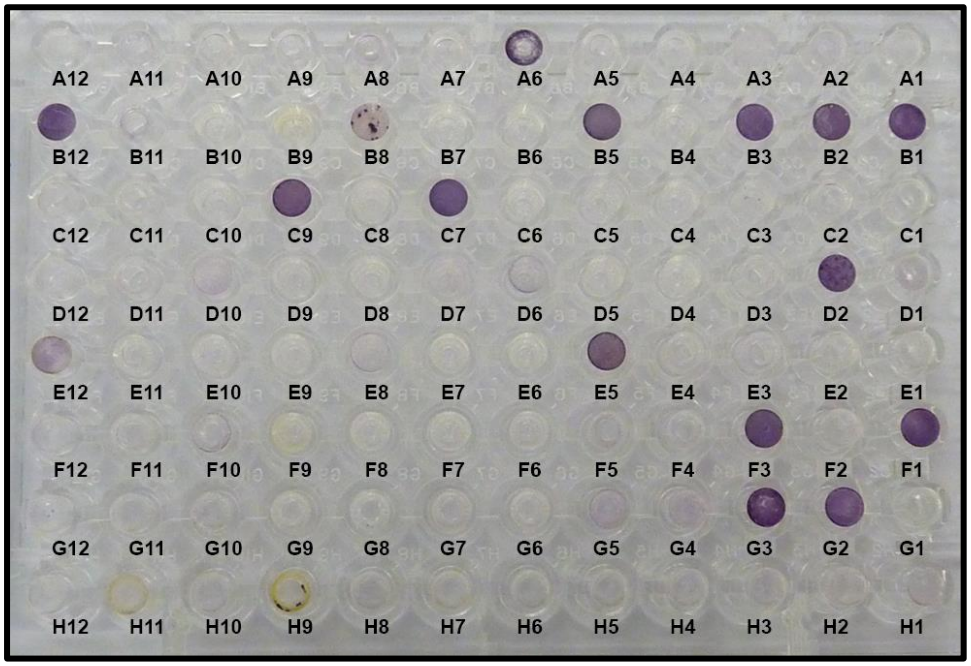

Figure 3.4. Biolog phenotypic array (PM2A) for WT. Each well contains a different carbon source (see appendix). The ability to utilize a carbon source is determined by purple colour formation. A1 is a negative control containing no source of carbon.

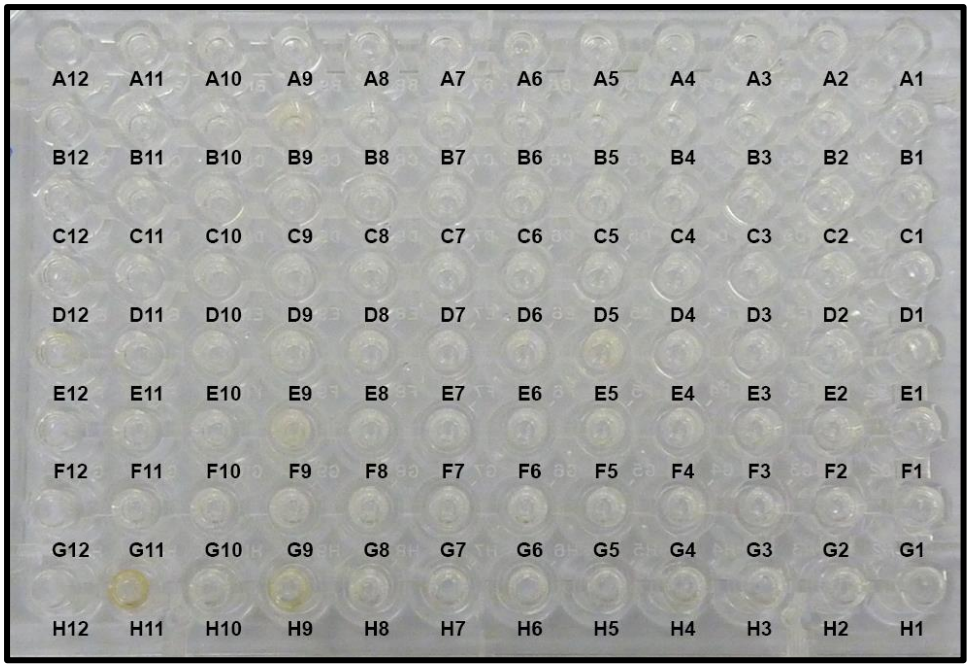

Figure 3.5. Biolog phenotypic array (PM2A) for BN50. Each well contains a different carbon source (see appendix). The ability to utilize a carbon source is determined by purple colour formation. A1 is a negative control containing no source of carbon.

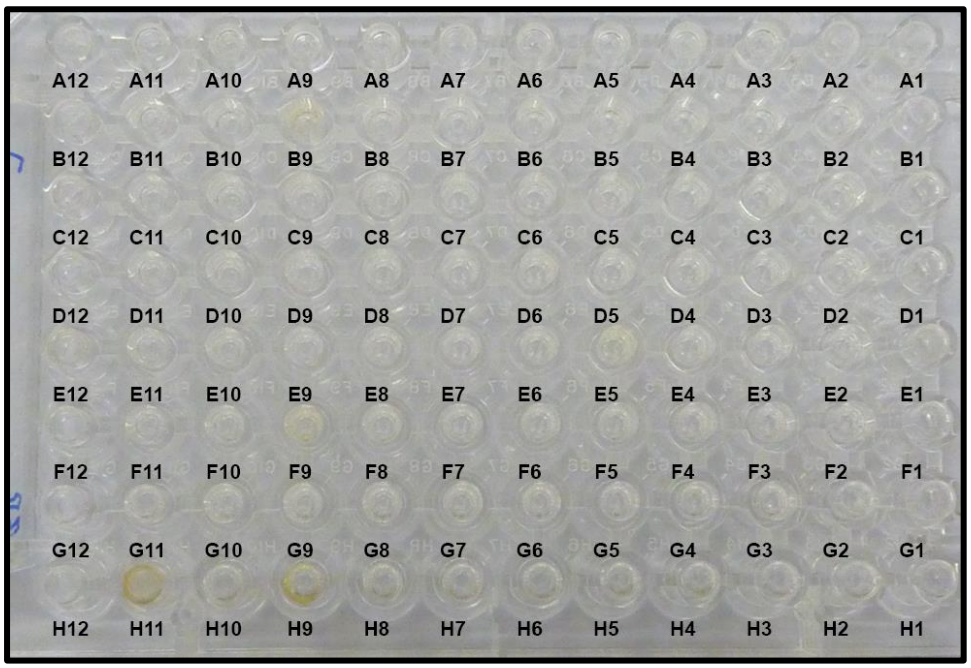

Figure 3.6. Biolog phenotypic array (PM2A) for BR50.1. Each well contains a different carbon source (see appendix). The ability to utilize a carbon source is determined by purple colour formation. A1 is a negative control containing no source of carbon.

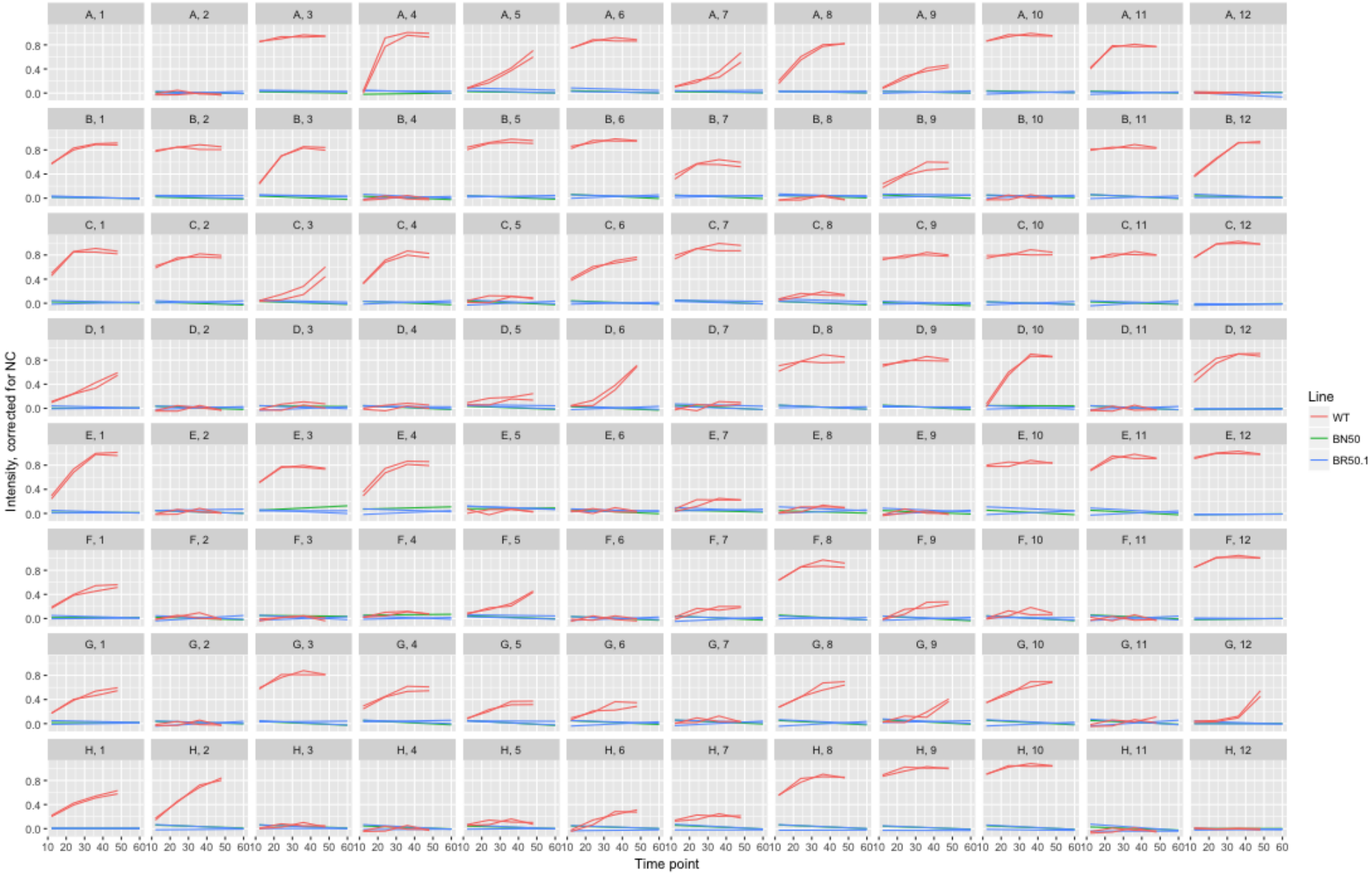

Figure 3.7. Kinetic data for WT, BN50 and BR50.1 tested on PM1. Change in purple colour formation was assessed by taking OD_{595} measurements every 12 hours. BN50 and BR50.1 were measured up to 60 hours. WT was measured to 48 hours. Two replicates for WT were performed. Each well is corrected by subtracting absorbance values from the negative control.

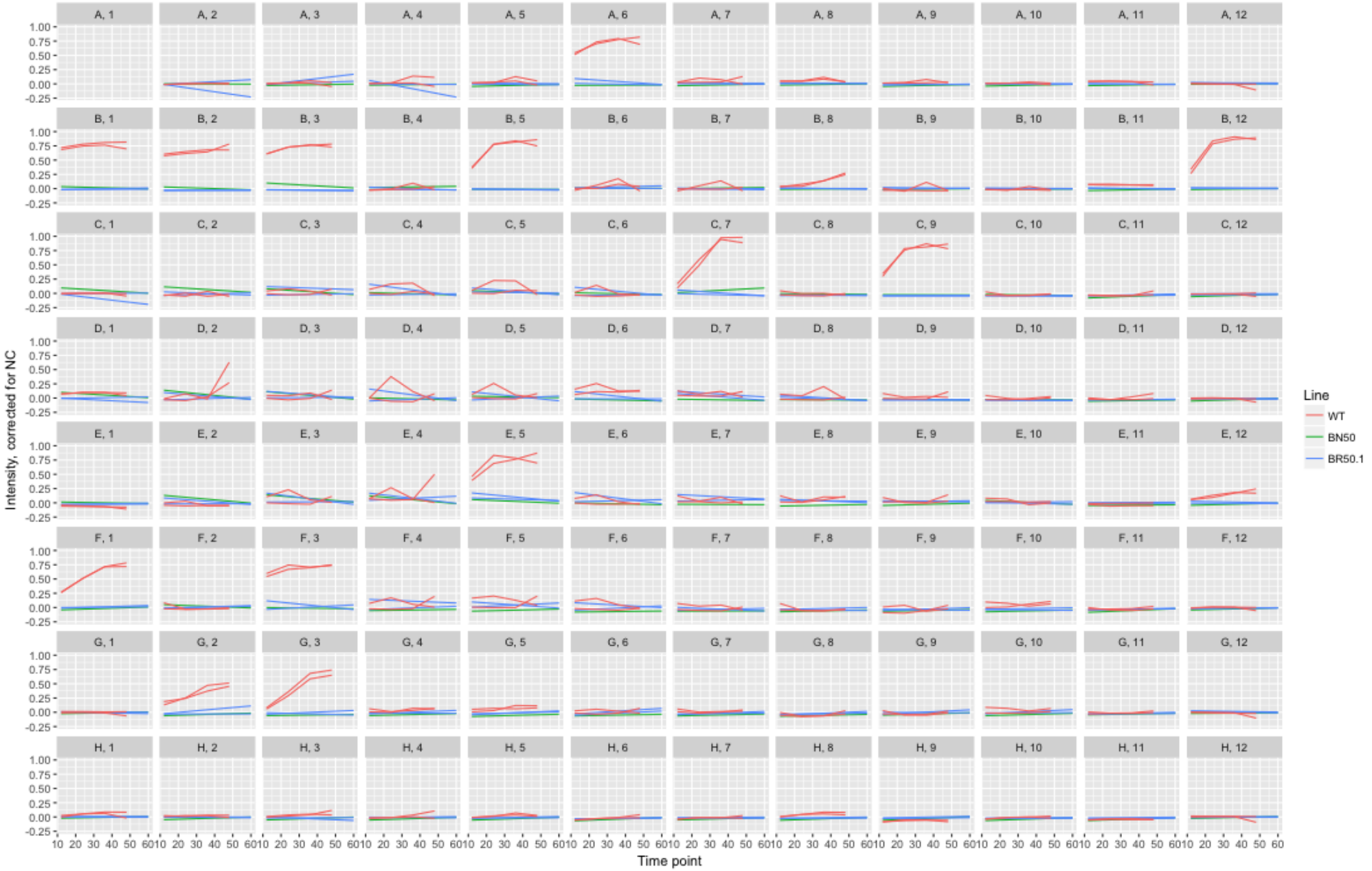

Figure 3.8. Kinetic data for WT, BN50 and BR50.1 tested on PM2A. Change in purple colour formation was assessed by taking OD_{595} measurements every 12 hours. BN50 and BR50.1 were measured up to 60 hours. WT was measured to 48 hours. Two replicates for WT were performed. Each well is corrected by subtracting absorbance values from the negative control.

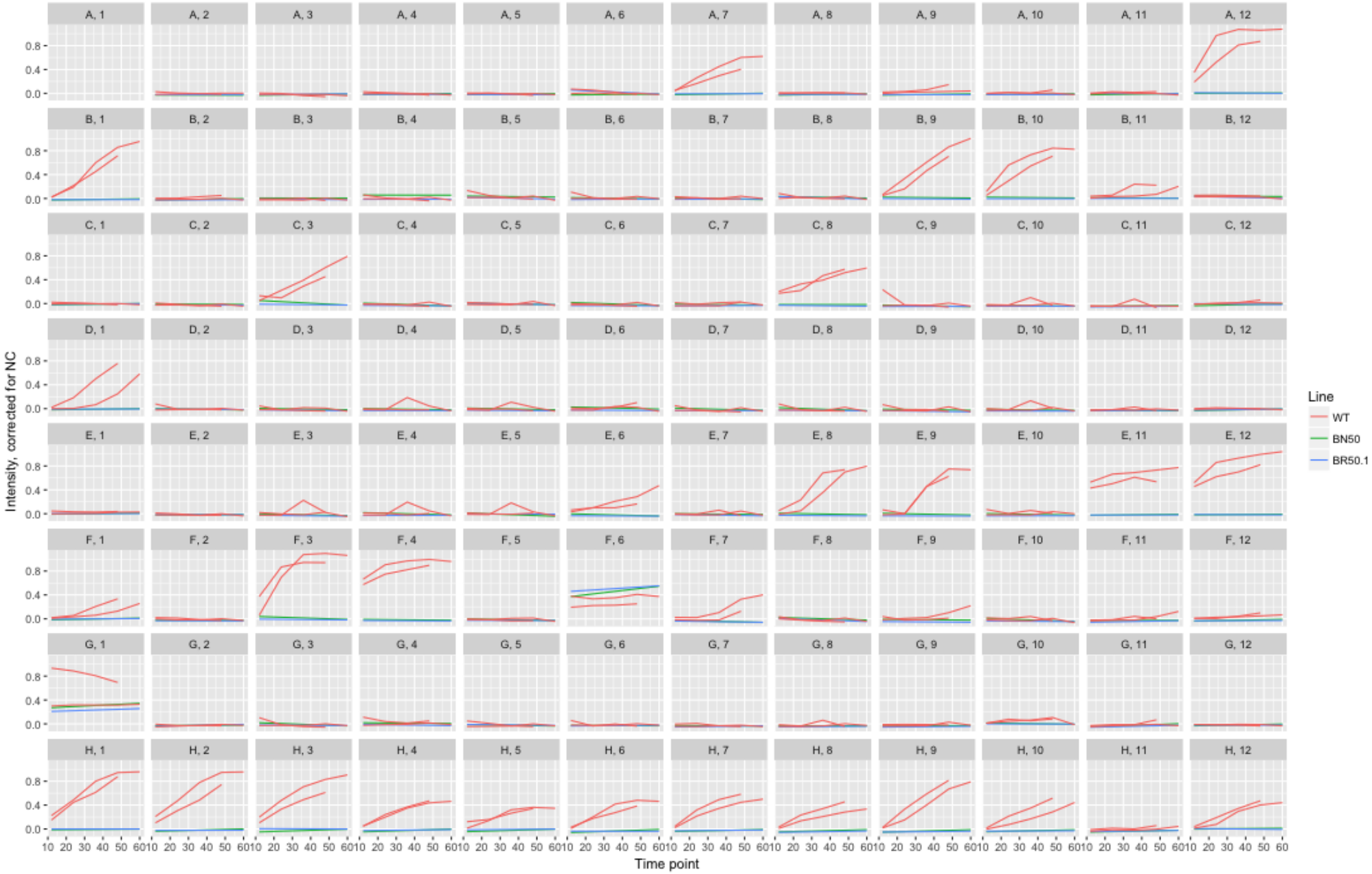

Figure 3.9. Kinetic data for WT, BN50 and BR50.1 tested on PM3B. Change in purple colour formation was assessed by taking OD_{595} measurements every 12 hours. BN50 and BR50.1 were measured up to 60 hours. Two replicates for WT were performed; 1 replicate was measured to 48 hours and the other to 60 hours. Each well is corrected by subtracting absorbance values from the negative control.

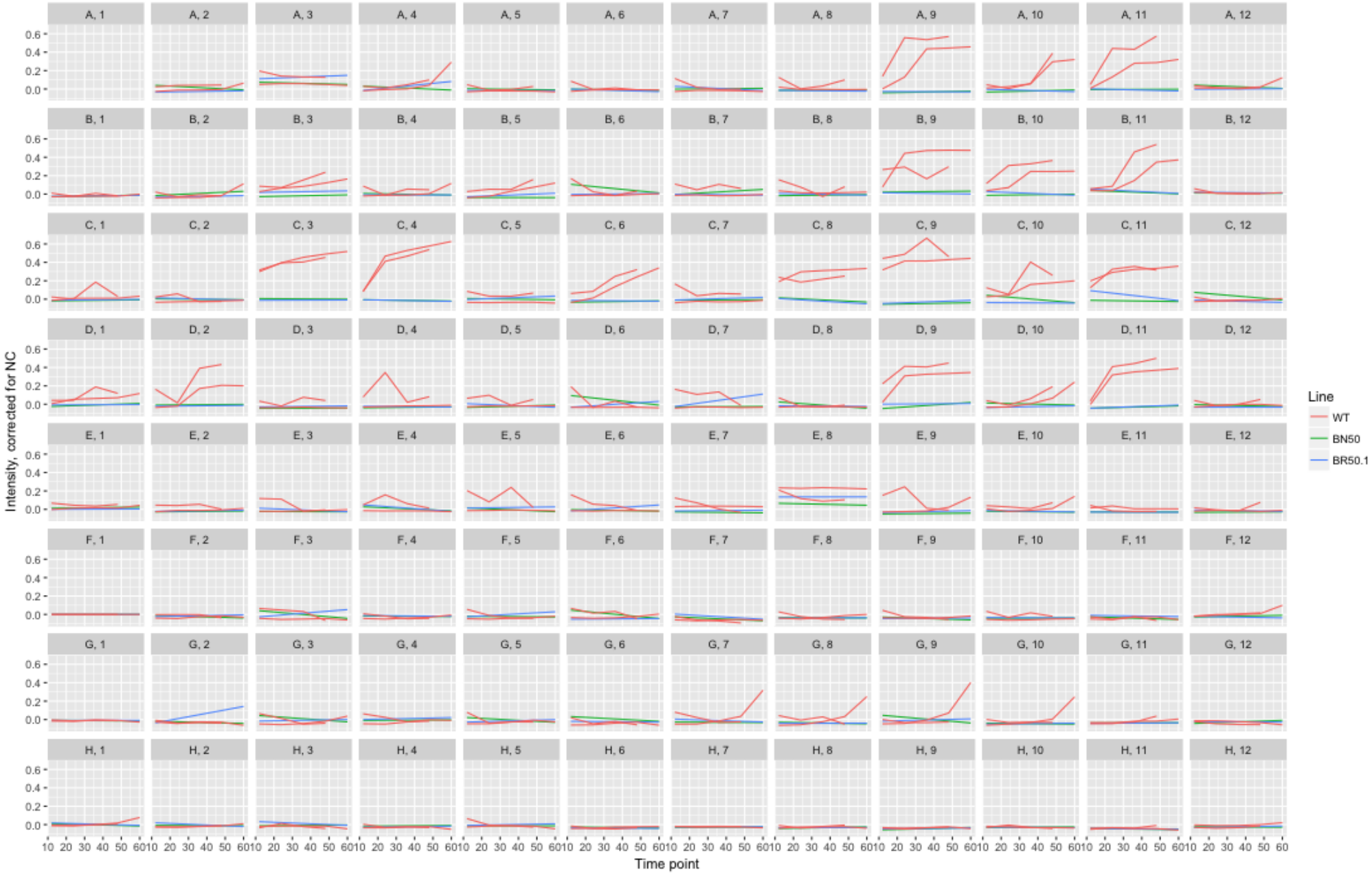

Figure 3.10. Kinetic data for WT, BN50 and BR50.1 tested on PM4A. Change in purple colour formation was assessed by taking OD_{595} measurements every 12 hours. BN50 and BR50.1 were measured up to 60 hours. Two replicates for WT were performed; 1 replicate was measured to 48 hours and the other to 60 hours. Each well is corrected by subtracting absorbance values from the negative control.

Biolog Data reveals differences in respiration kinetics between bottleneck and bottleneck relief control lines (BNC50 and BRC50.1)

To gauge whether long-term culturing itself can cause significant changes between lineages, we also tested bottleneck controls and bottleneck relief controls on Biolog plates. As a starting point, the number of wells per plate calculated to have an endpoint OD595 absorbance value greater than 0.1 was calculated. This value is often used as a threshold to indicate active metabolic activity. For PM1, we found that results were similar between wild-type, the bottleneck control (BNC50) and the bottleneck relief control (BRC50.1) (Figure 3.11), while for PM2A, BNC50 appears to show reduced activity (Figure 3.12). Differences are minor between control lines tested on plate PM3B (Figure 3.13) while for PM4A, BNC50 and BRC50.1 appear to show significantly reduced activity compared to wild-type (Figure 3.14). Further inspection of kinetic data reveals large differences in levels of respiration between control and wild-type lineages. For example, we observed a decrease in activity in BNC50 for utilization of carbon sources N-acetyl-D-glucosamine, L-proline, D-mannose, D-galactonic acid-γ-Lactone, L-rhamnose, D-fructose, maltose, Thymidine, uridine, maltotriose, glycyl-L-proline, p-Hydroxy phenyl acetic acid, L-galactonic acid-γ-lactone and D-galacturonic Acid (Supplementary figure 3.1). For BRC50.1, we observed some decreases in activity for utilization of succinic acid, maltose, uridine, L-threonine, L-galactonic acid-γ-lactone and D-galacturonic acid (Supplementary figure 3.1).

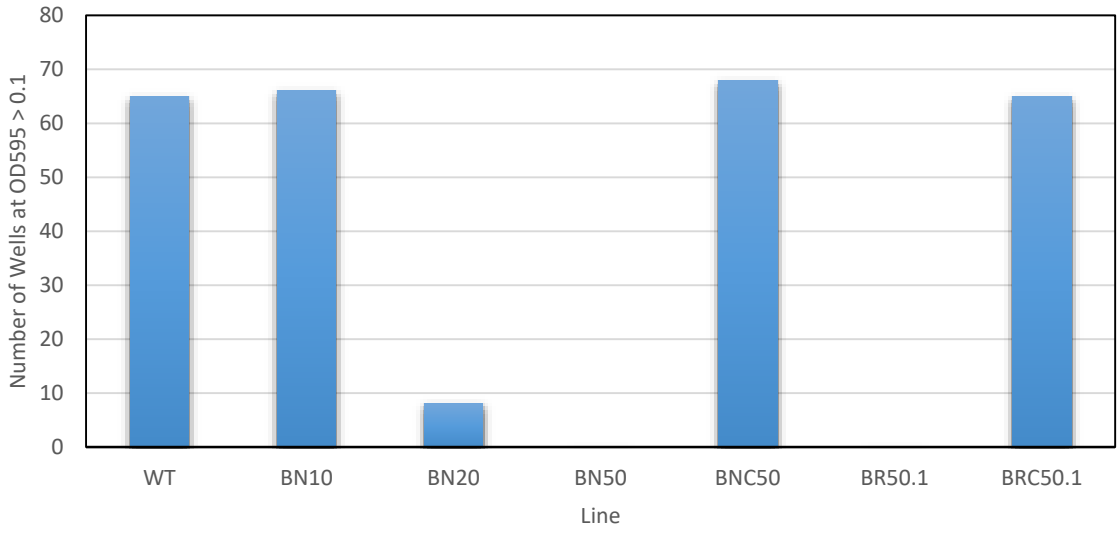

Figure 3.11. PM1: Number of wells with an endpoint absorbance (OD595) value greater than 0.1. Endpoint data was calculated at 48hrs for WT, BNC50 and BRC50.1. For all other lines, endpoint data was calculated at 60hrs to account for slow growth. Data was corrected with the negative control. Where replicates were performed, mean optical density values for each well-type were calculated.

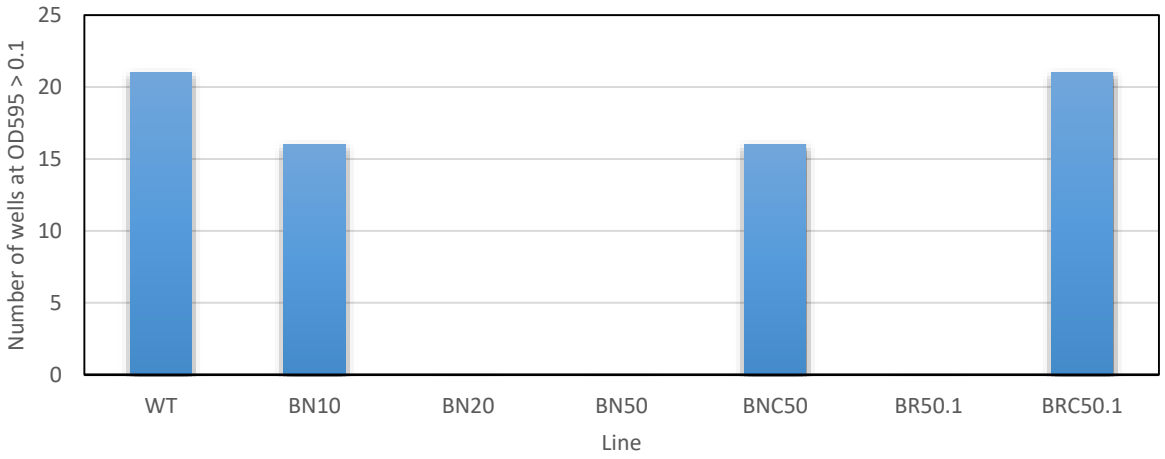

Figure 3.12. PM2A: Number of wells with an endpoint absorbance (OD595) value greater than 0.1. Endpoint data was calculated at 48hrs for WT, BNC50 and BRC50.1. For all other lines, endpoint data was calculated at 60hrs to account for slow growth. Data was corrected with the negative control. Where replicates were performed, mean optical density values for each well-type were calculated.

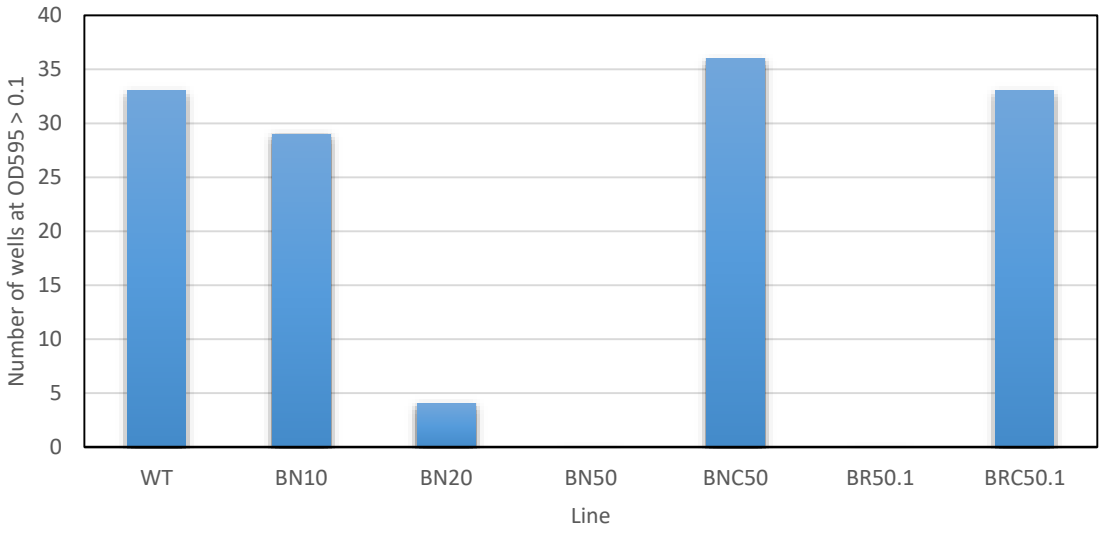

Figure 3.13. PM3B: Number of wells with an endpoint absorbance (OD595) value greater than 0.1. Endpoint data was calculated at 60 hours for all lines. Data was corrected with the negative control. Where replicates were performed, mean optical density values for each well-type were calculated. Note that BNC50 appears to have acquired a gain-of-function phenotype. However, absorbance > 0.1 is used only as an arbitrary threshold to indicate active respiration. In some cases inactive wells may produce values that exceed this threshold.

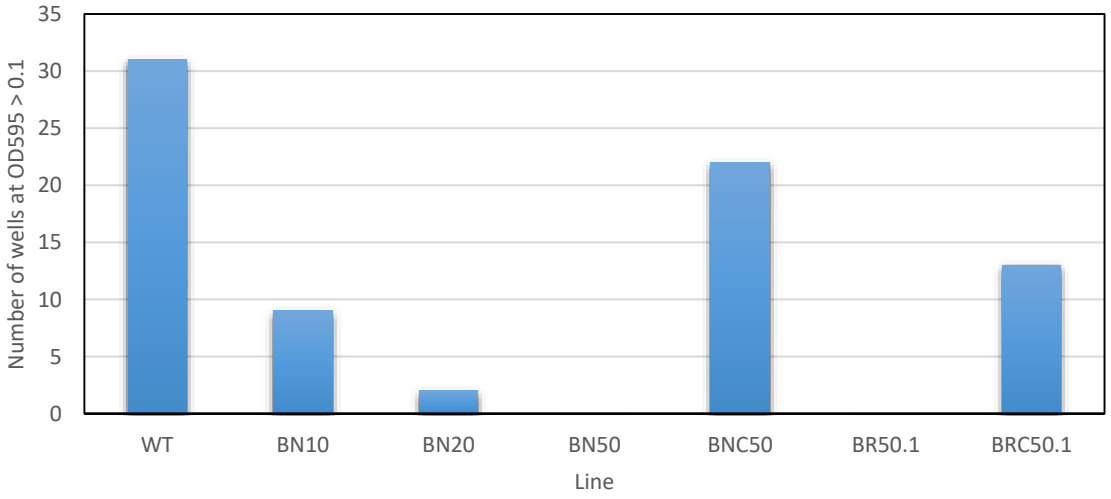

Figure 3.14. PM4A: Number of wells with an endpoint absorbance (OD595) value greater than 0.1. Endpoint data was calculated at 60 hours for all lines. Data was corrected with the negative control. Where replicates were performed, mean optical density values for each well-type were calculated.

Widespread metabolic erosion occurred between Bottleneck days 10-20

As evident above (Figure 3.11, 3.12, 3.13, 3.14), the most prominent metabolic changes occur between days 10 – 20 of the bottleneck regime. Closer examination of purple colour formation for each Biolog plate and kinetic data supports this. For example, inspection of PM1 plates revealed about 57 phenotypes that were eroded between days 10-20 (Figure 3.15, 3.16, Table 3.1). PM2A, PM3B and PM4A also show a significant number of loss-of-function phenotypes (Table 3.1, Supplementary figure 3.5, 3.6, 3.7).

Table 3.1. Loss of function phenotypes observed between days 10-20 of the bottleneck regime

Well	PM1 - Loss of Function Phenotypes	Well	PM2A - Loss of Function Phenotypes
A4	D-Saccharic acid	A6	Dextrin
A5	Succinate Acid	B1	N-Acetyl-D-Galactosamine
A6	D-Galactose	B3	β-D-Allose
A7	L-Aspartic Acid	B5	D-Arabinose
A8	L-Proline	B12	3-0-β-D-Galacto-pyranosyl-D-Arabinose
A9	D-Alanine	C9	β-Methyl-D-Glucoronic Acid
A10	D-Trehalose	D6	D-Tagatose
A11	D-Mannose	E12	5-Keto-D-Gluconic Acid
B1	D-Serine	F3	Melibionic Acid
B2	D-Sorbitol	G2	L-Alaninamide
B3	Glycerol	G3	N-Acetyl-L-Glutamic Acid
B5	D-Glucuronic acid	**Well**	**PM3B - Loss of Function Phenotypes**
B9	L-Lactic Acid	A7	L-Alanine
C1	D-Glucose-6-Phosphate	B1	L-Glutamine
C2	D-Galactonic Acid-γ-Lactone	B9	L-Proline
C3	D,L-Malic Acid	B10	L-Serine
C4	D-Ribose	C3	D-Alanine
C6	L-Rhamnose	C8	D-Serine
C7	D-Fructose	D1	N-Acetyl-L-Glutamic acid
C8	Acetic Acid	E8	D-Glucosamine
C9	α -D-glucose	E9	D-Galactosamine
C10	Maltose	E11	N-Acetyl-D-Glucosamine
C11	D-Melibiose	E12	N-Acetyl-D-Galactosamine
C12	Thymidine	F1	N-Acetyl-D-Mannosamine
D1	L-Asparagine	F4	Cytidine

D6	α-Keto-Glutaric acid
D8	α-Methyl-D-Galactosidase
D9	α-D-Lactose
D10	Lactulose
D12	Uridine
E4	D-Fructose-6-Phosphate
E8	β-Methyl-D-Glucoside
E10	Maltotriose
E11	2-Deoxy Adenosine
E12	Adenosine
F1	Glycyl-L-Aspartic Acid
F5	Fumaric Acid
F7	Propionic Acid
F8	Muicic Acid
F9	Glycolic Acid
F12	Glyoxylic acid
G1	Glycyl-L-Glutamic acid
G3	L-Serine
G4	L-Threonine
G5	L-Alanine
G6	L-Alanyl-Glycine
G8	N-Acetyl- β-D-Mannosamine
G9	Mono Methyl Succinate
G10	Methyl Pyruvate
G11	D-Malic Acid
G12	L-Malic Acid
H2	p-Hydroxy Phenyl Acetic Acid
H6	L-Lyxose
H7	Glucuronamide
H8	Pyruvic acid
H9	L-Galacturonic Acid-y-Lactone
H10	D-Galacturonic Acid
F7	Guanosine
H1	Ala-Asp
H4	Ala-Gly
H5	Ala-His
H6	Ala-Leu
H7	Ala-Thr
H8	Gly-Asn
H10	Gly-Glu
H12	Met-Ala

Well	**PM4A - Loss of Function Phenotypes**
A2	Phosphate
A3	Pyrophosphate
A4	Trimeta-phosphate
A5	Tripoly-phosphate
B5	Carbamyl Phosphate
B9	Guanosine-3'-monophosphate

For PM1, carbon sources D-mannitol (well B11) and L-glutamic acid (well B12) are some of the few remaining carbon sources clearly able to be utilized by BN20 (Figure 3.15, 3.16). Others might include N-acetyl-D-glucosamine, D-gluconic acid, D,L-α-glycerol-phosphate, L-glutamine, D-glucose-1-phosphate and glycyl-L-proline however utilization of these compounds is very weak (Figure 3.15, 3.16) and confirmation requires further testing.

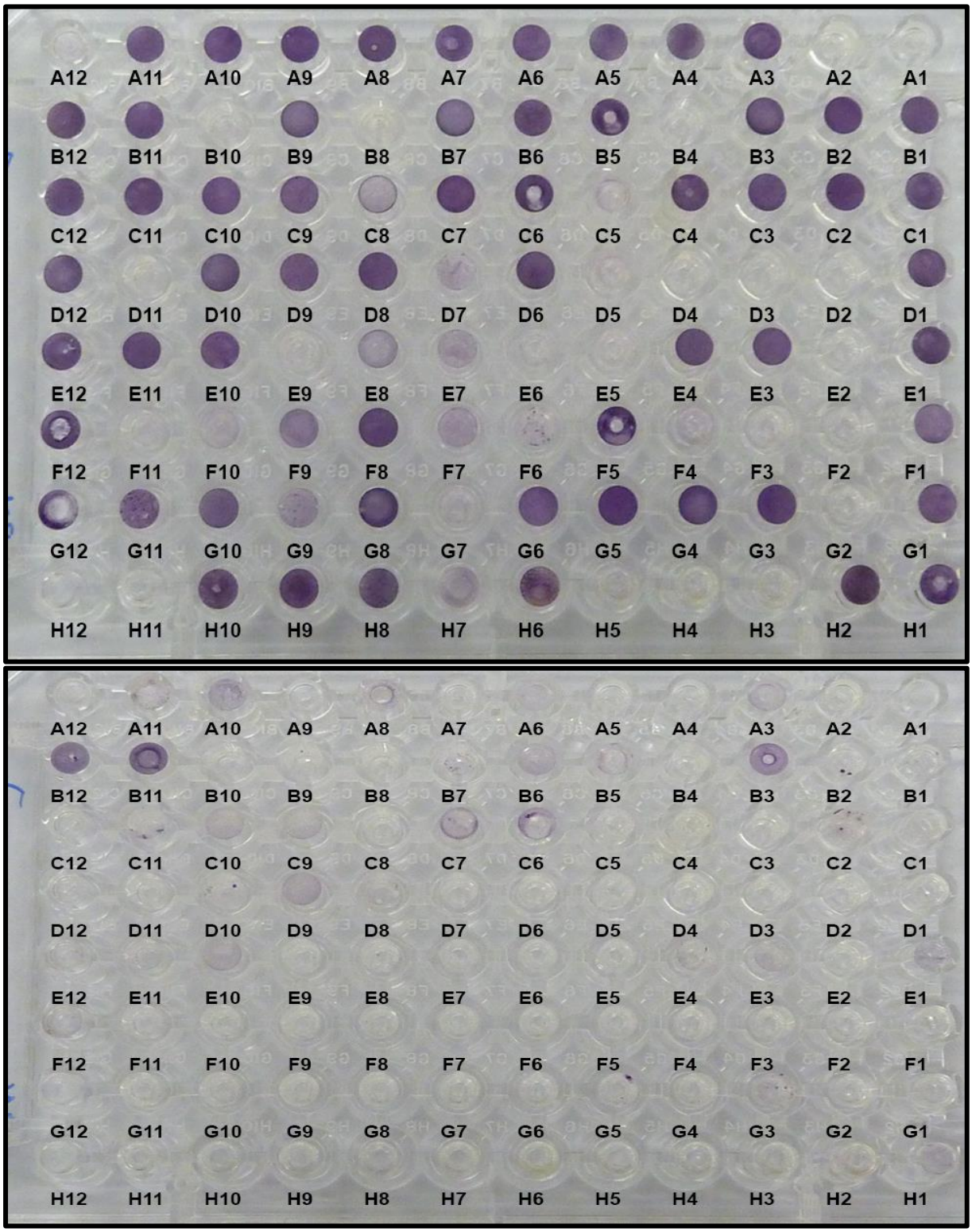

Figure 3.15. Comparison between BN10 (top) and BN20 (bottom) tested on BIOLOG plate PM1. Each well contains a different carbon source. The ability to utilize a carbon source is determined by purple colour formation. A1 is a negative control containing no source of carbon. Note that B11 and B12 represent D-mannitol and L-glutamic Acid – based Biolog wells.

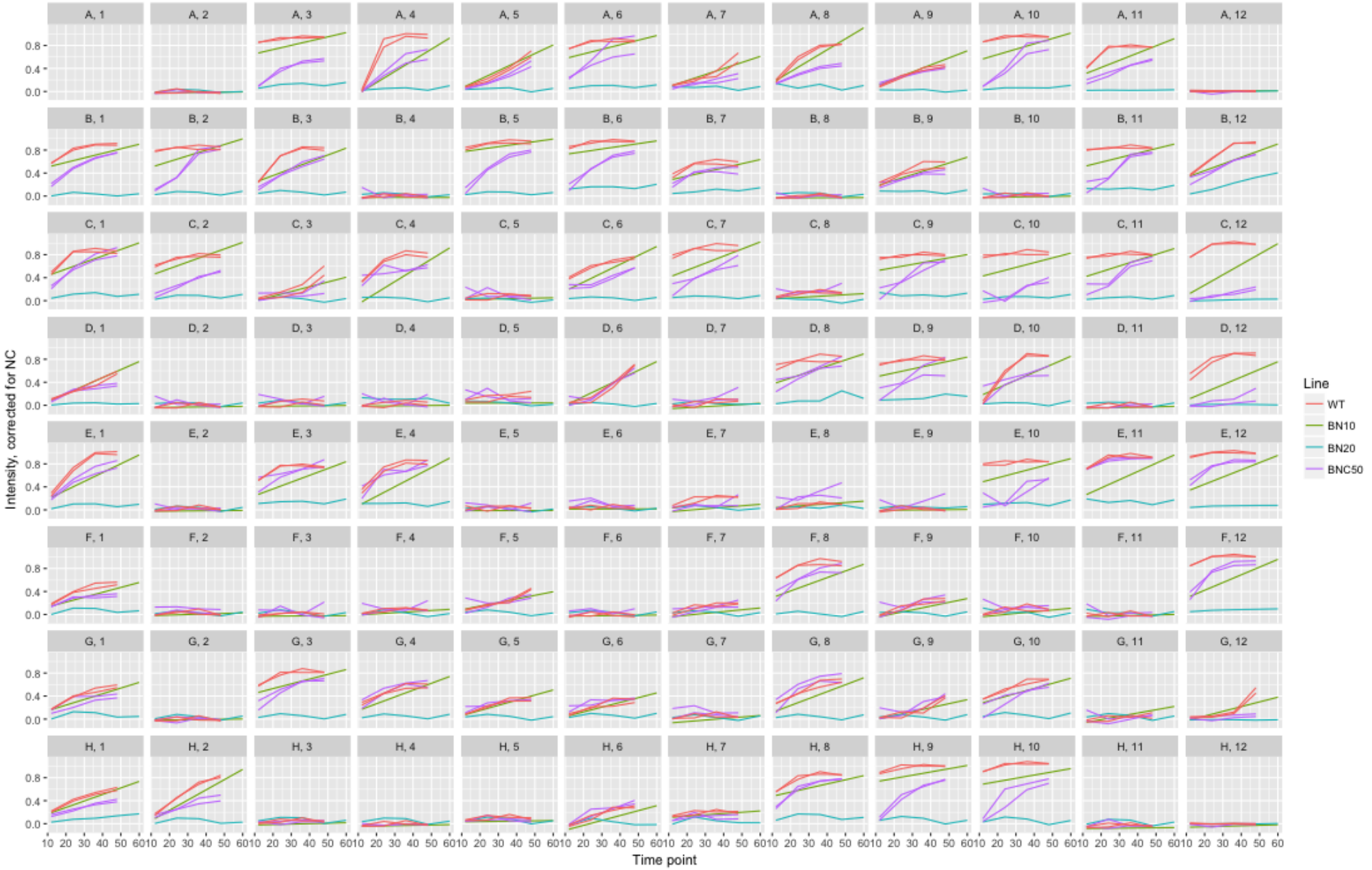

Figure 3.16. Kinetic data for WT, BN10, BN20 and BNC50 tested on plate PM1. Purple colour formation is assessed by taking OD_{595} measurements every 12 hours. Measurements were taken up to 60 hours for slow-growers BN10 and BN20 and 48 hours for WT and BNC50. Each well is corrected by subtracting absorbance values from the negative control. Data is from duplicate trials for WT and BNC50. BN10 and BN20 were tested once only

To examine whether mutations correlate with loss of metabolic function, the genomes of BN10 and BN20 were analysed to disentangle the mutational basis for widespread metabolic erosion that occurred between these two time points in the bottleneck regime. Genes encoding key enzymes that are involved in metabolic pathways associated with the utilization of carbon sources found in PM1 were examined. In some cases, sequences encoding enzymes remained mutation-free or if a mutation was present, the mutational impact was minimal. For example, we found that while an inability to utilize carbon sources such as D-Galactose, D-Alanine and D-Mannose was apparent for BN20 (Table 3.1), sequences encoding enzymes directly involved in utilizing these carbon sources remain intact (Table 3.2). Even in sequences where a mutation has occurred, delta-bitscore values associated with these mutations are normally less than 5 suggesting minimal impairment on protein function. For example, *PutA* and *PutP* genes carry mutations due to substitutions that have associated DBS values of 2 and 1.6, respectively (Table 3.2). Nevertheless, further testing is required to determine exactly the impact of these mutations for the metabolic reactions tested (see chapter 2 for limitations of the DBS method). What these results are indicating however is that metabolic losses are not necessarily attributable to mutations in protein-coding regions directly involved in the degradation of specific Biolog sources (Table 3.2). Therefore, mutations in promoters or regulatory regions could be involved. Testing such cases are beyond the scope of this project however.

Table 3.2. Mutational changes to key enzymes involved in various metabolic processes that were impaired between days 10 and 20 of the bottleneck regime

Biolog well	Energy Source	Key enzymes	Mutations	Amino-acid change	Protein effect	DBS
A6	D-Galactose	GalM, GalK, GalU, GalT, GalE	none			
A8	L-Proline	PutA, PutP	T -> A Substitution(PutA)	D -> V	Substitution	2
			A -> G Substitution (PutP)	K -> E	Substitution	1.6
A9	D-Alanine	DdlA,DdlB	none			
A11	D-Mannose	ManA,ManX,ManY,ManZ	none			
B1	D-Serine	DsdC, DsdX, DsdA	A -> G Substitution (dsdA)	none	none	0
			T -> C Substitution (dsdX)	S -> P	Substitution	0.5
B2	D-Sorbitol	SrlA,SrlE,SrlB,SrlD	T -> C Substitution (srlB)	V -> A	Substitution	3.2
B3	Glycerol	GlpA, GlpB, GlpC, GlpK	A -> G Substitution (glpB)	S -> G	Substitution	3.1
			G -> A Substitution (glpB)	R -> H	Substitution	3.1
C4	D-Ribose	RbsD, RbsK	none			
C6	L-Rhamnose	YiiL,RhaD, RhaA, RhaB, RhaS, RhaR, RhaT	T -> C Substitution (yiiL)	T -> A	Substitution	0
			T -> C Substitution (rhaB)	D -> G	Substitution	2.7
			A -> T Substitution (rhaR)	S -> C	Substitution	1.6
C7	D-Fructose	FruA, FruK, FruB	C -> T Substitution (fruB)	A -> T	Substitution	3.1
C10	Maltose	MalG,MalF,MalE,MalK,LamB,MalM	none			
D1	L-Asparagine	AnsB	T -> C substitution (ansB)	none	none	0
D9	α-D-Lactose	LacA,LacY,LacZ,LacI	none			
D10	Lactulose	LacA,LacY,LacZ,LacI	none			
G3	L-Serine	SdaA, SdaB, SdaC,TdcC,TdcG	none			
G4	L-Threonine	TdcR, TdcA, TdcB, TdcC, TdcD,TdcE, TdcG	none			
G5	L-Alanine	DadX, DadA	none			

The genome of BN20 was analysed to determine if widespread loss of metabolic function that occurred between days 10 and 20 of the bottleneck regime was due to mutations in key enzymes involved in those impaired phenotypes. Here are some examples of carbon sources that were not usable by BN20. Shown are mutations (or lack of) that occurred in sequences encoding key enzymes, amino-acid changes resulting from mutations, the effect on the associated protein and overall DBS value for that sequence. Enzymes here represent essential components for the utilization of the various Biolog sources tested.

Large-effect mutations might explain widespread metabolic erosion observed in BN20

Based on our initial observations presented above, we decided to investigate whether mutations predicted to have significant functional implications may be the cause of widespread metabolic erosion observed between bottleneck days 10 - 20. These include sequences that carry DBS values greater than 5, which is often indicative that

a particular SNP is having a functionally significant impact on protein function (Wheeler et al., 2015).

Some of the most impacted protein encoding sequences are associated with energy production and carbohydrate transport/metabolism (Table 3.3). Alpha-xylosidase and oxidoreductase, for example, have associated DBS scores of 1224.2 and 1136 (Table 3.3). Several cell membrane associated sequences were also hit by functionally-severe mutations in BN20, such as those encoding a cellulose synthase regulator protein, membrane protein and alanine racemase (Table 3.3). There appears to be no COG category for which protein sequences were hit substantially more than others, and several sequences encoding proteins of unknown function show high DBS scores, indicating the cause for widespread metabolic degradation occurring between days 10 – 20 of the bottleneck regime is not clear-cut. These observations imply that pinpointing such causes is beyond the scope of this project however in the discussion and also in chapter 4 I discuss possible ways one might approach this.

Table 3.3. The most severely impacted protein-encoding sequences identified in the genome of BN20

Product	Mutation	Protein effect	DBS	Cog Category
alpha-xylosidase	(C)5 -> (C)6 Insertion (tandem repeat)	Frame Shift	1224.2	G
oxidoreductase subunit	(G)3 -> (G)2 Deletion (tandem repeat)	Frame Shift	1136	C
cellulose synthase regulator protein	(T)7 -> (T)8 Insertion (tandem repeat)	Frame shift	944.5	M
D-allose import ATP-binding protein	(T)7 -> (T)8 Insertion (tandem repeat)	Frame shift	874.4	P
acyltransferase/acyl-ACP synthetase	G -> A Substitution	Truncation	799.5	I
membrane protein	G -> T Substitution	Truncation	633	M
type II citrate synthase	(T)4 -> (T)5 Insertion (tandem repeat)	Frame Shift	596.7	C
phosphoethanolamine transferase	(T)7 -> (T)8 Insertion (tandem repeat)	Frame shift	594.4	S
hypothetical protein	(A) insertion	Frame shift	401.4	S
xanthine permease	T -> A substitution	Truncation	356.7	F
DNA-binding transcriptional regulator	C -> T Substitution	Truncation	342.3	K
protease modulator	(A)3 -> (A)2 Insertion (tandem repeat)	Frame Shift	338	0
ethanolamine utilization cobalamin adenosyltransferase	(T)6 -> (T)7 Insertion (tandem repeat)	Frame shift	326.3	E
alanine racemase	C -> T Substitution	Truncation	317.1	M
NADPH quinone reductase	C -> T Substitution	Truncation	304	S
putative crotonobetaine/carnitine-CoA ligase	(A) insertion	Frame shift	195.7	I and Q
arginine ABC transporter substrate-binding protein	(T)6 -> (T)5 Deletion (tandem repeat)	Frame shift	179.6	E
rRNA (cytosine-C(5)-)-methyltransferase	C -> T Substitution (truncation)	Truncation	165.7	J
	(A)3 -> (A)2 Deletion (tandem repeat)	Frame shift	165.7	J
ultifunctional fatty acid oxidation complex subunit alpha	(T)6 -> (T)7 Insertion (tandem repeat)	Frame shift	140.6	I
putative oxidoreductase	(A)8 -> (A)7 Deletion (tandem repeat)	Frame shift	118.9	S
LysR family transcriptional regulator	(G)5 -> (G)6 Insertion (tandem repeat)	Frame Shift	92.8	K
hypothetical protein	(C)6 -> (C)7 Insertion (tandem repeat)	Frame shift	68.3	M
RNA-directed DNA polymerase	(A)8 -> (A)9 Insertion (tandem repeat)	Frame Shift	59.4	L
zince protease	G -> A Substitution	Truncation	53.8	O
sensory histidine kinase	G -> A Substitution	Substitution	37	T
fimbrial usher protein	G -> A Substitution	Truncation	20.9	M
sulfite reductase subunit alpha	A -> G Substitution	Substitution	9.2	I
	G -> A Substitution	Substitution	9.2	I
maltodextrin phosphorylase	A -> T Substitution	Substitution	7.2	G
hypothetical protein	G -> A Substitution	Substitution	7	S
hydrogenase 2 large subunit	G -> A Substitution	Substitution	6.8	C
	C -> T Substitution	Substitution	6.8	C
reactive intermediate detoxifying aminoacrylate hydrolase	A -> T Substitution	Substitution	6.4	F
TPM domain protein phosphatase	G -> A Substitution	Substitution	6.4	S
hybrid sensory histidine kinase in two-componentregulatory system	A -> C Substitution	Substitution	6.3	T
lysine decarboxylase	C -> T Substitution	Substitution	5.8	E
glucan biosynthesis protein G	T -> C Substitution	Substitution	5.6	P
glutamate synthase	G -> A Substitution	Substitution	5.4	E
DNA-binding transcriptional dual regulator, repressor of N-acetylglucosamine	T -> A Substitution	Substitution	5.3	K

Shown here are the most functionally-deleterious mutations in the genome of BN20. The specific mutation responsible for severally impacted protein-encoding sequences are displayed, their effect, associated DBS score and COG category that the protein encoding sequences belong to.

Key enzymes involved in various metabolic pathways accumulate functionally severe mutations throughout the bottleneck regime and these persist in the relief Lines.

Further inspection of SNPs that have accumulated up to bottleneck day 50, and whether these show any signs of reverting at bottleneck relief day 50, indicates the capacity for the evolving populations to utilize many of the Biolog sources tested might be impaired irreversibly (Figure 3.17, Figure 2.12 chapter 2). Figure 3.17 depicts an abundance of mutations in protein-coding genes associated with various metabolic processes identified in the genome of BN50. Additionally, comparing this figure to 2.12 in chapter 2 suggests very few of these mutations are reverting. Moreover, we discussed in chapter 2 how the relief lines continue to accumulate mutations including in sequences associated with metabolism, some of which are even predicted to be functionally severe.

To illustrate some examples, table 3.4 depicts some enzymes involved in metabolic pathways that have been impacted by mutation, some of which have significantly high associated DBS scores (e.g. GalU). Additionally, inspection of these sequences in the relief genomes reveals mutations in most cases do not revert, and in some cases more mutations have accumulated in the same genes in the relief lines (Figure 2.12, chapter 2). For example, parallel truncations in the *putA* gene (responsible for proline utilization) identified in all relief genomes suggests recapturing the capacity to utilize L-proline that wild-type populations can perform is unlikely (Figure 3.18).

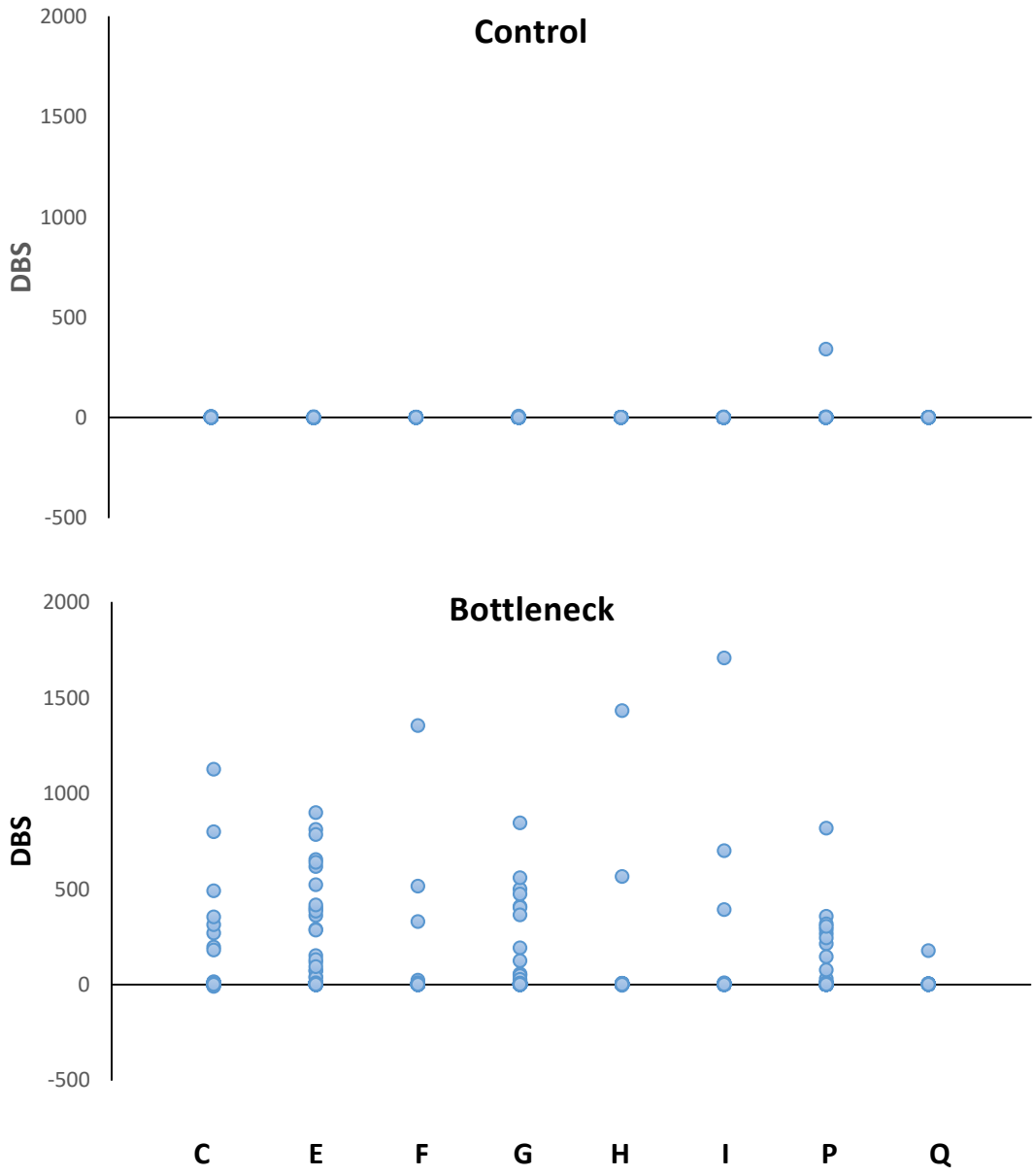

Figure 3.17. Scatterplot showing DBS values calculated for BNC50 (top) and BN50 (bottom) relative to WT. This depicts the abundance of functionally severe mutations that were predicted to occur over the 50-day bottleneck regime in protein sequences associated with metabolism. The bottom figure shows DBS values calculated based on analysis of protein encoding sequences in the genome of BN50 while the top figure shows DBS values calculated for the genome of BNC50 which represents the day 50 non-bottleneck control line. The letters represent COG categories that associated protein sequences belong to. C = energy production, E = amino acid transport metabolism, F = Nucleotide transport/metabolism, G = carbohydrate transport/metabolism, H = coenzyme transport/metabolism, I = Lipid transport/metabolism, P = Inorganic ion transport/metabolism, Q = secondary metabolites.

Table 3.4. Examples of mutations that have accumulated throughout the course of the bottleneck regime in enzymes critical in metabolic pathways.

Energy Source	Key enzymes	Mutations	Amino-acid change	Protein effect	DBS	Present in BR lines?
D-Galactose	GalM	C -> T Substitution	G -> S	Substitution	2.1	All
	GalK	none				
	GalU	C -> T Substitution		Truncation	266.5	All
	GalT	C -> T Substitution	none	none	0	All
	GalT	T -> A Substitution	none	none	0	All
	GalE	none				
L-Proline	PutA	C -> T Substitution	G -> S	Substitution	7.4	All
	PutA	G -> A Substitution	S -> L	Substitution	7.4	All
	PutA	C -> T Substitution	none	none	7.4	All
	PutA	G -> A Substitution	P -> L	Substitution	7.4	All
	PutA	A -> G Substitution	I -> T	Substitution	7.4	All
	PutA	T -> A Substitution	D -> V	Substitution	7.4	All
	PutP	C -> T Substitution	none	none	3.4	All
	PutP	G -> A Substitution	A -> T	Substitution	3.4	All
	PutP	A -> G Substitution	K -> E	Substitution	3.4	All
	PutP	G -> A Substitution	none	none	3.4	All
α-D-Lactose	LacA	none				
	LacZ	C -> T Substitution	none	none	0	All
	LacZ	G -> A Substitution	none	none	0	All
	LacI	C -> T Substitution	G -> E	Substitution	0.5	All
Maltose	MalG	none				
	MalF	G -> A Substitution	A -> V	Substitution	4.8	All
	MalF	C -> T Substitution	A -> T	Substitution	4.8	All
	MalE	C -> T Substitution		Truncation	517	All
	MalE	C -> T Substitution	A -> T	Substitution	517	All
	LamB	C -> T Substitution	none	none	0	All
	MalK	G -> A Substitution	E -> K	Substitution	0.1	All
	MalM	none				

Shown are some examples of mutations identified in the genome of BN50 as well as the effects of these mutations on protein function and whether they are present in the BR lines.

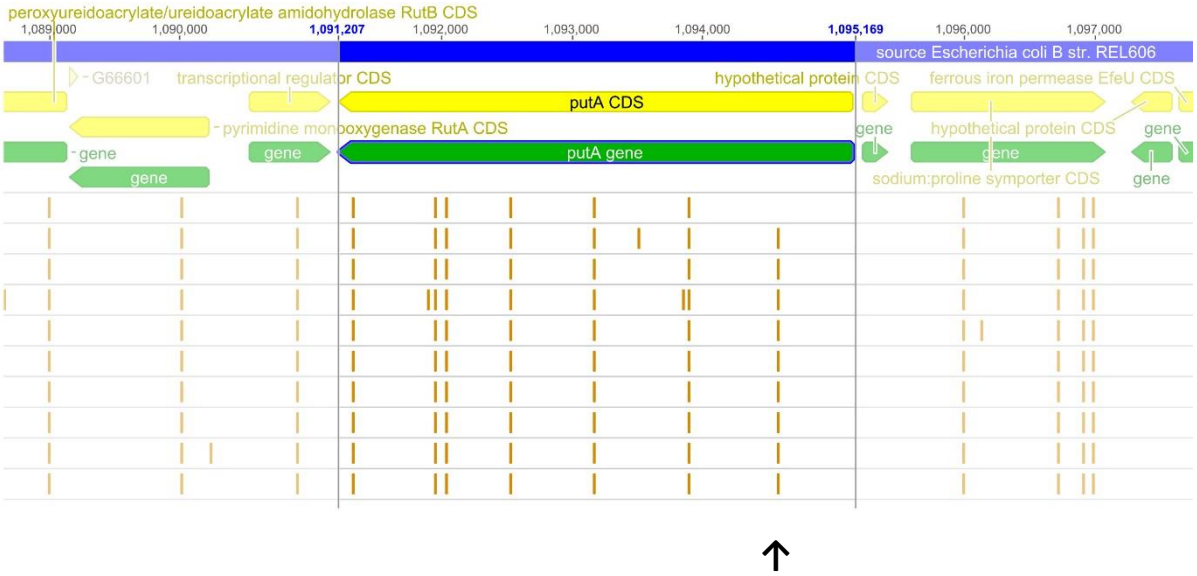

Figure 3.18. Depiction of SNPs in the *putA* gene identified in the genome of BN50 and also in the relief lines. Shown here is the *putA* gene (green bar), CDS (yellow bar) and surrounding sequences. In blue is the WT REL606 genome for which reads were mapped to. Orange dashes represent SNPs and each white horizontal segment represents a BR line. BN50 is the top white horizontal line. The SNPs shown by the black arrow are responsible for premature stop codons which have resulted in a truncated protein for each of the nine BR lines sequenced. In the top white horizontal segment this SNP is absent – this segment represents the genome of BN50 for which this mutation is absent. PutA is a proline dehydrogenase that acts as a bifunctional enzyme catalyzing reactions in the proline degradation pathway.

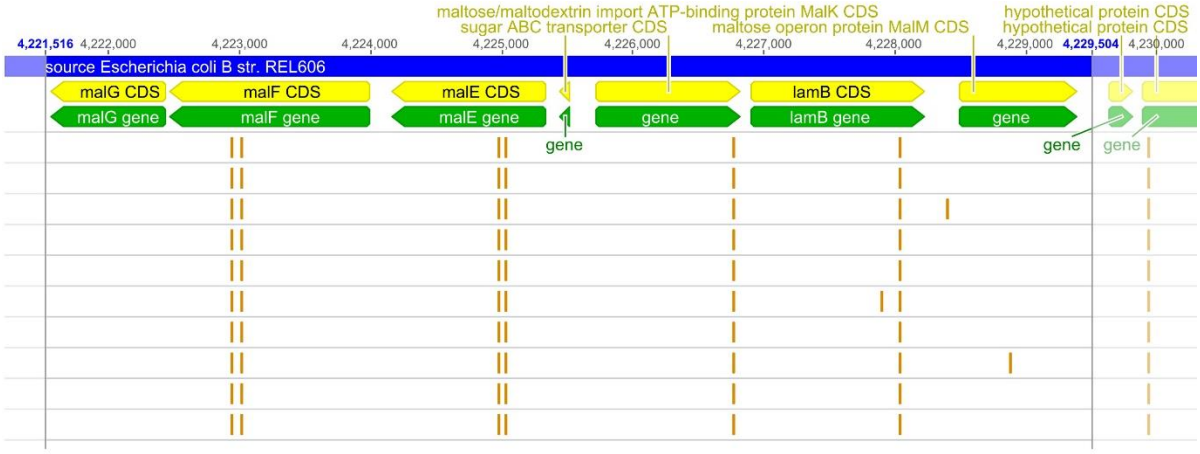

Figure 3.19. Depiction of SNPs in the *mal* genes identified in the genome of BN50 and also in the relief lines. Shown here is the maltose regulon (green bars), CDS regions (yellow bars) and surrounding sequences. In blue is the WT REL606 genome for which reads were mapped to. Orange dashes represent SNPs. Each white horizontal segment represents a BR line. BN50 is the top white horizontal line.

Discussion

The aim for this part of the project was to assess the phenotypic effects of Muller's ratchet on populations of *E.coli* REL606 + pGEM::*mutD5*. Few studies to date have examined how populations subjected to the ratchet respond to specific metabolic environments, and even fewer have tested what happens when populations are allowed to recover under a relief-type regime. Moreover, few studies have tracked the genomic changes that occur over such regimes, and related these changes to phenotypic changes. The aim here was to achieve exactly that. Specifically, we tested bottlenecked MA lines and relieved lines on Biolog plates containing hundreds of different carbon, nitrogen, sulphur and phosphorous sources.

Consistent with a previous study (Funchain et al., 2000), we found that repeated bottlenecking rapidly eroded the metabolic capacity of the bottlenecked populations, and this capacity did not appear to change under a relief regime. Based on the Biolog colour change assay, which measures substrate-dependent respiration, and rates-based measurements collected through time, we counted a total loss of 150 phenotypes that wild-type populations could undergo. This includes a loss of capacity to utilize about 85 different carbon sources, 35 different nitrogen sources and 30 different phosphorous and sulphur sources. We tested populations following 50 cycles of single-cell bottlenecking and for each type of Biolog plate, no purple colour formation was observed (Figure 3.2, 3.5, 3.7, 3.8 3.9, 3.10). Likewise, when

populations were allowed to evolve under a relief regime for 50 cycles we observed exactly the same pattern (Figure 3.3, 3.6, 3.7, 3.8, 3.9, 3.10).

Extensive, although less substantial, loss of phenotypic functions were also reported in Funchain et al. (2000). In this study it was observed that following 40 cycles of bottlenecking mutator *E.coli* populations on rich media, several catabolic defects were observed based on tests using carbon-based Biolog plates. For example, they reported that in 11% of lineages glycolic acid utilization was impaired and in 10% of lineages L-threonine utilization was also impaired. Additionally, they found that D-galacturonic acid metabolism was impaired in only 1% of the lines tested. Overall they report that 70% of lines experienced a defect in at least one sugar pathway. These results are less substantial than those reported in our study, which is probably due to the differences in mutation rate. For instance in Funchain et al. (2000) they introduced a defective *mutS* gene into lines to elevate mutation rates whereas this study involved the introduction of an impaired *mutD5* allele. MA lines experiencing phenotypic erosion is also reported elsewhere (Escarmís et al., 2009; Estes & Lynch, 2003; Leiby & Marx, 2014b; Uchimura et al., 2015). For example, in Leiby & Marx (2014), it was argued that metabolic erosion primarily occurs through mutation accumulation, as opposed to physiological trade-offs. They tested this hypothesis on Biolog plates and found metabolic erosion was more substantial in lines that showed elevated mutation rates compared to lines with lower mutation rates. Overall, the results presented here are consistent with previous MA studies – that is, elevated mutation rates tends to result

in the impairment of metabolic pathways if conditions favour genetic drift and minimise the efficiency of selection.

The extent to which impaired phenotypic functions are able to be recaptured in mutation accumulation lines remains poorly understood. Previous studies have typically focused on general fitness recovery as opposed to recovery of specific phenotypes (e.g. Bull et al., 2003; Burch & Chao, 1999; Estes & Lynch, 2003). In this study, we found that recapturing impaired metabolic phenotypes is unlikely in severely bottlenecked MA lines, even when populations become fitter overall. This is evident in figures 3.3, 3.6, 3.7, 3.8, 3.9 and 3.10 which shows no indication that bottleneck relief line BR50.1 can utilize any carbon, nitrogen, phosphorous or sulphur sources contained in Biolog plates PM1, PM2A, PM3B and PM4A. Overall, the widespread loss-of-function phenotypes observed in the bottlenecked lines, and the inability of the relief populations to recapture such phenotypes is consistent with several arguments in evolutionary biology. Firstly, that it is easier to lose a function than to gain one. This is exemplified here by how rapidly phenotypic functions were lost and how populations failed to recapture these phenotypes over an equivalent time period. Secondly, that elevated mutation rates are typically attenuated in natural populations to avoid significant functional impairment such as that observed here (McDonald, Hsieh, Yu, Chang, & Leu, 2012; Wielgoss et al., 2013). For instance, we initially hypothesized to observe at least one or two novel gain-of-function phenotypes as a result of elevated mutation rates that populations experienced under the bottlenecking regime. However, we found no such case. It is likely that under our

experimental regime that the deleterious effects of elevated mutation rates has outweighed any chance for a rare beneficial mutation to emerge in some functional capacity (Denamur & Matic, 2006). Fine-tuning mutation rates to avoid error catastrophe has been shown to be important for mutator populations adapting to new environments (Tanaka et al., 2003; Travis & Travis, 2002), as well as pathogens evolving rapidly in response to novel antibiotics (Bjorkholm et al., 2001; Eliopoulos & Blazquez, 2003). Further delta-bitscore analyses may allow the detection of novel gain-of-function phenotypes that are difficult to detect in growth impaired (bottleneck and relief) lineages, and this could be followed up by downstream tests of phenotype via gene replacement.

To gauge how lineages respond to different metabolic environments that have evolved via long-term culturing, though not under a bottleneck regime per se, we also tested bottleneck controls and bottleneck relief controls on Biolog plates. We observed large differences in respiration between wild-type and both control lines, however, inspection of endpoint data and kinetic data over time reveals that losses are mainly due to decreases in activity as opposed to complete loss of function. However, there are cases where loss of function activity was observed, particularly in plate PM4A in which control lines appear to show a limited capacity to utilize phosphorous and sulphur sources compared to wild-type populations (Figure 3.14, Supplementary Figure 3.4). We suspect that this general reduction in activity observed in the bottleneck and relief control lines could be due to both costs associated with elevated mutation rates as well as physiological trade-offs. As mutation rates remain high in

control lines (see chapter 2), it is likely that some mutations have impaired metabolic pathways, which is in line with other MA studies (e.g. Leiby & Marx, 2014). In terms of physiological trade-offs, we suspect that because cells are growing in rich media, some unused metabolic pathways are inevitably becoming eroded over time (Cooper & Lenski, 2000). As populations adapt to their environment, mutations will inevitably accumulate in genes that encode unused pathways, as these pathways are not under any selective pressure. As such, we suspect some decline in metabolic capacity observed in the control lines could be examples of antagonistic pleiotropy, whereby mutations beneficial in one environment are costly (or neutral) in another (Cooper & Lenski, 2000).

Intriguingly, we found that most metabolic activity was eroded between days 10 – 20 of the bottleneck regime. It appears that at day 10, a wild-type metabolic capacity remains largely intact, however, from day 20 we observed very few positive metabolic signals. For example, in plate PM1 we observed that utilization of D-mannitol and L-glutamic acid is possible while utilization of almost all other carbon sources is not (Figure 3.15, 3.16). This rapid and widespread erosion of metabolic function tends to support the argument that the general decline in function that occurs under Muller's ratchet is caused by mutations of large effect, compared to a "death by a thousand paper cuts" scenario. If the latter were true then we might expect to see a gradual decay of metabolic activity over an extended period of time. Instead, we found that significant metabolic erosion occurred in only 10 cycles of single-cell bottlenecking (i.e. between days 10 -20). Testing each day between days 10-20 using biolog plates, of

course, would provide more illumination into exactly how rapidly these functions erode, and whether such erosion occurs in parallel across different sources in different types of Biolog plates.

To explore this further, we compared genomes derived from days 10 and 20 of the bottleneck regime. Focusing on Biolog plate PM1, we looked at coding sequences in the genome of BN20 that are important for the utilization of carbon sources that are impaired at this time point. In general, we observed few mutations in these coding sequences, and for mutations that were present, their associated DBS scores were typically low. For example, no mutations were identified in genes encoding enzymes GalM, GalK, GalU, GalT and GalE that are essential in galactose metabolism (Table 3.2). Despite this, BN20 shows a reduced capacity to utilize D-galactose (Figure 3.15, 3.16, table 3.1). Moreover, BN20 is unable to utilize L-proline (Figure 3.15, 3.16, table 3.1) and although mutations were identified in *putA* and *putP* genes that are responsible for L-proline metabolism, the DBS scores associated with these mutations are 2 and 1.6 respectively, suggesting the impact of these mutations on protein function is minimal (Table 3.2). Overall, it appears that metabolic erosion is not caused by mutations of small effect accumulating in individual pathways. However, this possibility cannot be excluded, because mutations could be accumulating in surrounding regulatory or promoter regions and these could be impacting on metabolic pathways. Additionally, only a limited number of genes were assessed here. Clearly more extensive work is required to examine how mutations that accumulated

between days 10 to 20 of the bottleneck regime impact on individual metabolic pathways.

Because of this uncertainty, we decided to investigate large effect mutations in the genome of BN20, based on the largest DBS values calculated. We identified several enzymes predicted to be significantly impaired that are associated with carbohydrate metabolism and transport and energy production as well as several enzymes that are involved in cell membrane processes (Table 3.3). We suspect these could be reasonable candidates to decipher the mutational basis for the widespread metabolic erosion observed during days 10 to 20. For example, a frameshift mutation in a gene responsible for alpha-xylosidase has the largest associated DBS value (1224.2). The function of this enzyme is to catalyse the transfer of an alpha-xylosyl residue from alpha-xyloside to xylose, glucose, mannose, fructose, maltose and other carbon sources (Okuyama, Mori, Chiba, & Kimura, 2004). While it is not clear whether an impaired alpha-xylosidase eliminated the capacity for the bottlenecked populations to utilize the carbon sources tested, one study does report that the *yicJI* operon that encodes an alpha-xylosidase is important for overall fitness under different carbon-based conditions (Répérant et al., 2011). It is worth mentioning that this mutation reverted in line BR50.1 (see chapter 2), however, as it did not revert in other BR lines, it is difficult to determine how important this mutation is. Although these severely impaired enzymes that are listed in table 3.3 are reasonable candidates for determining the mutational basis for the widespread metabolic erosion observed between days 10 to 20, determining the causes by genomic analyses alone is limited.

In order to investigate this more rigorously, gene knock-out or knock-in experiments coupled with fitness experiments would be required. Moreover, as DBS analyses only considers protein-coding sequences, we leave ourselves vulnerable here to disregarding the impact that mutations in non-coding regions have on metabolism. Testing each time point via further biolog assays between days 10 to 20 coupled with genomic analyses might be a good approach to narrow-down the mutational basis for the widespread metabolic erosion that occurred over this time period.

As mentioned previously, it is not commonplace to find studies that have examined the phenotypic changes that occur to MA lines that have subsequently evolved under a relief regime. Perhaps the most relevant study is by Estes & Lynch (2003). This group propagated large population sizes of MA lines of *Caenorhabditis elegans* that had acquired several morphological defects as well as extreme body sizes. They found that over time these defects reverted to wild-type morphologies. Additionally, they observed that one MA line that acquired an uncoordinated (Unc) phenotype as well as a high incidence of males (Him) lost these abnormalities following 10 generations of fitness recovery. In our study, we found no such reversion of phenotypes, even after 50 cycles of bottleneck relief. However, when we examined the genome of bottleneck day 50 and the relief lineages, this is not all that surprising. We found numerous functionally-severe mutations in genes encoding enzymes that are essential for various aspects of metabolism (Figure 3.17, Figure 2.12 chapter 2). For example, we looked at the genome of BN50 and found that the gene encoding PutA, a multifunctional protein that functions in proline catabolism, as well as PutP, a proline

symporter, carry several mutations each. The DBS values for these mutations are high, with mutations in the *PutA* gene responsible for a significant DBS value (7.4) (Table 3.4). All these mutations were retained in the relief lines. Moreover, we found additional mutations in *putA* genes for all the relief lines (Figure 3.18). The DBS value associated with these mutations is 1616.2 due to predicted truncations. Additionally, upon inspection of the relief genomes, we found that mutations present in BN50 that are associated with metabolic function in most cases have not reverted (Figure 2.12, chapter 2). Furthermore, we found in some cases (e.g. the PutA example above), BR lines continue to accumulate functionally severe mutations in these metabolic pathways (Figure 3.18, Figure 2.12 chapter 2). As such, it is not surprising that we observed no evidence that BR50.1 recaptured any phenotype impaired in the bottleneck regime. Therefore, I suspect that for some phenotypes, the effect of Muller's ratchet has caused these evolving populations to cross the point of no return. Although further work is required, I will nevertheless put a stake in the ground and argue that some of these impaired metabolic functions are irreversibly impaired, and therefore unlikely to return to a functional wild-type state. I argue this for several reasons. Firstly, relief lines are continuing to accumulate functionally severe mutations at an elevated rate, and in genes associated with energy production and carbohydrate transport/metabolism (see figure 2.12 chapter 2). Secondly, the abundance of mutations in genes associated with these eroded pathways, and the rare occurrence of back mutations that would be necessary to restore functional activity in these pathways means that recapturing previously accessible phenotypes is unlikely.

At this point, the reader is probably wondering about compensatory mutations that could potentially mitigate these impaired phenotypes. However, when considering physiological trade-offs (Cooper & Lenski, 2000), I suspect that natural selection would not necessarily favour recapturing the functional capacity of these impaired phenotypes if relief lines were allowed to evolve even further in the same, rich media - why would relief populations evolving in rich LB media be under strong selection pressures to be able to utilize many of the highly specific biolog substrates tested? If some phenotypes are recaptured, and assuming back mutations are rare, I suspect that the overall trend would see phenotypes re-emerge in slow, 'hill-climbing' fashion analogous to Fisher's geometric model of adaptation (Fisher, 1930), and not in proportion to the massive parallel losses of phenotypes that occurred between bottleneck days 10 -20. Nevertheless, such speculation requires further testing and therefore it would be worth evolving relief lines further (beyond day 50) and testing multiple lines on Biolog plates.

Supplementary Material

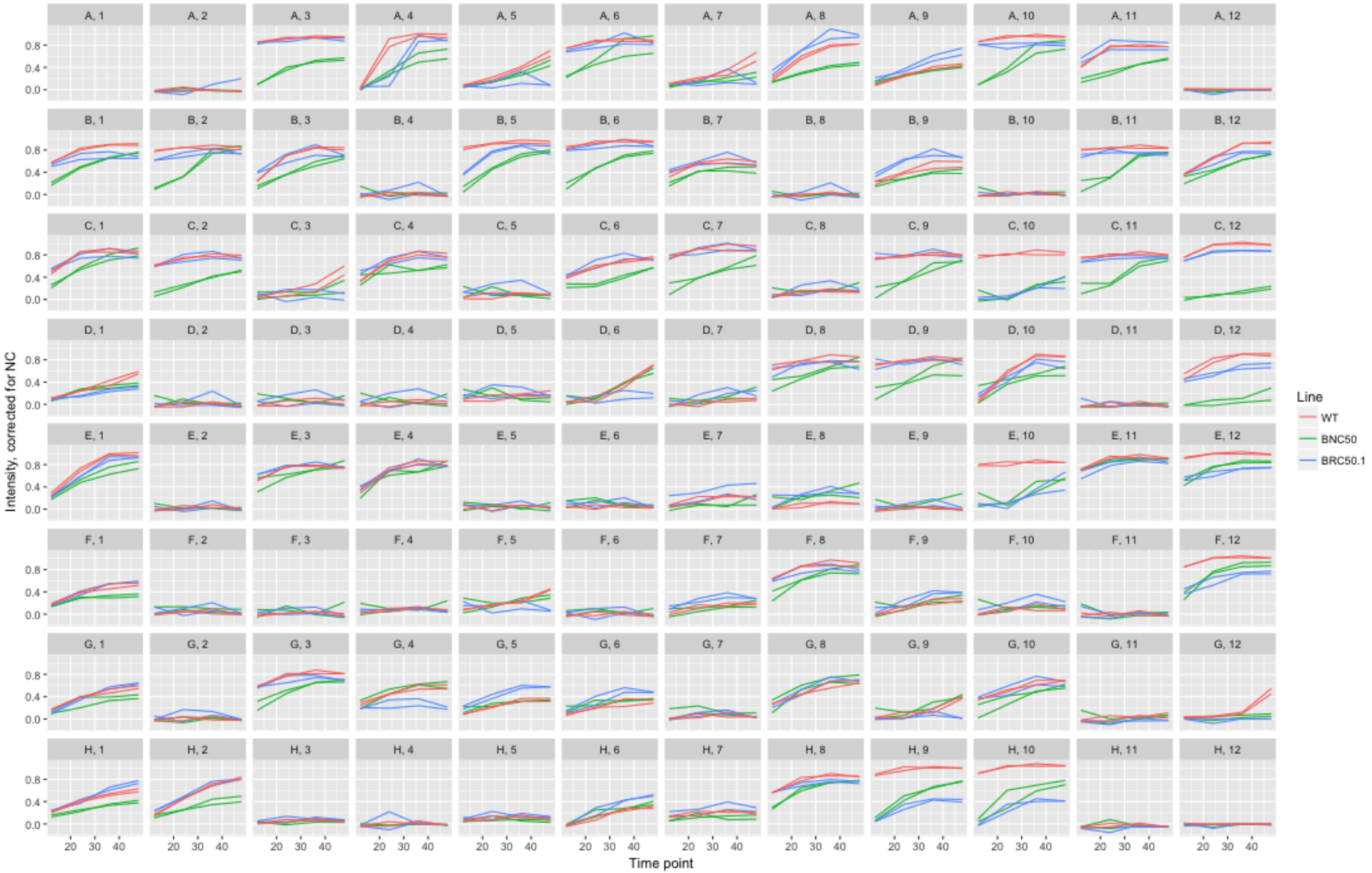

Supplementary Figure 3.1. Kinetic data for WT, BNC50 and BRC50.1 tested on Biolog plate PM1. Active respiration is assessed by taking OD_{595} measurements every 12 hours. Measurements were taken up to 60 hours. Each well is corrected by subtracting absorbance values from the negative control. Data is from duplicate trials

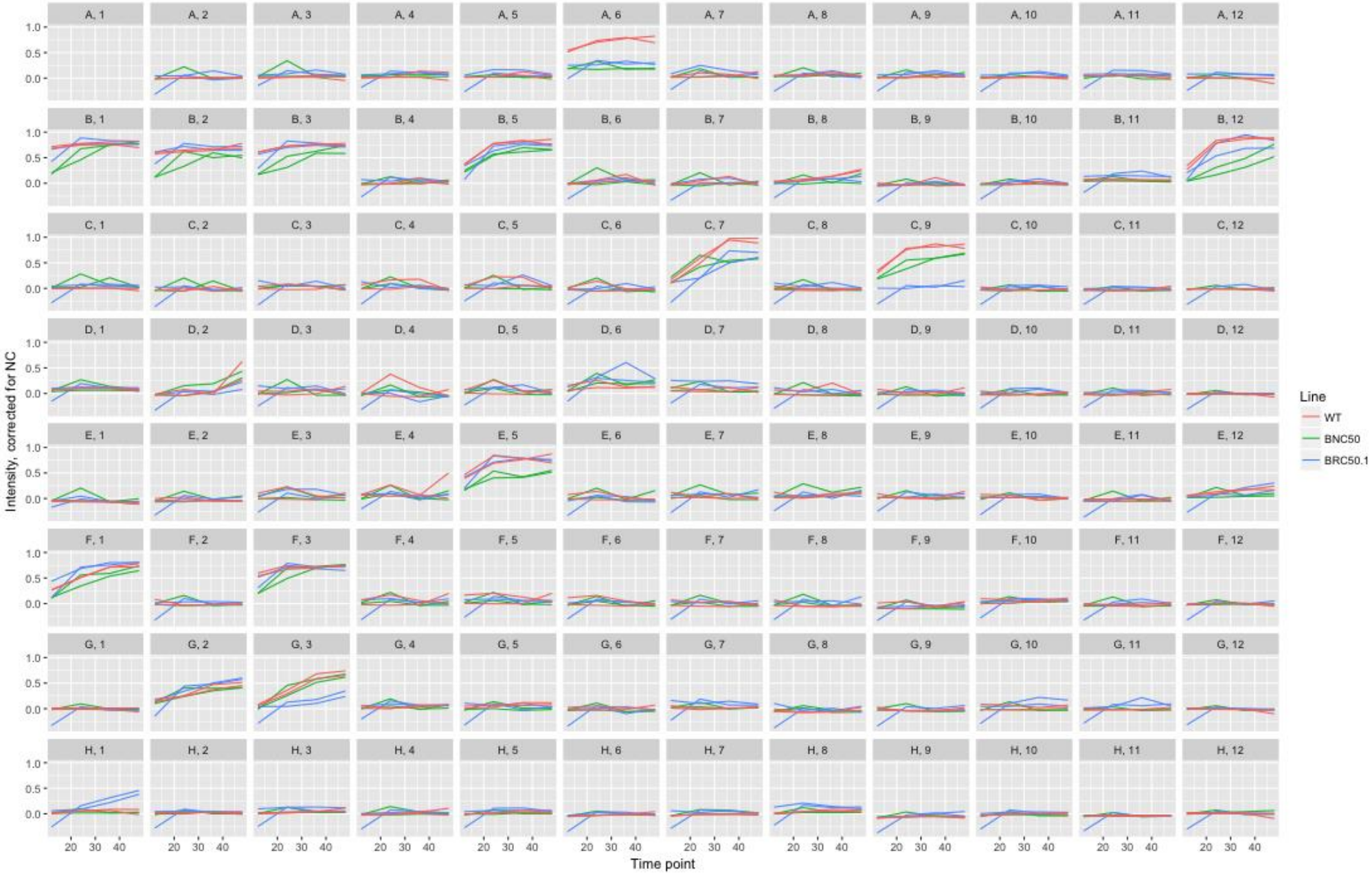

Supplementary Figure 3.2. Kinetic data for WT, BNC50 and BRC50.1 tested on Biolog plate PM2A. Active respiration is assessed by taking OD_{595} measurements every 12 hours. Measurements were taken up to 60 hours. Each well is corrected by subtracting absorbance values from the negative control. Data is from duplicate trials.

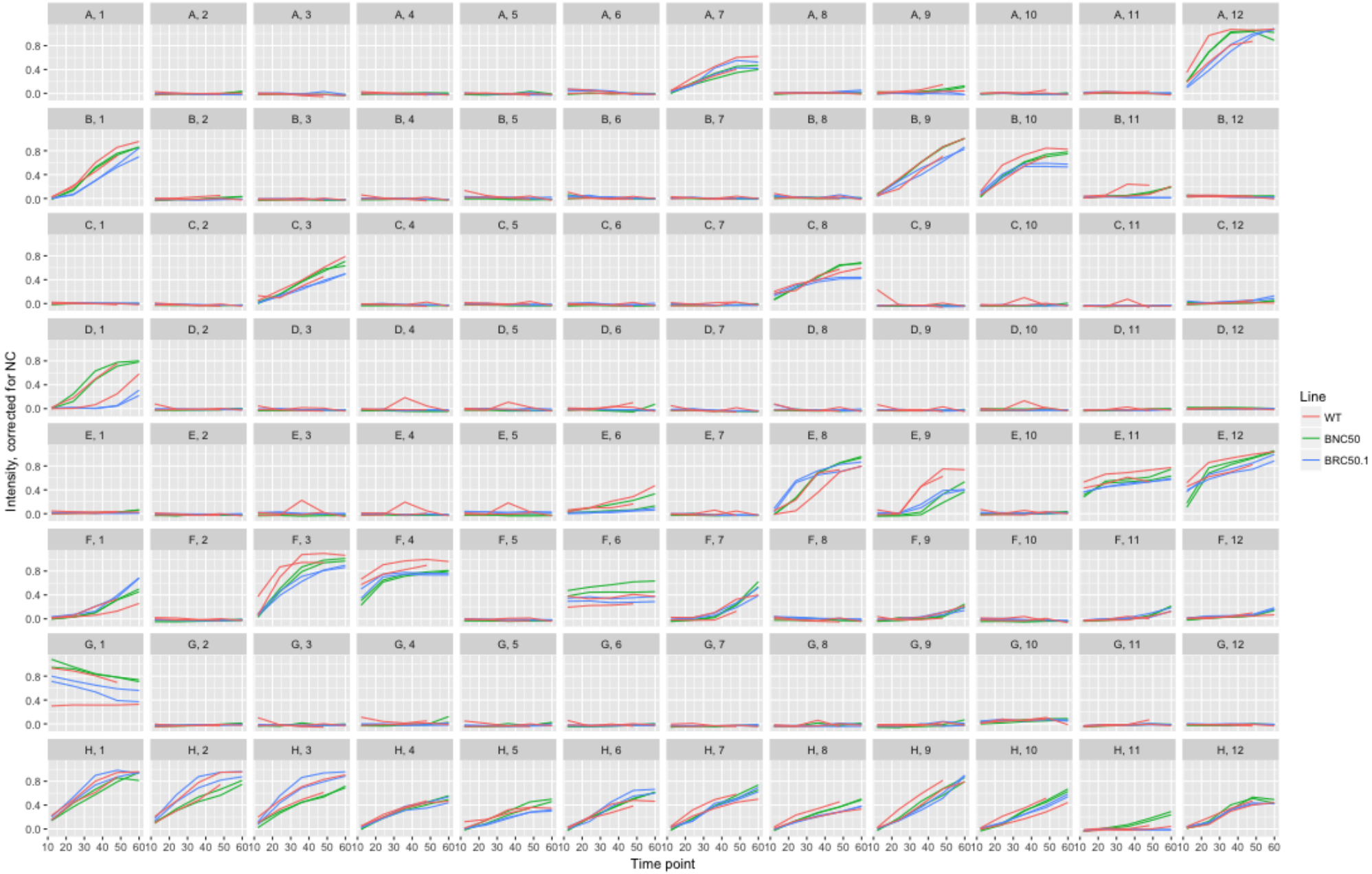

Supplementary Figure 3.3. Kinetic data for WT, BNC50 and BRC50.1 tested on Biolog plate PM3B. Active respiration is assessed by taking OD_{595} measurements every 12 hours. Measurements were taken up to 60 hours. Each well is corrected by subtracting absorbance values from the negative control. Data is from duplicate trials.

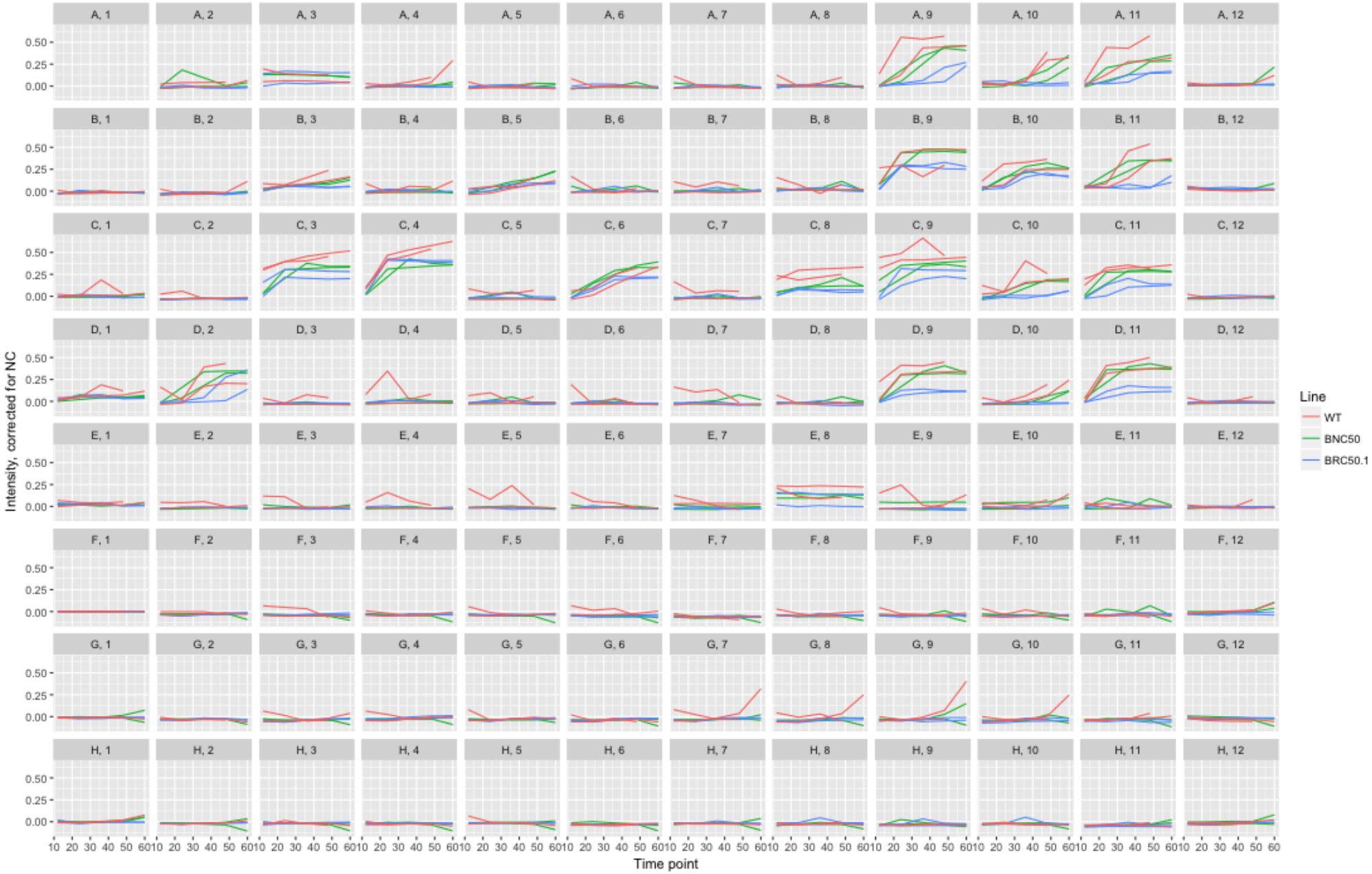

Supplementary Figure 3.4. Kinetic data for WT, BNC50 and BRC50.1 tested on Biolog plate PM4A. Active respiration is assessed by taking OD_{595} measurements every 12 hours. Measurements were taken up to 60 hours. Each well is corrected by subtracting absorbance values from the negative control. Data is from duplicate trials.

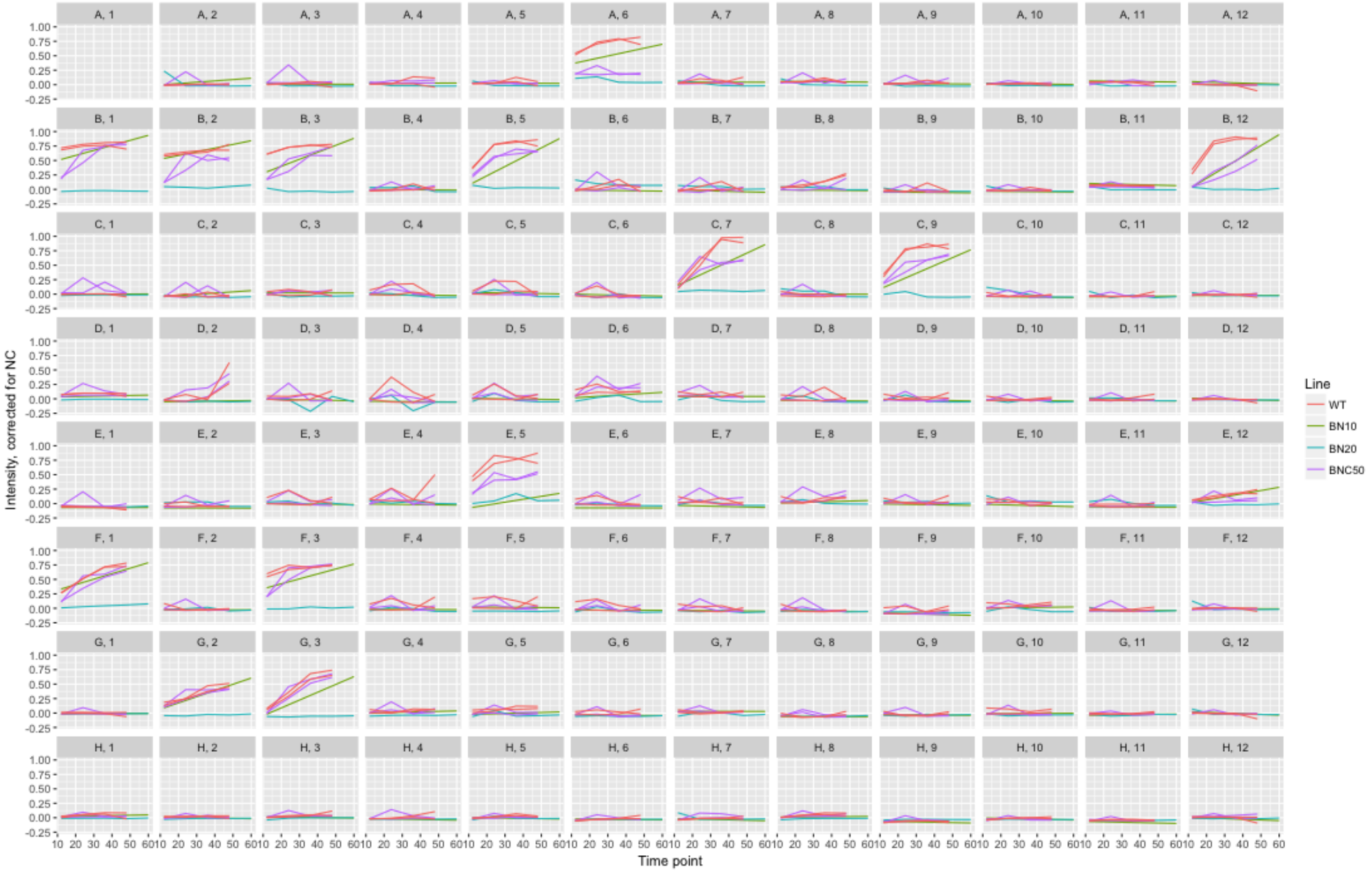

Supplementary Figure 3.5. Kinetic data for WT, BN10, BN20 and BNC50 on plate PM2A. Active respiration is assessed by taking OD_{595} measurements every 12 hours. Measurements were taken up to 60 hours for slow-growers BN10 and BN20 and 48 hours for WT and BNC50. Each well is corrected by subtracting absorbance values from the negative control. Data is from duplicate trials for WT and BNC50. BN10 and BN20 were tested once only.

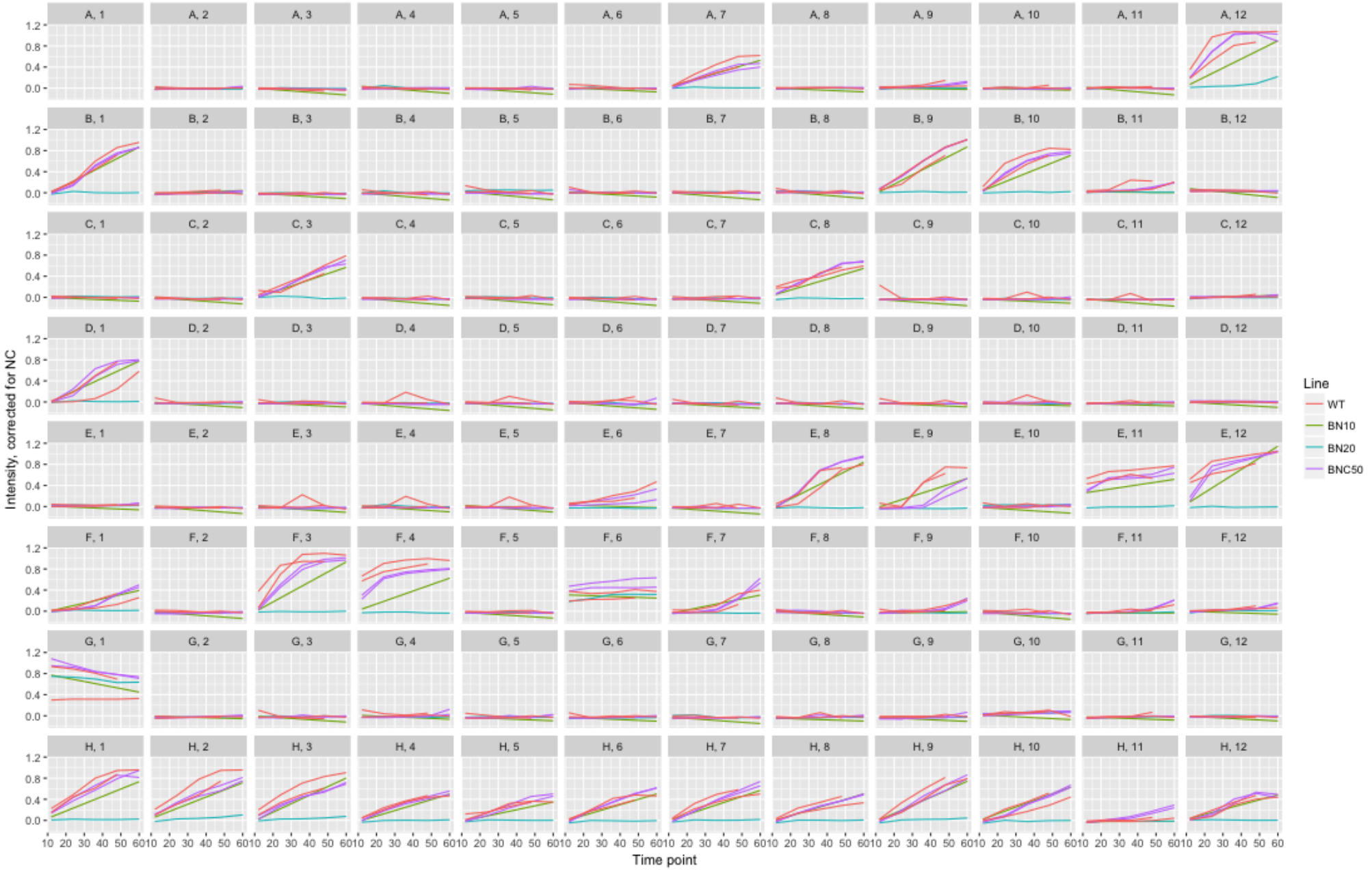

Supplementary Figure 3.6. Kinetic data for WT, BN10, BN20 and BNC50 on plate PM3B. Active respiration is assessed by taking OD_{595} measurements every 12 hours. Measurements were taken up to 60 hours. Each well is corrected by subtracting absorbance values from the negative control. Data is from duplicate trials for WT and BNC50. BN10 and BN20 were tested once only.

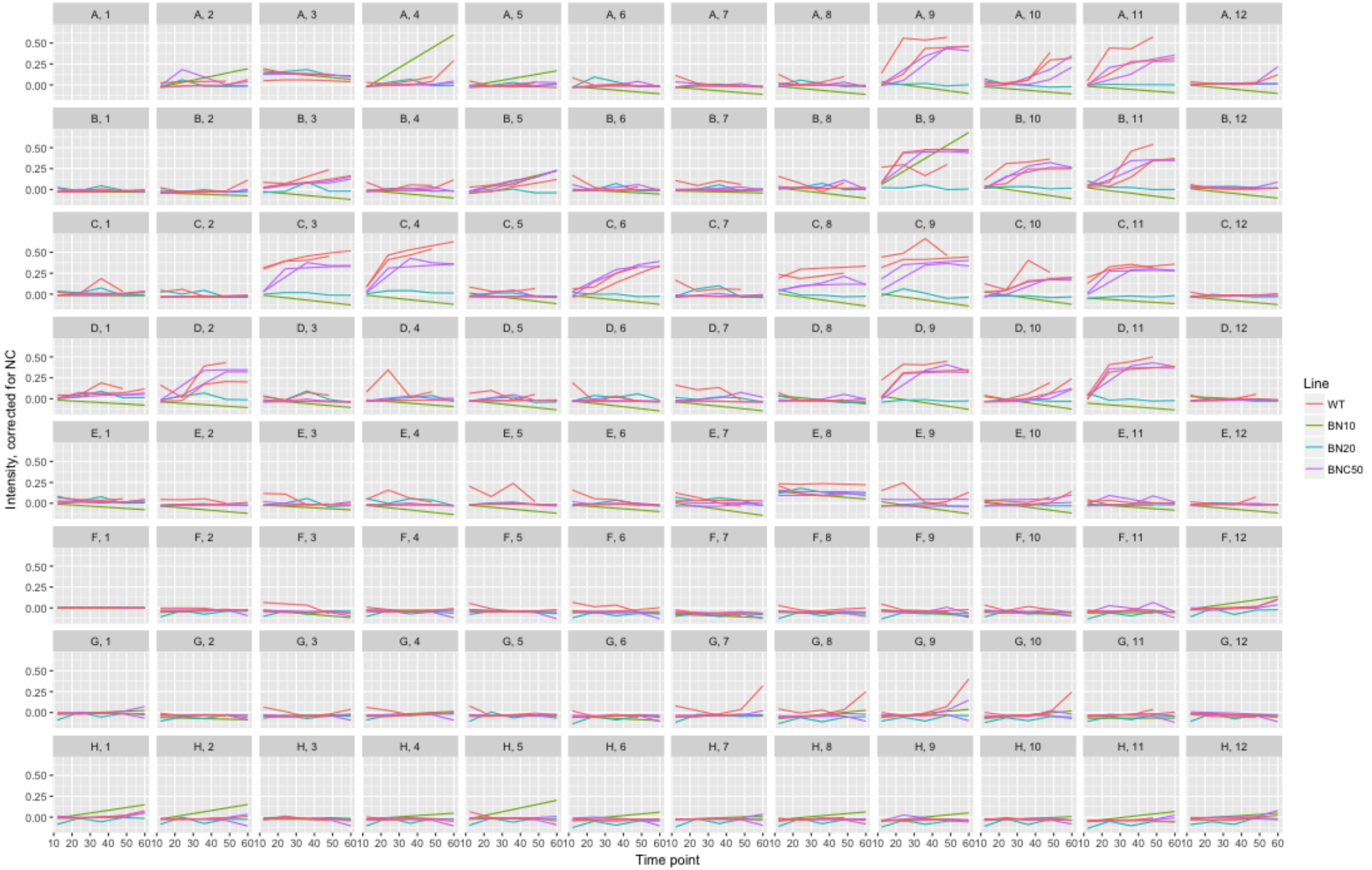

Supplementary Figure 3.7. Kinetic data for WT, BN10, BN20 and BNC50 on plate PM4A. Respiration is assessed by taking OD_{595} measurements every 12 hours. Measurements were taken up to 60 hours. Each well is corrected by subtracting absorbance values from the negative control. Data is from duplicate trials for WT and BNC50. BN10 and BN20 were tested once only.

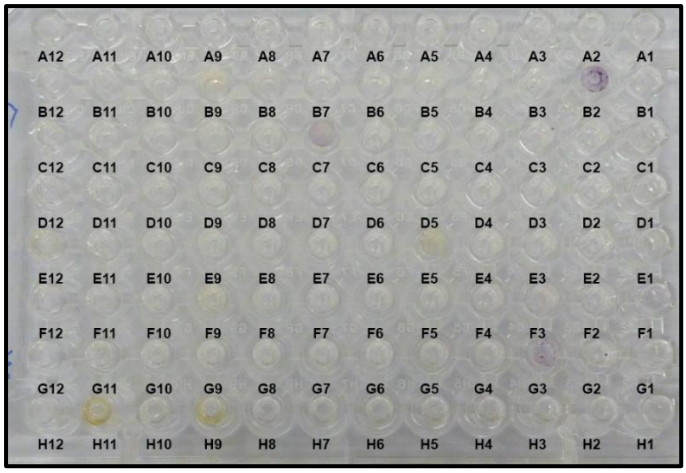

Supplementary Figure 3.8. BN20 tested on Biolog plate PM2A.

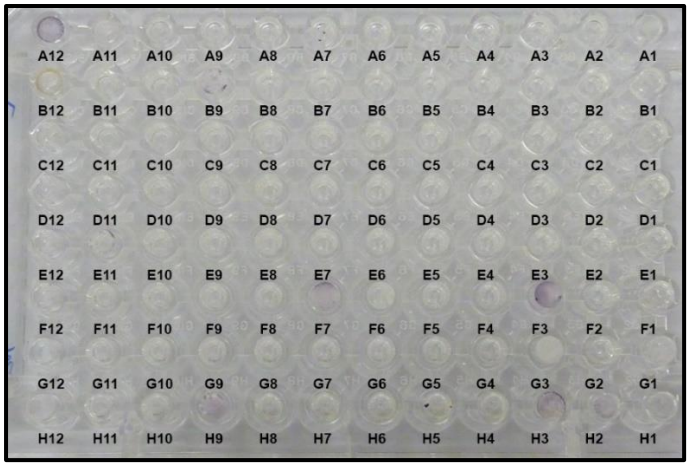

Supplementary Figure 3.9. BN20 tested on Biolog plate PM3B.

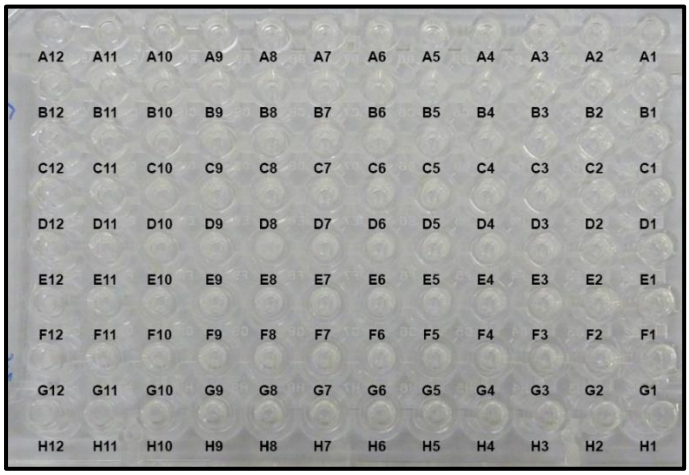

Supplementary Figure 3.10. BN20 tested on Biolog plate PM4A.

Appendix

PM1 Carbon Sources

	1	2	3	4	5	6	7	8	9	10	11	12
A	Negative Control	L-Arabinose	N-Acetyl-D-Glucosamine	D-Saccharic Acid	Succinic Acid	D-Galactose	L-Aspartic Acid	L-Proline	D-Alanine	D-Trehalose	D-Mannose	Dulcitol
B	D-Serine	D-Sorbitol	Glycerol	L-Fucose	D-Glucuronic Acid	D-Gluconic Acid	D,L-α-GlycerolPhosphate	D-Xylose	L-Lactic Acid	Formic Acid	D-Mannitol	L-Glutamic Acid
c	D-Glucose-6-Phosphate	D-Galactonic Acid-y-Lactone	D,L-Malic Acid	D-Ribose	Tween 20	L-Rhamnose	D-Fructose	Acetic Acid	α-D-Glucose	Maltose	D-Melibiose	Thymidine
d	L-Asparagine	D-Aspartic Acid	D-Glucosaminic Acid	1,2-Propanediol	Tween 40	α-Keto-Glutaric Acid	α-Keto-Butyric Acid	α-Methyl-D-Galactoside	α-D-Lactose	Lactulose	Sucrose	Uridine
e	L-Glutamine	m-Tartaric Acid	D-Glucose-1-Phosphate	D-Fructose-6-Phosphate	Tween 80	α-Hydroxy Glutaric Acid-y-Lactone	α-Hydroxy Butyric Acid	β-Methyl-D-Glucoside	Adonitol	Maltotriose	2-Deoxy Adenosine	Adenosine
f	Glycyl-L-Aspartic Acid	Citric Acid	m-Inositol	D-Threonine	Fumaric Acid	Bromo Succinic Acid	Propionic Acid	Mucic Acid	Glycolic Acid	Glyoxylic Acid	D-Cellobiose	Inosine
g	Glycyl-LGlutamic Acid	Tricarballylic Acid	L-Serine	L-Threonine	L-Alanine	L-Alanyl-Glycine	Acetoacetic Acid	N-Acetyl-β-D-Mannosamine	Mono Methyl Succinate	Methyl Pyruvate	D-Malic Acid	L-Malic Acid
h	Glycyl-L-Proline	p-Hydroxy Phenyl Acetic Acid	m-Hydroxy Phenyl Acetic Acid	Tyramine	D-Psicose	L-Lyxose	Glucuronamide	Pyruvic Acid	L-Galactonic Acid-y-Lactone	D-Galacturonic Acid	Phenylethylamine	2-Aminoethanol

PM2A Carbon Sources

	1	2	3	4	5	6	7	8	9	10	11	12
A	Negative Control	Chondroitin Sulfate C	α-Cyclodextrin	β-Cyclodextrin	y-Cyclodextrin	Dextrin	Gelatin	Glycogen	Inulin	Laminarin	Mannan	Pectin
B	N-Acetyl-DGalactosamine	N-AcetylNeuraminic Acid	β-D-Allose	Amygdalin	D-Arabinose	D-Arabitol	L-Arabitol	Arbutin	2-Deoxy-D-Ribose	i-Erythritol	D-Fucose	3-0-β-D-Galactopyranosyl-D-Arabinose
c	Gentiobiose	L-Glucose	Lactitol	D-Melezitose	Maltitol	a-Methyl-DGlucoside	β-Methyl-D-Galactoside	3-Methyl Glucose	β-Methyl-D-Glucuronic Acid	α-Methyl-D-Mannoside	β-Methyl-D-Xyloside	Palatinose
d	D-Raffinose	Salicin	Sedoheptulosan	L-Sorbose	Stachyose	D-Tagatose	Turanose	Xylitol	N-Acetyl-DGlucosaminitol	y-Amino Butyric Acid	Amino Valeric Acid	Butyric Acid
e	Capric Acid	Caproic Acid	Citraconic Acid	Citramalic Acid	D-Glucosamine	2-Hydroxy Benzoic Acid	4-Hydroxy Benzoic Acid	β-Hydroxy Butyric Acid	y-Hydroxy Butyric Acid	a-Keto-Valeric Acid	Itaconic Acid	5-Keto-D-Gluconic Acid
f	D-Lactic Acid Methyl Ester	Malonic Acid	Melibionic Acid	Oxalic Acid	Oxalomalic Acid	Quinic Acid	D-Ribono-1,4-Lactone	Sebacic Acid	Sorbic Acid	Succinamic Acid	D-Tartaric Acid	L-Tartaric Acid
g	Acetamide	L-Alaninamide	N-Acetyl-LGlutamic Acid	L-Arginine	Glycine	L-Histidine	L-Homoserine	Hydroxy-LProline	L-Isoleucine	L-Leucine	L-Lysine	L-Methionine
h	L-Ornithine	L-Phenylalanine	L-Pyroglutamic Acid	L-Valine	D,L-Carnitine	Sec-Butylamine	D.L-Octopamine	Putrescine	Dihydroxy Acetone	2,3-Butanediol	2,3-Butanone	3-Hydroxy 2-Butanone

PM3B Nitrogen Sources

	1	2	3	4	5	6	7	8	9	10	11	12
A	Negative Control	Ammonia	Nitrite	Nitrate	Urea	Biuret	L-Alanine	L-Arginine	L-Asparagine	L-Aspartic Acid	L-Cysteine	L-Glutamic Acid
B	L-Glutamine	Glycine	L-Histidine	L-Isoleucine	L-Leucine	L-Lysine	L-Methionine	L-Phenylalanine	L-Proline	L-Serine	L-Threonine	L-Tryptophan
c	L-Tyrosine	L-Valine	D-Alanine	D-Asparagine	D-Aspartic Acid	D-Glutamic Acid	D-Lysine	D-Serine	D-Valine	L-Citrulline	L-Homoserine	L-Ornithine
d	N-Acetyl-LGlutamic Acid	N-Phthaloyl-LGlutamic Acid	L-Pyroglutamic Acid	Hydroxylamine	Methylamine	N-Amylamine	N-Butylamine	Ethylamine	Ethanolamine	Ethylenediamine	Putrescine	Agmatine
e	Histamine	β-Phenylethylamine	Tyramine	Acetamide	Formamide	Glucuronamide	D,L-Lactamide	D-Glucosamine	D-Galactosamine	D-Mannosamine	N-Acetyl-DGlucosamine	N-Acetyl-DGalactosamine
f	N-Acetyl-DMannosamine	Adenine	Adenosine	Cytidine	Cytosine	Guanine	Guanosine	Thymine	Thymidine	Uracil	Uridine	Inosine
g	Xanthine	Xanthosine	Uric Acid	Alloxan	Allantoin	Parabanic Acid	D,L-α-Amino-N-Butyric Acid	γ-Amino-N-Butyric Acid	Amino-N-Caproic Acid	D,L-α-Amino-Caprylic Acid	Amino-N-Valeric Acid	α-Amino-N-Valeric Acid
h	Ala-Asp	Ala-Gln	Ala-Glu	Ala-Gly	Ala-His	Ala-Leu	Ala-Thr	Gly-Asn	Gly-Gln	Gly-Glu	Gly-Met	Met-Ala

PM4A Phosphorous and Sulphur Sources

	1	2	3	4	5	6	7	8	9	10	11	12
A	Negative Control	Phosphate	Pyrophosphate	Trimetaphosphate	Tripolyphosphate	Triethyl Phosphate	Hypophosphite	Adenosine-2′-monophosphate	Adenosine-3′-monophosphate	Adenosine-5′-monophosphate	Adenosine-2′,3′-cyclic monophosphate	Adenosine-3′,5′-cyclic monophosphate
B	Thiophosphate	Dithiophosphate	D,L-α-Glycerol Phosphate	β-Glycerol Phosphate	Carbamyl Phosphate	D-2-PhosphoGlyceric Acid	D-3-PhosphoGlyceric Acid	Guanosine-2′-monophosphat	Guanosine-3′-monophosphate	Guanosine-5′-monophosphate	Guanosine-2′,3′-cyclic monophosphate	Guanosine-3′,5′-cyclic monophosphate
c	Phosphoenol Pyruvate	PhosphoGlycolic Acid	D-Glucose-1-Phosphate	D-Glucose-6-Phosphate	2-Deoxy-DGlucose 6-Phosphate	D-Glucosamine-6-Phosphate	6-PhosphoGluconic Acid	Cytidine-2′-monophosphate	Cytidine-3′-monophosphate	Cytidine-5′-monophosphate	Cytidine-2′,3′-cyclic monophosphate	Cytidine-3′,5′-cyclic monophosphate
d	D-Mannose-1-Phosphate	D-Mannose-6-Phosphate	Cysteamine-SPhosphate	Phospho-LArginine	O-Phospho-DSerine	O-Phospho-LSerine	O-Phospho-LThreonine	Uridine-2′-monophosphate	Uridine-3′-monophosphate	Uridine-5′-monophosphate	Uridine-2′,3′-cyclic monophosphate	Uridine-3′,5′-cyclic monophosphate
e	O-Phospho-DTyrosine	O-Phospho-LTyrosine	Phosphocreatine	Phosphoryl Choline	O-PhosphorylEthanolamine	Phosphono Acetic Acid	2-Aminoethyl Phosphonic Acid	Methylene Diphosphonic Acid	Thymidine-3′-monophosphate	Thymidine-5′-monophosphate	Inositol Hexaphosphate	Thymidine 3′,5′-cyclic monophosphate
f	Negative Control	Sulfate	Thiosulfate	Tetrathionate	Thiophosphate	Dithiophosphate	L-Cysteine	D-Cysteine	L-CysteinylGlycine	L-Cysteic Acid	Cysteamine	L-Cysteine Sulfinic Acid
g	N-Acetyl-LCysteine	S-Methyl-LCysteine	Cystathionine	Lanthionine	Glutathione	D,L-Ethionine	L-Methionine	D-Methionine	Glycyl-LMethionine	N-Acetyl-D,LMethionine	L-Methionine Sulfoxide	L-Methionine Sulfone
h	L-Djenkolic Acid	Thiourea	1-Thio-β-DGlucose	D,L-Lipoamide	Taurocholic Acid	Taurine	Hypotaurine	p-Amino Benzene Sulfonic Acid	Butane Sulfonic Acid	2-Hydroxyethane Sulfonic Acid	Methane Sulfonic Acid	Tetramethylene Sulfone

Chapter 4

Conclusions, Limitations, and Future Directions

Conclusions

We tracked the genomic and phenotypic changes to populations of *E.coli* that have evolved under both a bottleneck regime and bottleneck relief regime. A previous member of our lab group, Alicia Lai, reported fitness decline, elevated mutation rates as well as impaired protein function that worsened over the course of 50 cycles of single-cell bottlenecking on rich media (Lai, 2017). In turn, this system resembled what is predicted to occur under Muller's ratchet. As reported in chapter 2, I found that evolving fitness-impaired lineages further via a bottleneck relief regime provided an escape route from the continual decline in function and fitness that is expected under the ratchet. I found that while fitness clearly improved, as measured by growth rates, protein function appeared to worsen, at least according the delta-bitscore analyses we performed. However, we came to the conclusion that the pathway to protein and fitness restoration may lie in untapped territory at the genomic level, and not strictly in the direction of the ancestor per se. This gives the false impression that protein function is not improving when in it fact it probably is. We argued that mutations that have rarely occurred in the history of the sequences that went into the profile hidden

markov models are responsible for fitness improvements. We argue this for several reasons. Firstly, because the DBS method calculates the functional severity of mutations based on sequence conservation. As there are many ways in which a single mutation may be compensated for, it is likely that the abundance of mutations that occurred in populations throughout the bottleneck regime has opened doorways to novel genomic landscapes that selection would normally restrict. Deleterious mutations were not strongly selected against in the bottleneck period and their continual accumulation was later mitigated via the emergence of compensatory mutations in the subsequent relief regime, many of which have probably rarely occurred before - at least in the context of the gamma-proteobacterial sequences that went into the profile HMM. This echoes arguments that propose the importance of compensatory evolution in facilitating aspects of biological complexity; for example, the emergence of antibiotic resistance in some cases that, without some form of compensatory suppression to minimise deleterious side-effects, can result in fitness costs (Maisnier-Patin & Andersson, 2004; Zuckerkandl, 1997; Zuckerkandl, 2001).

In addition to the accumulation of compensatory mutations that may be restoring protein function and fitness, we argued that because mutation rates remain high in the relief lines, some protein encoding sequences have probably accumulated slightly deleterious mutations to some degree throughout the relief regime. Additionally, we suspect that some compensatory mutations themselves may have fitness costs in a wild-type background. These conclusions are not uncommon in evolutionary biology (Denamur & Matic, 2006; Poon & Chao, 2005; Szamecz et al., 2014) . In our case, we

argue that these explain at least some of the seemingly paradoxical figure presented in chapter 2 (Figure 2.12) that appears to show no improvement in protein function in the relief lines under the assumption that the principle of the delta-bitscore metric is to assess the functional severity of mutations.

Our next aim was to assess how populations respond to different metabolic environments throughout the course of the bottleneck regime and also at the end of the relief regime. For all phenotypes that were observed in wild-type lines, we found complete erosion of these phenotypes throughout the bottleneck regime, none of which were recaptured in the relief lines. Additionally, we found that these losses were rapid, with most occurring within 20 cycles of bottlenecking. These observations reflect the consequences of elevated mutation rates and the general dilemma that organisms experience – that is, balancing adequate mutation rates to facilitate adaptation with fine-tuned repair systems to prevent an over-accumulation of deleterious mutations (Denamur & Matic, 2006) . In line with other studies, we found that MA can drive metabolic erosion (Funchain et al., 2000.; Leiby & Marx, 2014). However, as few studies have examined how recovering populations respond to different metabolic environments, we present a novel result here showing that extreme MA can cause long-term losses in overall metabolic capacity even as lineages become fitter. We determined this by looking at how relief lines respond to the various environments in each Biolog plate tested. Visual inspection of plates and kinetic data shows no evidence for active respiration in any of the 379 environments tested.

Genomic analyses also provided intriguing insight. For instance, we found an accumulation of functionally-severe mutations in bottleneck day 50 and relief genomes in sequences associated with metabolism (Figure 3.17 and 2.12, respectively). Closer inspection of some of these genes revealed mutations were in genes that are essential for the utilization of some of the Biolog sources tested. In addition, some of these mutations did not appear to revert in the relief lines and even more mutations in some of these genes had accumulated throughout the relief regime. Therefore, I argue that unless compensatory mutations allow these impaired phenotypes to be recaptured, I suspect some are irreversibly impaired. Moreover, assuming relief lines were evolved even further (beyond 50 cycles) under the same constant conditions, I doubt there would be strong selective pressures to recapture some of these impaired phenotypes when considering antagonistic pleiotropy and the idea that deleterious mutations in unused genes can even confer a selective advantage under some circumstances (Cooper & Lenski, 2000; Elena & Lenski, 2003).

Overall, the results presented here suggest that the genomic and phenotypic landscape for lineages escaping the deleterious effects of Muller's ratchet is novel compared to that of ancestral lineages, and might be quite complex, in fact. Additionally, the molecular mechanisms that sent populations into fitness decline are not proportional to the molecular mechanisms that allowed populations to escape the ratchet.

Project Overview

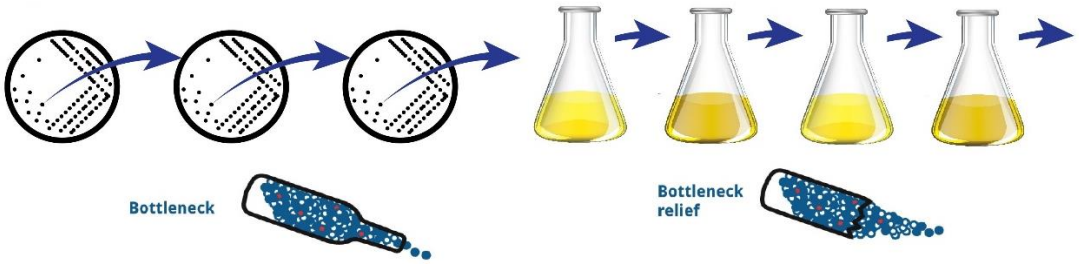

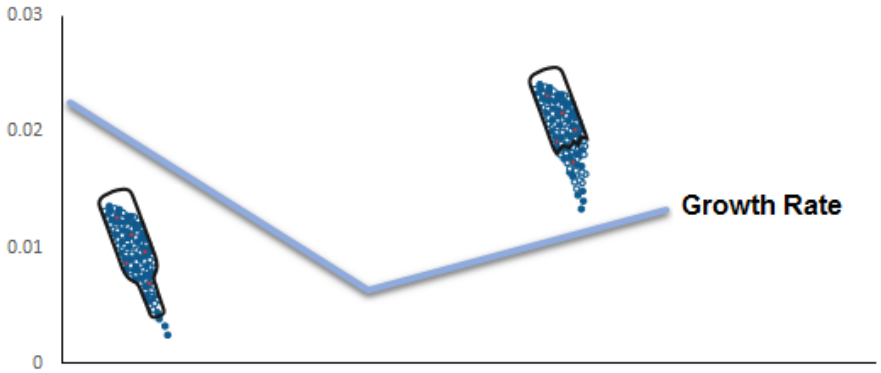

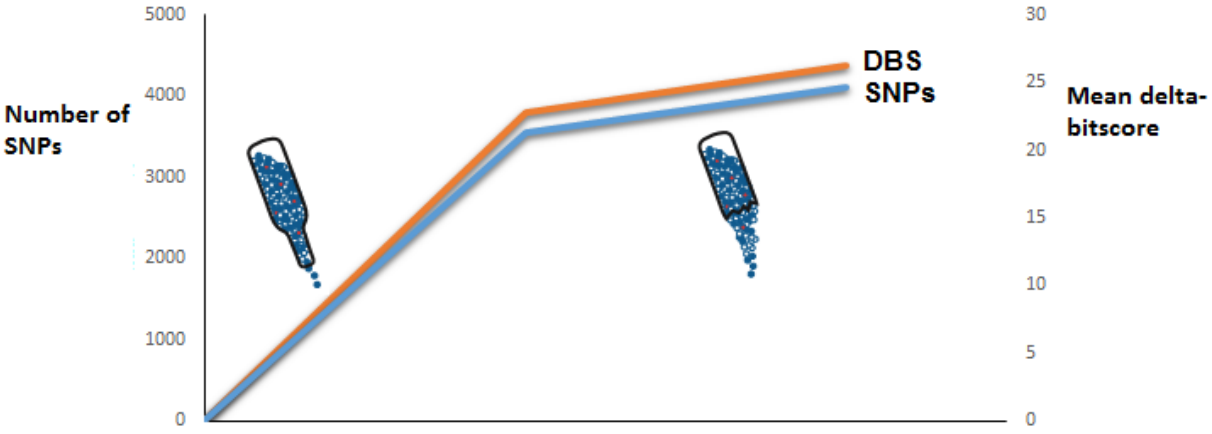

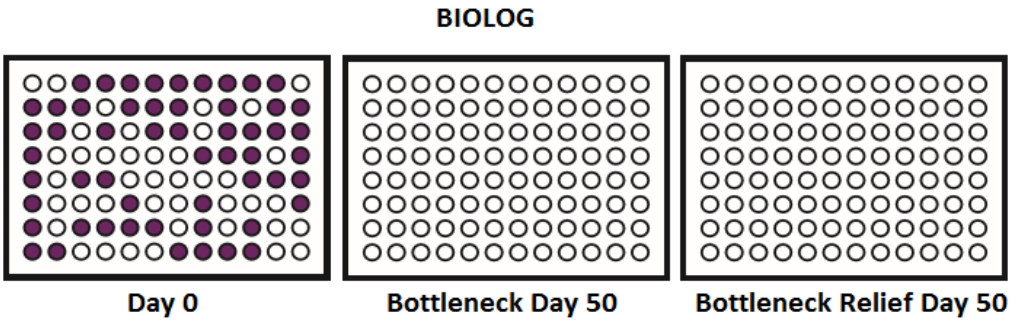

Limitations

Chapter 2

Throughout chapter 2, I argued that novel compensatory mutations probably account for fitness recovery observed in the relief lineages. However, I provided very few examples showing how compensatory mutations may be interacting with, and reducing the effects of, other mutations that have deleterious effects. Nevertheless, based on DBS analyses, I am confident that a substantial proportion of fitness recovery is accounted for via compensatory mutations. If reversion mutations were common then figure 2.12 would show DBS values distributed mainly below zero however we found this is not the case. Moreover, it is commonplace in the literature to find arguments that place importance on compensatory evolution for mitigating the effects of deleterious mutations compared to reversion mutations (Bull et al., 2003; Burch & Chao, 1999; Estes & Lynch, 2003; Maisnier-Patin & Andersson, 2004). Furthermore, this is argued to be particularly true for populations that have gene defects that are responsible for causing populations to be at a significant distance from a fitness peak (Szamecz et al., 2014). Overall, although I have not provided many examples of compensatory interactions under this system, I am nevertheless confident that their occurrence has accounted for important aspects of protein function improvement and fitness recovery.

I mentioned several times throughout chapter 2 that the delta-bitscore method does not capture information on sequences outside coding regions of a genome. This of course is a significant limitation because fitness restoration could be partly explained

by mutational changes outside of coding regions. Such regions are critical for many aspects of cellular function such as rRNA and tRNA genes that are essential for translation. I suspect that these essential genes would be under strong selection pressures in the relief regime if mutations were impairing their activity. As the DBS method does not consider these changes, we fail to capture the complete picture as to how fitness recovery is occurring. Nevertheless, we did find some degree of correlation between delta-bitscore and doubling time implying that mutations in protein-coding regions contribute to fitness to some degree. Additionally, delta-bitscore represents the most relevant tool for this type of study. Other approaches such as the dN/dS method are less reliable over short evolutionary timescales and fail to score indels (Kryazhimskiy et al., 2008; Wheeler et al., 2016).

Another limitation to this study is that we sequenced genomes that represent populations from day 50 of the bottleneck relief regime only. This means that we did not capture the full extent of genomic changes that occurred throughout the 50 cycle relief period. Therefore, assessing the mutational causes for fitness changes that occurred at earlier time points via genomic changes that are detected by examining day 50 genomes is somewhat limited. This is particularly of concern when interpreting changes that occurred between days 10 and 20 of the relief regime because during this time period the most significant improvements in fitness were observed. Any mutational changes that contributed to this rapid fitness improvement can only be interpreted in the day 50 genomes if such changes remained unaltered up until day 50 of the experiment.

Contamination that is possible between populations is also worth mentioning. Experiments were undertaken in two sets of 12-well culture plates in a shaking environment. Because wells are close together, there is a possibility that liquid from one well (which represents a single lineage) can transfer to another well close by (that represents a different lineage). However, our lab group has previously tested the speed limits in which plates should be shaking. We have found that agitating 2ml cultures at 160rpm does not allow liquid spill-over. Therefore, I am confident that spill-over did not occur. Finally, external sources of contamination were readily screened for using the various approaches described in the methods section of chapter 2.

Chapter 3

The Biolog results presented were based on visual inspection of plates and kinetic data. As such, the lack of statistical power to support our results, and the element of human error that comes with visual inspection is certainly a limitation to consider. Nevertheless, there are certainly benefits to these approaches. For instance some wells contain material that appears very thick at the bottom of the plates. We found that some of these wells were calculated at a high absorbance even though no colour change was identified following visual inspection - these types of occurrences can only be reported through visual inspection alone. Other factors that may contribute to false positives can also be detected through visual inspection. For example condensation may also cause optical density readings to be high even if no purple colour formation occurs. Additionally, inspection of kinetic data over time allows one to identify a reading at a particular time point that might not makes sense relative to the rest of

the time period. For example, as the purple colour formation that occurs is irreversible in wells that populations are respiring in, absorbance readings that decrease suggests background noise could be having an impact. Where absorbance values increase then decrease rapidly it could be that the readings that appeared to show an increase are actually false positive readings. Observing kinetic data allows one to tease apart change that is due to respiration as opposed to changes that are due to background noise.

There are several statistical tests that could have been performed here to improve statistical power. Some groups for example divide absorbance readings by the average well colour development (AWCD) while other groups perform principle component analyses (Garland, 1996; Hackett & Griffiths, 1997). In-house procedures are readily adopted also, or basic statistical procedures such as an ANOVA can be performed (Gryta, Frąc, & Oszust, 2014; Mackie et al., 2014; Vehkala, Shubin, Connor, Thomson, & Corander, 2015) However, our primary objective was to test for loss-of-function and gain-of-function phenotypes rather than decreases or increases in metabolic activity, per se. We argue that inspecting kinetic data and observing purple colour formation (or lack of) is a reasonably robust approach for this type of study. Additionally, as time limitations prevented us performing replicates for some lines (e.g. BN10 and BN20), statistical measures would not have been appropriate in these instances regardless. Finally, there is some debate about how robust these commonly adopted statistical tools are. For example, many argue against the reliability of the commonly used AWCD approach (e.g. Hackett & Griffiths, 1997; Sturino et al., 2010).

Future Directions

As cultures were frozen down on a daily basis, significant improvements could be made to provide more insight from this experiment. Here, I discuss some of these before offering suggestions as to how this work could be expanded even further.

Based on the limitations presented above, there are multiple ways in which this research could be improved. For example, we could better relate mutational changes to fitness changes through gene knock-out or knock-in experiments coupled with fitness assays. Such procedures would enable us to better understand the effect of single mutations on overall fitness. The delta-bitscore metric we employed only gives us clues as to the impact of mutations, and because mutations have different effects depending on the environmental context, there is no way of knowing with absolute certainty how mutations effect populations evolving in different environments. Of course, one benefit the delta-bitscore provides is a starting point as to which mutations should be candidates for knock-in/knock-out experiments. Under this experiment particularly, there were thousands of mutations to consider. What the DBS method does is aid in teasing apart mutations that are likely to have an impact versus those that are redundant.

Other ways to improve on this research would be to sequence more genomes at different time points of the relief regime. In particular, sequencing genomes for days 10 through to 20 would enable us to better understand the mutational basis that caused significant fitness increases for all relief lines during this period. At this point

we have no indication as to whether back mutation or compensatory mutations are responsible for fitness increases. Furthermore, we are unsure if mutations occurred inside or outside protein encoding genes. To facilitate this, fitness experiments could be performed on populations from day 10 through to 20. This would allow us to correlate mutational changes with fitness changes more precisely than that reported in this study. In turn, this would provide a better opportunity to pinpoint the exact causes for fitness improvements.

The Biolog experiments could be significantly improved. For example, only seven time points throughout the bottleneck and bottleneck relief regime were tested. Testing time points between days 10 – 20 of the bottleneck regime would be particularly useful because over this time period significant metabolic losses were reported (see chapter 3). To test whether these losses are due to a small number of mutations with large effect ('death by knockout') or many mutations of small effect ('death by a thousand paper cuts') we could perform Biolog screens at all time points from days 10 to 20 then follow this up with genomic analyses at these time points also. Additionally, for the relief lines, only line BR50.1 was tested. Although we found no evidence for metabolic activity in any of the Biolog wells tested, it could be that other relief lines are able to respire in some wells. Finally, we could perform more replicates and follow these up with statistical analyses to ensure results are more robust. Already mentioned are principle component analyses, AWCD analyses, or simple ANOVA tests that could bring more clarity to results. Another possibility is implementation of a recently described pipeline that adopts a three-step grouping, normalization, and

effect identification procedure (Vehkala et al., 2015). One advantage of this tool, the authors claim, is that it treats actively respiring wells and non-actively respiring wells separately while normalizing (Vehkala et al., 2015). This is important because bacteria that respire have completely different metabolisms from inactive bacteria.

Testing for the Emergence of Complex Features

Throughout this thesis I have mentioned several times that one of the aims of this experiment was to screen for rare gain-of-function phenotypes that might emerge as a by-product of elevated mutation rates that occur under Muller's ratchet. However, testing bottlenecked lines and relief lines in 379 metabolic environments revealed no novelty. Nevertheless, this does not rule out the possibility of that some type of novel gain-of-function mutation has occurred - it could be that the capacity for such a function to emerge phenotypically is hidden as a result of the bottlenecked and relief lines being growth impaired. As such, I propose that extending the bottleneck relief regime further may allow us to better assess the phenotypic capacity of these recovering populations. It could be that at the present cells are unable to utilize Biolog media in general, irrespective of what particular metabolic environment is being tested. By evolving relief lines for another 200 cycles, for instance, we might expect to see fitness improvements as well as a heightened metabolic capacity. Of course, as cells continue to adapt to a constant environment it could be that their metabolic capacity remains limited, however, it is difficult to know for sure and whatever the outcome would be an intriguing result regardless. Moreover, additional phenotypes could be tested such as phage sensitivity, antibiotic resistance, chemical sensitivity etc.

Ultimately, the long-term goal of this experiment is to test for the emergence of complex features that emerge via mutation and drift. The idea that these forces can drive biological complexity with natural selection of secondary importance is underpinned in many hypotheses, such as Constructive neutral evolution (Stoltzfus, 1999) , the new mutation theory of phenotypic evolution (Nei, 2007), coadaptional drive (Zuckerkandl, 2001) and the Zero Force evolutionary Law (McShea & Brandon, 2010). However elegant these theories may seem, few studies have experimentally tested for the emergence of complex systems that emerge via mutation and drift. MA experiments coupled with recovery experiments circumvent these issues by generating conditions that reduce natural selection then allow it to re-emerge. Our lab group previously discovered the emergence of slippage-type editing under this type of regime and found that its origins were rooted in selectively neutral processes (Lai, 2017). Here, we wondered whether novel phenotypes may emerge via processes of mutation and drift. Evolving relief lines further may help us to answer this. Assuming we were to discover a novel phenotype, we could then test the fitness costs of mutations responsible for this phenotype via gene replacement experiments using wild-type lines, and competing these lines with evolved populations. If there are fitness costs (or no benefits, at least) associated with this phenotype in a wild-type background then we could argue that such a phenotype emerged more or less neutrally, rather than through the action of positive selection per se. Such insight could provide answers to previous ideas such as those that argue conditions that minimise the efficiency of selection may allow the emergence of complex features that would

previously be inaccessible due to constraints imposed by natural selection (Doolittle, 2012; Lynch, 2007). By combining experimental evolution with genome sequencing, the latter of which is becoming increasingly accessible, we have the tools at our disposal to test these long-standing evolutionary theories that bring about widespread debate while remaining largely untested.

References

Abel, S., Abel zur Wiesch, P., Davis, B. M., Waldor, M. K., & Baranowski, C. (2015). Analysis of Bottlenecks in Experimental Models of Infection. PLOS Pathogens, 11(6), e1004823.

Akashi, H., Osada, N., & Ohta, T. (2012). Weak selection and protein evolution. Genetics, 192(1), 15–31.

Akins, R. A., & Lambowitz, A. M. (1987). A protein required for splicing group I introns in Neurospora mitochondria is mitochondrial tyrosyl-tRNA synthetase or a derivative thereof. Cell, 50(3), 331–345.

Allen, J. M., Light, J. E., Perotti, M. A., Braig, H. R., & Reed, D. L. (2009). Mutational Meltdown in Primary Endosymbionts: Selection Limits Muller's Ratchet. PLoS ONE, 4(3), e4969.

Andersson, D. I., & Hughes, D. (1996). Muller's ratchet decreases fitness of a DNA-based microbe. Proceedings of the National Academy of Sciences of the United States of America, 93(2), 906–7.

Andersson, D. I., Hughest, D., & Smith, J. M. (1996). Muller's ratchet decreases fitness of a DNA-based microbe. Evolution, 93, 906–907.

Barrick, J. E., & Lenski, R. E. (2013). Genome dynamics during experimental evolution. Nature Reviews Genetics, 14(12), 827–839.

Baurén, G., & Wieslander, L. (1994). Splicing of Balbiani ring 1 gene pre-mRNA occurs simultaneously with transcription. Cell, 76(1), 183–92.

Bergstrom, C. T., McElhany, P., & Real, L. A. (1999). Transmission bottlenecks as determinants of virulence in rapidly evolving pathogens. Proceedings of the National Academy of Sciences of the United States of America, 96(9), 5095–100.

Beyer, A. L., & Osheim, Y. N. (1988). Splice site selection, rate of splicing, and alternative splicing on nascent transcripts. Genes & Development, 2(6), 754–65.

Bjorkholm, B., Sjolund, M., Falk, P. G., Berg, O. G., Engstrand, L., & Andersson, D. I. (2001). Mutation frequency and biological cost of antibiotic resistance in Helicobacter pylori. Proceedings of the National Academy of Sciences, 98(25), 14607–14612.

Bjrkman, J., Hughes, D., Andersson, D. I., & Roth, J. R. (1998). Virulence of antibiotic-resistant Salmonella typhimurium. Microbiology, 95, 3949–3953.

Blin, C., Passet, V., Touchon, M., Rocha, E. P. C., & Brisse, S. (2017). Metabolic diversity of the emerging pathogenic lineages of Klebsiella pneumoniae. Environmental Microbiology.

Blount, Z. D., Barrick, J. E., Davidson, C. J., & Lenski, R. E. (2012). Genomic analysis of a key innovation in an experimental *Escherichia coli* population. Nature, 489(7417), 513–518.

Bochner, B. R. (2009). Global phenotypic characterization of bacteria. FEMS Microbiology Reviews, 33(1), 191–205.

Bull, J. J., Badgett, M. R., Rokyta, D., & Molineux, I. J. (2003). Experimental Evolution Yields Hundreds of Mutations in a Functional Viral Genome. Journal of Molecular Evolution, 57(3), 241–248.

Burch, C. L., & Chao, L. (1999). Evolution by small steps and rugged landscapes in the RNA virus phi6. Genetics, 151(3), 921–7.

Ceapa, C., Lambert, J., van Limpt, K., Wels, M., Smokvina, T., Knol, J., & Kleerebezem, M. (2015). Correlation of Lactobacillus rhamnosus Genotypes and Carbohydrate Utilization Signatures Determined by Phenotype Profiling. Applied and Environmental Microbiology, 81(16), 5458–70.

Chao, L. (1990). Fitness of RNA virus decreased by Muller's ratchet. Nature, 348(6300), 454–455.

Charlesworth, B. (2009). Fundamental concepts in genetics: Effective population size and patterns of molecular evolution and variation. Nature Reviews Genetics, 10(3), 195–205.

Clarke, D. K., Duarte, E. A., Moya, A., Elena, S. F., Domingo, E., & Holland, J. (1993a). Genetic bottlenecks and population passages cause profound fitness differences in RNA viruses. Journal of Virology, 67(1), 222–8.

Clarke, D. K., Duarte, E. A., Moya, A., Elena, S. F., Domingo, E., & Holland, J. (1993b). Genetic bottlenecks and population passages cause profound fitness differences in RNA viruses. Journal of Virology, 67(1), 222–8.

Cooper, V. S., & Lenski, R. E. (2000). The population genetics of ecological specialization in evolving *Escherichia coli* populations. Nature, 407(6805), 736–739.

Darwin, C. (1859). *The Origin of Species by Means of Natural Selection*. London: John Murray.

Degnen, G. E., & Cox, E. C. (1974). Conditional mutator gene in *Escherichia coli*: isolation, mapping, and effector studies. Journal of Bacteriology, 117(2), 477–87.

Denamur, E., & Matic, I. (2006). Evolution of mutation rates in bacteria. Molecular Microbiology, 60(4), 820–827.

Denver, D. R., Morris, K., Streelman, J. T., Kim, S. K., Lynch, M., & Thomas, W. K. (2005). The transcriptional consequences of mutation and natural selection in *Caenorhabditis elegans*. Nature Genetics, 37(5), 544–548.

Doolittle, W. F. (2012). Evolutionary biology: A ratchet for protein complexity. Nature, 481(7381), 270.

Elena, S. F., & Lenski, R. E. (2001). Epistasis between new mutations and genetic background and a test of genetic canalization. Evolution; International Journal of Organic Evolution, 55(9), 1746–52.

Elena, S. F., & Lenski, R. E. (2003). Microbial genetics: Evolution experiments with microorganisms: the dynamics and genetic bases of adaptation. Nature Reviews Genetics, 4(6), 457–469.

Eliopoulos, G. M., & Blazquez, J. (2003). Hypermutation as a Factor Contributing to the Acquisition of Antimicrobial Resistance. Clinical Infectious Diseases, 37(9), 1201–1209.

Escarmís, C., Dávila, M., & Domingo, E. (1999). Multiple molecular pathways for fitness recovery of an RNA virus debilitated by operation of Muller's ratchet. Journal of Molecular Biology, 285(2), 495–505.

Escarmís, C., Perales, C., & Domingo, E. (2009). Biological effect of Muller's Ratchet: distant capsid site can affect picornavirus protein processing. Journal of Virology, 83(13), 6748–56.

Estes, S., & Lynch, M. (2003). Rapid fitness recovery in mutationally degraded lines of *Caenorhabditis elegans*. Evolution, 57(5), 1022–1030.

Felsenstein, J. (1974). The evolutionary advantage of recombination. Genetics, 78(2), 737–56.

Finnigan, G. C., Hanson-Smith, V., Stevens, T. H., & Thornton, J. W. (2012). Evolution of increased complexity in a molecular machine. Nature, 481(7381), 360.

Fisher, R.A. (1930b). The Genetical Theory of Natural Selection. Oxford University Press. Revised Edition (1958), Dover Publications.

Fleming, L., & McShea, D. W. (2013). *Drosophila* mutants suggest a strong drive toward complexity in evolution. Evolution & Development, 15(1), 53–62.

Foster, P. L., Lee, H., Popodi, E., Townes, J. P., & Tang, H. (2015). Determinants of spontaneous mutation in the bacterium *Escherichia coli* as revealed by whole-genome sequencing. Proceedings of the National Academy of Sciences, 112(44), E5990–E5999.

Funchain, P., Yeung, A., Lee Stewart, J., Lin, R., Slupska, M. M., & Miller, J. H. (2000). The Consequences of Growth of a Mutator Strain of *Escherichia coli* as Measured by Loss of Function Among Multiple Gene Targets and Loss of Fitness. Genetics, 154(3), 959-970.

Garland, J. L. (1996). Analytical approaches to the characterization of samples of microbial communities using patterns of potential C source utilization. Soil Biology and Biochemistry, 28(2), 213–221.

Gould, S.J. (1996). Full House: The spread of excellence from Plato to Darwin. Three Rivers Press, New York, NY.

Gryta, A., Frąc, M., & Oszust, K. (2014). The application of the Biolog EcoPlate approach in ecotoxicological evaluation of dairy sewage sludge. Applied Biochemistry and Biotechnology, 174(4), 1434–43.

Guard-Bouldin, J., Morales, C. A., Frye, J. G., Gast, R. K., & Musgrove, M. (2007). Detection of Salmonella enterica subpopulations by phenotype microarray antibiotic resistance patterns. Applied and Environmental Microbiology, 73(23), 7753–6.

Hackett, C. A., & Griffiths, B. S. (1997). Statistical analysis of the time-course of Biolog substrate utilization. Journal of Microbiological Methods, 30(1), 63–69.

Hahn, M. W. (2008). Toward a selection theory of molecular evolution. Evolution, 62(2), 255–265.

Haigh, J. (1978). The accumulation of deleterious genes in a population--Muller's Ratchet. Theoretical Population Biology, 14(2), 251–67.

Haldane, J.B.S. (1957b). The cost of natural selection. J. Genet. 55, 511-24.

Halligan, D. L., & Keightley, P. D. (2009). Spontaneous Mutation Accumulation Studies in Evolutionary Genetics. Annu. Rev. Ecol. Evol. Syst, 40, 151–72.

Hedge, P. J., & Spratt, B. G. (1985). Resistance to beta-lactam antibiotics by re-modelling the active site of an *E. coli* penicillin-binding protein. Nature, 318(6045), 478–80.

Hickey, D. A. (1982). Selfish DNA: a sexually-transmitted nuclear parasite. Genetics, 101(3-4), 519–31.

Hsieh, P. (2001). Molecular mechanisms of DNA mismatch repair. Mutation Research/DNA Repair, 486(2), 71–87.

Huerta-Cepas, J., Szklarczyk, D., Forslund, K., Cook, H., Heller, D., Walter, M. C., … Bork, P. (2016). eggNOG 4.5: a hierarchical orthology framework with improved functional annotations for eukaryotic, prokaryotic and viral sequences. Nucleic Acids Research, 44(D1), D286–93.

Jaramillo, N., Domingo, E., Munoz-Egea, M. C., Tabares, E., & Gadea, I. (2013). Evidence of Muller's ratchet in herpes simplex virus type 1. Journal of General Virology, 94(Pt_2), 366–375.

Kearse, M., Moir, R., Wilson, A., Stones-Havas, S., Cheung, M., Sturrock, S., … Drummond, A. (2012). Geneious Basic: An integrated and extendable desktop software platform for the organization and analysis of sequence data. Bioinformatics, 28(12), 1647–1649.

Keymer, D. P., Miller, M. C., Schoolnik, G. K., & Boehm, A. B. (2007). Genomic and phenotypic diversity of coastal Vibrio cholerae strains is linked to environmental factors. Applied and Environmental Microbiology, 73(11), 3705–14.

Kibota, T. T., & Lynch, M. (1996). Estimate of the genomic mutation rate deleterious to overall fitness in E. coll. Nature, 381(6584), 694–696.

Kimura, M. (1968). Evolutionary Rate at the Molecular Level. Nature, 217(5129), 624–626.

Kimura, M. (1991). The neutral theory of molecular evolution: A review of recent evidence. The Japanese Journal of Genetics, 66(4), 367–386.

King, J. L., & Jukes, T. H. (1969). Non-Darwinian evolution. Science (New York, N.Y.), 164(3881), 788–98.

Kryazhimskiy, S., Plotkin, J. B., Smith, D., Simonsen, L., & Miller, M. (2008). The Population Genetics of dN/dS. PLoS Genetics, 4(12), e1000304.

Lai, A. (2017). The Emergence of Slippage-Type Editing in an Evolution Experiment. PhD thesis. University of Canterbury.

Langmead, B., & Salzberg, S. L. (2012). Fast gapped-read alignment with Bowtie 2. Nature Methods, 9(4), 357–359.

Lappin, T. R. J., Grier, D. G., Thompson, A., & Halliday, H. L. (2006). HOX genes: seductive science, mysterious mechanisms. The Ulster Medical Journal, 75(1), 23–31.

Leiby, N., & Marx, C. J. (2014). Metabolic Erosion Primarily Through Mutation Accumulation, and Not Tradeoffs, Drives Limited Evolution of Substrate Specificity in *Escherichia coli*. PLoS Biology, 12(2), e1001789.

Lenski, R. E., Ofria, C., Pennock, R. T., & Adami, C. (2003). The evolutionary origin of complex features. Nature, 423, 139-144.

Lenski, R. E., Rose, M. R., Simpson, S. C., & Tadler, S. C. (1991). Long-Term Experimental Evolution in *Escherichia coli*. I. Adaptation and Divergence During 2,000 Generations. The American Naturalist, 138(6), 1315–1341.

Levin, B. R., Perrot, V., & Walker, N. (2000). Compensatory mutations, antibiotic resistance and the population genetics of adaptive evolution in bacteria. Genetics, 154(3), 985–97.

Lewis, J. (1990). Sex and death in protozoa: The history of an obsession. Trends in Biochemical Sciences, 15(2), 77.

Lukeš, J., Archibald, J. M., Keeling, P. J., Doolittle, W. F., & Gray, M. W. (2011). How a neutral evolutionary ratchet can build cellular complexity. IUBMB Life, 63(7), 528–537.

Lynch, M. (1996). Mutation accumulation in transfer RNAs: molecular evidence for Muller's ratchet in mitochondrial genomes. Molecular Biology and Evolution, 13(1), 209–220.

Lynch, M. (2007). The frailty of adaptive hypotheses for the origins of organismal complexity. Proceedings of the National Academy of Sciences of the United States of America, 104(1), 8597–604.

Lynch, M., Ackerman, M. S., Gout, J.-F., Long, H., Sung, W., Thomas, W. K., & Foster, P. L. (2016). Genetic drift, selection and the evolution of the mutation rate. Nature Reviews Genetics, 17(11), 704–714.

Lynch, M., Bürger, R., Butcher, D., & Gabriel, W. The mutational meltdown in asexual populations. The Journal of Heredity, 84(5), 339–44.

Maciver, S. K. (2016). Asexual Amoebae Escape Muller's Ratchet through Polyploidy. Trends in Parasitology, 32(11), 855–862.

Mackie, A., Paley, S., Keseler, I. M., Shearer, A., Paulsen, I. T., & Karp, P. D. (2014). Addition of *Escherichia coli* K-12 growth observation and gene essentiality data to the EcoCyc database. Journal of Bacteriology, 196(5), 982–8.

Maisnier-Patin, S., & Andersson, D. I. (2004). Adaptation to the deleterious effects of antimicrobial drug resistance mutations by compensatory evolution. Research in Microbiology, 155(5), 360–369.

Maisnier-Patin, S., Berg, O. G., Liljas, L., & Andersson, D. I. (2002). Compensatory adaptation to the deleterious effect of antibiotic resistance in Salmonella typhimurium. Molecular Microbiology, 46(2), 355–66.

Maynard Smith, J. (1968). "Haldane's dilemma" and the rate of evolution. Nature, Lond. 219, 1114-16.

Mayr, E. (1962). Animal Species and Evolution. HUP.

McDonald, M. J., Hsieh, Y.-Y., Yu, Y.-H., Chang, S.-L., & Leu, J.-Y. (2012). The evolution of low mutation rates in experimental mutator populations of Saccharomyces cerevisiae. Current Biology : CB, 22(13), 1235–40.

McShea, D. W., & Brandon, R. N. (2010). Biology's first law : the tendency for diversity and complexity to increase in evolutionary systems. University of Chicago Press.

Moore, F. B.-G., Rozen, D. E., & Lenski, R. E. (2000). Pervasive compensatory adaptation in *Escherichia coli.* Proceedings of the Royal Society B: Biological Sciences, 267(1442), 515–522.

Moran, N. A. (1996). Accelerated evolution and Muller's rachet in endosymbiotic bacteria. Proceedings of the National Academy of Sciences of the United States of America, 93(7), 2873–8.

Muller, H. J. (1932). Some Genetic Aspects of Sex. The American Naturalist, 66(703), 118–138.

Muller, H. J. (1964). The relation of recombination to mutational advance. Mutation Research, 106, 2–9.

Naas, T., Blot, M., Fitch, W. M., & Arber, W. (1995). Dynamics of IS-related genetic rearrangements in resting *Escherichia coli* K-12. Molecular Biology and Evolution, 12(2), 198–207.

Nei, M. (1969). Gene duplication and nucleotide substitution in evolution. Nature, 221(5175), 40–2.

Nei, M. (2005). Selectionism and neutralism in molecular evolution. Molecular Biology and Evolution, 22(12), 2318–42.

Nei, M. (2007). The new mutation theory of phenotypic evolution. Proceedings of the National Academy of Sciences of the United States of America, 104(30), 12235–42.

Nei, M., Suzuki, Y., & Nozawa, M. (2010). The Neutral Theory of Molecular Evolution in the Genomic Era. Annual Review of Genomics and Human Genetics, 11(1), 265–289.

Nilsen, T. W. (2003). The spliceosome: the most complex macromolecular machine in the cell? BioEssays, 25(12), 1147–1149.

Notley-McRobb, L., & Ferenci, T. (1999a). Adaptive mgl-regulatory mutations and genetic diversity evolving in glucose-limited *Escherichia coli* populations. Environmental Microbiology, 1(1), 33–43.

Notley-McRobb, L., & Ferenci, T. (1999b). The generation of multiple co-existing mal-regulatory mutations through polygenic evolution in glucose-limited populations of *Escherichia coli*. Environmental Microbiology, 1(1), 45–52.

Ohno, S. (1970). Evolution by Gene Duplication. Berlin, Heidelberg: Springer Berlin Heidelberg.

Ohta, T. (1972). Evolutionary rate of cistrons and DNA divergence. Journal of Molecular Evolution, 1(2), 150–157.

Ohta, T. (1973). Slightly Deleterious Mutant Substitutions in Evolution. Nature, 246(5428), 96–98.

Ohta, T. (1992). The Nearly Neutral Theory of Molecular Evolution. Annual Review of Ecology and Systematics, 23(1), 263–286.

Okuyama, M., Mori, H., Chiba, S., & Kimura, A. (2004). Overexpression and characterization of two unknown proteins, YicI and YihQ, originated from *Escherichia coli*. Protein Expression and Purification, 37(1), 170–9.

Overballe-Petersen, S., Harms, K., Orlando, L. A. A., Mayar, J. V. M., Rasmussen, S., Dahl, T. W., … Willerslev, E. (2013). Bacterial natural transformation by highly fragmented and damaged DNA. Proceedings of the National Academy of Sciences of the United States of America, 110(49), 19860–5.

Overballe-Petersen, S., & Willerslev, E. (2014). Horizontal transfer of short and degraded DNA has evolutionary implications for microbes and eukaryotic sexual reproduction. BioEssays, 36(10), 1005–1010.

Paukstelis, P. J., & Lambowitz, A. M. (2008). Identification and evolution of fungal mitochondrial tyrosyl-tRNA synthetases with group I intron splicing activity. Proceedings of the National Academy of Sciences of the United States of America, 105(16), 6010–5.

Perfeito, L., Sousa, A., Bataillon, T., & Gordo, I. (2014). Rates of fitness decline and rebound suggest pervasive epistasis. Evolution; International Journal of Organic Evolution, 68(1), 150–62.

Perutz, M. F. (1983). Species adaptation in a protein molecule. Molecular Biology and Evolution, 1(1), 1–28.

Pfaffelhuber, P., Staab, P. R., & Wakolbinger, A. (2012). Muller's ratchet with compensatory mutations. The Annals of Applied Probability, 22(5), 2108–2132.

Pires-daSilva, A., & Sommer, R. J. (2003). The evolution of signalling pathways in animal development. Nature Reviews Genetics, 4(1), 39–49.

Poon, A., & Chao, L. (2005). The rate of compensatory mutation in the DNA bacteriophage phiX174. Genetics, 170(3), 989–99.

Poon, A., & Otto, S. P. (2000). Compensating for our load of mutations: freezing the meltdown of small populations. Evolution; International Journal of Organic Evolution, 54(5), 1467–79.

Raeside, C., Gaffe, J., Deatherage, D. E., Tenaillon, O., Briska, A. M., Ptashkin, R. N., … Schneider, D. (2014). Large Chromosomal Rearrangements during a Long-Term Evolution Experiment with *Escherichia coli*. mBio, 5(5): e01377-14.

Répérant, M., Porcheron, G., Rouquet, G., & Gilot, P. (2011). The yicJI metabolic operon of *Escherichia coli* is involved in bacterial fitness. FEMS Microbiology Letters, 319(2), 180–186.

Repoila, F., & Darfeuille, F. (2009). Small regulatory non-coding RNAs in bacteria: physiology and mechanistic aspects. Biology of the Cell, 101(2), 117–131.

Rifkin, S. A., Houle, D., Kim, J., & White, K. P. (2005). A mutation accumulation assay reveals a broad capacity for rapid evolution of gene expression. Nature, 438(7065), 220–223.

Rispe, C., & Moran, N. A. (2000). Accumulation of Deleterious Mutations in Endosymbionts: Muller's Ratchet with Two Levels of Selection. The American Naturalist, 156(4), 425–441.

Rocha, E. P. C., Smith, J. M., Hurst, L. D., Holden, M. T. G., Cooper, J. E., Smith, N. H., & Feil, E. J. (2006). Comparisons of dN/dS are time dependent for closely related bacterial genomes. Journal of Theoretical Biology, 239(2), 226–235.

Schmidt, U., Podar, M., Stahl, U., & Perlman, P. S. (1996). Mutations of the two-nucleotide bulge of D5 of a group II intron block splicing in vitro and in vivo: phenotypes and suppressor mutations. RNA (New York, N.Y.), 2(11), 1161–72.

Simpson, G. G. (1964). Organisms and Molecules in Evolution. Science, 146(3651).

Stoltzfus, A. (1999). On the Possibility of Constructive Neutral Evolution. Journal of Molecular Evolution, 49(2), 169–181.

Sturino, J., Zorych, I., Mallick, B., Pokusaeva, K., Chang, Y.-Y., Carroll, R. J., & Bliznuyk, N. (2010). Statistical Methods for Comparative Phenomics Using High-Throughput Phenotype Microarrays. The International Journal of Biostatistics, 6(1).

Szamecz, B., Boross, G., Kalapis, D., Kovács, K., Fekete, G., Farkas, Z., … Pál, C. (2014). The Genomic Landscape of Compensatory Evolution. PLoS Biology, 12(8), e1001935.

Taddei, F., Godelle, B., Radman, M., Maynard-Smith, J., Toupance, B., & Gouyon, P. H. (1997). Role of mutator alleles in adaptive evolution. Nature, 387(6634), 700–702.

Takeuchi, N., Kaneko, K., & Koonin, E. V. (2014). Horizontal gene transfer can rescue prokaryotes from Muller's ratchet: benefit of DNA from dead cells and population subdivision. G3 (Bethesda, Md.), 4(2), 325–39.

Tanaka, M. M., Bergstrom, C. T., & Levin, B. R. (2003). The evolution of mutator genes in bacterial populations: the roles of environmental change and timing. Genetics, 164(3), 843–54.

Tenaillon, O. (2014). The Utility of Fisher's Geometric Model in Evolutionary Genetics. Annual Review of Ecology, Evolution, and Systematics, 45, 179–201.

Tenaillon, O., Barrick, J. E., Ribeck, N., Deatherage, D. E., Blanchard, J. L., Dasgupta, A., … Lenski, R. E. (2016). Tempo and mode of genome evolution in a 50,000-generation experiment. Nature, 536(7615), 165–170.

Travis, J. M. J., & Travis, E. R. (2002). Mutator dynamics in fluctuating environments. Proceedings of the Royal Society B: Biological Sciences, 269(1491), 591–597.

Uchimura, A., Higuchi, M., Minakuchi, Y., Ohno, M., Toyoda, A., Fujiyama, A., … Yagi, T. (2015). Germline mutation rates and the long-term phenotypic effects of mutation accumulation in wild-type laboratory mice and mutator mice. Genome Research, 25(8), 1125–34.

Vehkala, M., Shubin, M., Connor, T. R., Thomson, N. R., & Corander, J. (2015). Novel R Pipeline for Analyzing Biolog Phenotypic Microarray Data. PLOS ONE, 10(3), e0118392.

Viana, D., Comos, M., McAdam, P. R., Ward, M. J., Selva, L., Guinane, C. M., … Penadés, J. R. (2015). A single natural nucleotide mutation alters bacterial pathogen host tropism. Nature Genetics, 47(4), 361–366.

Wheeler, N. E., Barquist, L., Ashari Ghomi, F., Kingsley, R. A., & Gardner, P. P. (2015). A Profile-Based Method for Measuring the Impact of Genetic Variation. bioRxiv. Cold Spring Harbor Labs Journals.

Wheeler, N. E., Barquist, L., Kingsley, R. A., & Gardner, P. P. (2016). A profile-based method for identifying functional divergence of orthologous genes in bacterial genomes. Bioinformatics, 32(23), 3566-3574.

Whitlock, & Otto. (1999). The panda and the phage: compensatory mutations and the persistence of small populations. Trends in Ecology & Evolution, 14(8), 295–296.

Wielgoss, S., Barrick, J. E., Tenaillon, O., Wiser, M. J., Dittmar, W. J., Cruveiller, S., … Schneider, D. (2013). Mutation rate dynamics in a bacterial population reflect tension between adaptation and genetic load. Proceedings of the National Academy of Sciences of the United States of America, 110(1), 222–7.

Winkler, W. C., & Breaker, R. R. (2005). Regulation of bacterial gene expression by riboswitches. Annual Review of Microbiology, 59(1), 487–517.

Wright, S. (1977). Evolution and the Genetics of populations, vol. 3, Experimental Results and Evolutionary Deductions. University of Chicago press.

Wright, S. I., & Andolfatto, P. (2008). The Impact of Natural Selection on the Genome: Emerging Patterns in *Drosophila* and *Arabidopsis*. Annual Review of Ecology, Evolution, and Systematics, 39(1), 193–213.

Yuste, E., Sánchez-Palomino, S., Casado, C., Domingo, E., & López-Galíndez, C. (1999). Drastic fitness loss in human immunodeficiency virus type 1 upon serial bottleneck events. Journal of Virology, 73(4), 2745–51.

Zhang, E., & Ferenci, T. (1999). OmpF changes and the complexity of *Escherichia coli* adaptation to prolonged lactose limitation. FEMS Microbiology Letters, 176(2), 395–401.

Zhang, J. (2016). Neutral Theory. Oxford Bibliographies.

Zhang, J., & al., et. (2003). Evolution by gene duplication: an update. Trends in Ecology & Evolution, 18(6), 292–298.

Zuckerkandl, E. (1997). Neutral and nonneutral mutations: the creative mix--evolution of complexity in gene interaction systems. Journal of Molecular Evolution, 44 Suppl 1, S2–8.

Zuckerkandl, E. (2001). Intrinsically Driven Changes in Gene Interaction Complexity. I. Growth of Regulatory Complexes and Increase in Number of Genes. Journal of Molecular Evolution, 53(4-5), 539–554.

Zuckerkandl, E., & Pauling, l. (1965). Evolutionary Divergence and Convergence in Proteins. In Evolving Genes and Proteins (pp. 97–166).